Biosynthesis of Aromatic Amino Acids in Yeast and Aspergillus

Mechanisms Controlling the Flux of Chorismate

Dissertation
zur Erlangung des Doktorgrades
der Mathematisch-Naturwissenschaftlichen Fakultäten
der Georg-August-Universität zu Göttingen

vorgelegt von
Sven Kurt Krappmann
aus Hanau

Göttingen 2000

Die vorliegende Arbeit wurde in der Arbeitsgruppe von Prof. Dr. Gerhard H. Braus in der Abteilung Molekulare Mikrobiologie des Institutes für Mikrobiologie & Genetik der Georg-August-Universität Göttingen angefertigt.

Teile dieser Arbeit wurden veröffentlicht in:

Krappmann, S., R. Pries, G. Gellissen, M. Hiller, and G.H. Braus (2000) *HARO7* Encodes Chorismate Mutase of the Methylotrophic Yeast *Hansenula polymorpha* and Is Derepressed upon Methanol Utilization. *J. Bacteriol.* **182:** 4188-4197.

Krappmann, S., K. Helmstaedt, T. Gerstberger, S. Eckert, B. Hoffmann, M. Hoppert, G. Schnappauf, and G.H. Braus (1999) The *aroC* Gene of *Aspergillus nidulans* Codes for a Monofunctional, Allosterically Regulated Chorismate Mutase. *J. Biol. Chem.* **274:** 22275-22282.

D 7
Referent: Prof. Dr. G. H. Braus
Korreferent: Prof. Dr. G. Gottschalk
Tag der mündlichen Prüfung: 31. Oktober 2000

The books of the great scientists are gathering dust on the shelves of learned libraries. And rightly so. The scientist addresses an infinitesimal audience of fellow composers. His message is not devoid of universality but its universality is disembodied and anonymous. While the artist's communication is linked forever with its original form, that of the scientist is modified, amplified, fused with the ideas and results of others, and melts into the stream of knowledge and ideas which forms our culture. The scientist has in common with the artist only this: that he can find no better retreat from the world than his work and also no stronger link with his world than his work.

Max Delbrück, 1969

ACKNOWLEDGMENTS

Special thanks to Gerhard Braus for supervising and supporting this thesis with continous and inspiring interest.

I thank Prof. G. Gottschalk for accepting to co-examine this thesis.

I especially appreciate the works of Kerstin Helmstaedt, Thomas Gerstberger, and Ralph Pries who contributed to this work in their diploma theses.

Thanks to all present members of the group – Meike Andermann, Matthias Bäumer, Silke Busch, Oliver Draht, Olav Grundmann, Markus Hartmann, Gabi Heinrich, Stefan Irniger, Tim Köhler, Maria Meyer, Heidi Northemann, Axel Strittmatter, Naimeh Taheri, and Oliver Valerius – for discussions, ideas, and a very comfortable working atmosphere.
Especially, I thank Hans-Ueli Mösch who taught me a lot about molecular biology.

Additionally, I have to thank former colleagues – Gerd Albrecht, Sabine Eckert, Katrin Düvel, Bernd Hoffmann, Georg Schnappauf, Christhoph Springer, Christoph Wanke – who supported me in the initial phase of my works and beyond it.

I am thankful to Prof. G. Gellissen for the fruitful collaboration with Rhein Biotech GmbH, to Dr. Ch. Urbanke, Hannover, for analyses of AROC on an analytical ultracentrifuge, to Dr. M. Hoppert for assistance on electron microscopy, and to all other people at the Institute of Microbiology & Genetics of the Georg-August-University, Göttingen.

Finally, I want to thank my parents and all my friends for giving me a lot of general support all the time…

The Deutsche Forschungsgemeinschaft, the Fond der Chemischen Industrie, the Volkswagen-Stiftung, Rhein Biotech GmbH, and the Niedersächsischen Vorab der Volkswagen-Stiftung (Forschungsstelle für nachwachsende Rohstoffe) have granted financial support.

Table of Contents

Abbreviations

3AT	3-amino-1,2,4-triazole
5FOA	5-fluoroorotic acid
5MT	5-methyl-tryptophan
AA	anthranilic acid
AAS	anthanilate synthase
ADIC	2-amino-2-deoxyisochorismate
AGN	arogenic acid
ATP	adenosine-5'-triphosphate
bp	base pair(s)
BSA	bovine serum albumin
CA	chorismic acid
CDRP	carboxy-phenylamino-1-deoxyribulose-5-phosphate
CM	chorismate mutase
CPRE	cross pathway control recognition element
DAHP	3-deoxy-*D*-arabino-heptulosonate-7-phosphate
DHQ	3-dehydroquinate
DHS	3-dehydroshikimic acid
DON	6-diazo-5-oxo-*L*-norleucine
DTT	*DL*-dithiothreitol
E4P	erythrose-4-phosphate
EDTA	ethylenediaminetetraacetate
EPSP	5-enolpyruvylshikimate-3-phosphate
G3P	glyceraldehyde-3-phosphate
GAT	glutamine amidotransferase
GCRE	general control recognition element
HPP	4-hydroxyphenylpyruvic acid
IGP	indoleglycerole phosphate
NMR	nuclear magnetic resonance
nt	nucleotide(s)
OD	optical density
PA	prephenic acid
PAGE	polyacrylamide gel electrophoresis
PCR	polymerase chain reaction
PEP	phosphoenolpyruvic acid
PMSF	phenylmethylsulfonyl fluoride
PPY	phenylpyruvic acid
PRA	phosphoribosylanthranilic acid
SDS	sodium dodecylsulfate
S3P	shikimate-3-phosphate
UV	ultraviolet
wt	wild type
YEPD	yeast extract peptone dextrose
μ	growth rate

Summary

Chorismate mutases (E.C. 5.4.99.5) catalyse the Claisen rearrangement of chorismic acid to prephenate, the first reaction of the tyrosine/phenylalanine-specific branch of aromatic amino acid biosynthesis. Within this biosynthetic pathway they compete with the anthranilate synthase complex for the common substrate chorismate and both enzymes define the first branch point of that metabolic pathway. The *ARO7*-encoded chorismate mutase of the baker's yeast *Saccharomyces cerevisiae* which has previously been characterized in detail serves as model system for allosteric regulation of catalytic activity. Other chorismate mutases of fungi are hardly characterized.

In this thesis, the mechanisms regulating the enzymatic activities that channel chorismate into the two main branches in *S. cerevisiae* were analysed. The impact of an allosterically unregulated chorismate mutase was investigated in combination with genetically engineered variations in transcriptional regulation of expression of both branch point genes. It turned out that only the regulatory pattern as it exists at the branch point is sufficient under amino acid starvation conditions. The results imply that in the baker's yeast transcriptional and allosteric regulation have evolved in accordance to guarantee optimal flux of the intermediate compound into both branches. For comparison, the chorismate mutase activity of a methylotrophic yeast, the *HARO7* gene product of *Hansenula polymorpha*, was characterized. The allosteric enzyme is strictly regulated by the end products tyrosine and tryptophan. In the presence of methanol as sole carbon source, transcription of the encoding gene is induced, whereas under amino acid starvation conditions no additional transcriptional regulation is present. In order to characterize the chorismate mutase of a filamentous fungus, the *aroC*-encoded enzyme of *Aspergillus nidulans* was investigated. Here, again no transcriptional regulation upon starvation conditions is present, but allosteric regulation by the heterotropic effectors tyrosine and tryptophan. Catalytic properties of the gene product were determined as well as its quaternary structure. Furthermore, it was shown that the allosteric intramolecular signal transduction pathway is not conserved with respect to the baker's yeast enzyme.

Zusammenfassung

Chorismatmutasen (E.C. 5.4.99.5) katalysieren die Claisen-Umlagerung von Chorisminsäure in Prephenat, die erste Reaktion des Tyrosin/Phenylalanin-spezifischen Astes der Biosynthese aromatischer Aminosäuren. Innerhalb des Biosyntheseweges konkurrieren sie dabei mit dem Anthanilatsynthase-Komplex um das gemeinsame Substrat Chorismat, und beide Enzyme definieren den ersten Verzweigungspunkt innerhalb des metabolischen Stoffwechselweges. Die *ARO7*-kodierte Chorismatmutase der Bäckerhefe *Saccharomyces cerevisiae* wurde in vorangegangenen Arbeiten eingehend charakterisiert und stellt ein Modellsystem in Hinblick auf allosterische Regulation katalytischer Aktivität dar. Chorismatmutasen aus anderen Pilzen sind jedoch kaum charakterisiert.

In der vorliegenden Arbeit wurden die Mechanismen untersucht, die die enzymatischen Aktivitäten am ersten Verzweigungspunkt innerhalb der Biosynthese aromatischer Aminosäuren in *S. cerevisiae* regulieren. Der Einfluß einer allosterisch unregulierten Chorismatmutase wurde im Wechselspiel transkriptioneller Regulation der Genexpression beider Verzweigungspunktenzyme untersucht. Dabei zeigte sich, daß das regulatorische Muster, wie es am Verzweigungspunkt der Bäckerhefe vorliegt, unter Aminosäuremangelbedingungen notwendig ist. Die Ergebnisse legen nahe, daß in diesem Organismus im Zuge der Evolution transkriptionelle und allosterische Regulation der Chorismatmutaseaktivität ausgeprägt wurden, um einen optimalen Fluß des Intermediates in beide Hauptzweige zu gewährleisten. Darüber hinaus wurde die Chorismatmutaseaktivität einer methylotrophen Hefe, das *HARO7*-Genprodukt aus *Hansenula polymorpha*, charakterisiert. Das allosterische Enzym unterliegt strikter Regulation durch die Endprodukte Tyrosin und Tryptophan. In Gegenwart von Methanol als alleiniger C-Quelle wird die Transkription des kodierenden Gens induziert, während unter Aminosäuremangelbedingungen keine zusätzliche transkriptionelle Regulation vorliegt. Um die Chorismatmutase eines filamentösen Pilzes zu charakterisieren, wurde das *aroC*-kodierte Enzym aus *Aspergillus nidulans* eingehend untersucht. Auch hier liegt keine transkriptionelle Regulation unter Mangelbedingungen vor, jedoch allosterische Regulation durch die heterotropen Effektoren Tyrosin und Tryptophan. Die katalytischen Eigenschaften des Genproduktes wurden bestimmt, ebenso wie dessen Quartärstruktur. Darüber hinaus konnte für dieses Enzym gezeigt werden, daß der allosterische intramolekulare Signaltransduktionsweg im Vergleich zum Bäckerhefeenzym nicht konserviert ist.

Chapter 1

Introduction

1. Biosynthesis of Aromatic Amino Acids

Synthesis of amino acids in general is an essential process for a living cell as it leads to precursors of polypeptides as well as to primary and secondary metabolites. In the last five decades the biosynthetic cascade resulting in the aromatic amino acids *L*-phenylalanine, *L*-tyrosine, and *L*-tryptophan has gained increasing attention in biochemical research as it constitutes a model system for a complex and strictly regulated pathway that links carbohydrate metabolism to biosynthesis of aromatic compounds. With respect to energy expense, biosynthesis of aromatic amino acids is one of the most costly pathways in a living system. Synthesis of 1 mol of tryptophan, phenylalanine, and tyrosine requires 78, 65, and 62 mol ATP, respectively. Whereas animals are only able to form tyrosine by hydroxylation of phenylalanine and therefore require this amino acid together with tryptophan in their diet, archea, eubacteria, plants, and fungi are competent to synthesize all three aromatic amino acids *de novo*. Therefore this particular pathway has become an important target for herbicides, antibiotics and live vaccines. The reaction cascades resulting in phenylalanine, tyrosine and tryptophan are generally separated into seven invariable steps constituting the main trunk of the shikimate pathway and two branches emerging from chorismic acid, the central intermediate of the biosynthetic pathway (Pittard, 1996) (Fig 1).

1.1 The Shikimate Pathway

The enzymatic conversions resulting in the last common intermediate of the pathway were originally discovered through studies on *Escherichia coli* and *Salmonella typhimurium* about 40 years ago. Condensation of two carbohydrate metabolites, phosphoenolpyruvate (PEP) derived from glycolysis and erythrose-4-phosphate (E4P) derived from ribulose-5-phosphate, one product of the pentosephosphate cycle, to yield 3-deoxy-*D-arabino*-heptulosonate-7-phosphate (DAHP) and inorganic phosphate determines the first enzymatic step of the cascade and is enzymatically catalysed by a DAHP synthase activity (E.C. 4.1.2.15). By five enzymatic conversions DAHP is converted via 3-dehydroquinate (DHQ), 3-dehydroshikimate (DHS), shikimate, and shikimate-3-phosphate (S3P) to 5-enolpyruvylshikimate-3-phosphate (EPSP). The latter reaction is catalysed by an EPSP

synthase activity (E.C. 2.5.1.19) which is the major target of N-[phosphomono-methyl]glycine, the active ingredient of the broad-spectrum herbicide glyphosphate. This well-established EPSP synthase inhibitor has also been successfully tested in mice as therapeutic agent against pathogenic protozoans to combat toxoplasmosis or malaria (Roberts *et al*., 1998). In bacteria the five reactions from DAHP to EPSP are catalysed by separate enzymes, whereas in fungi a single multifunctional polypeptide, the so-called AROM complex, fulfils all five catalytic steps (reviewed by Coggins *et al*., 1985). AROM complexes have been studied extensively in fungi like *Neurospora crassa*, *Aspergillus nidulans*, or *Saccharomyces cerevisiae*. An evolutionary gene fusion event has been proposed to form the *arom* locus by sequence comparison of encoding genes to their prokaryotic counterparts (Catcheside *et al*., 1985; Charles *et al*., 1986; Duncan *et al*., 1987). As last step in the shikimate pathway main trunk the trans-1,4-elimination of phosphate from EPSP leading to chorismic acid (CA) has been identified. This reaction is catalysed by a chorismate synthase activity (E.C. 4.6.1.4) and requires reduced flavin although no oxidation or reduction process is involved in the catalytic reaction. Chorismate mutases are either monofunctional and therefore require addition of reduced flavin in *in vitro* assays or bifunctional carrying an NADPH-driven flavin reductase (diaphorase) activity associated within the same protein. The bacterial CA synthase enzymes from *E. coli* and *Bacillus subtilis* appear to be monofunctional (Hasan and Nester, 1978; White *et al*., 1988), opposite to fungal enzymes like from *N. crassa* or *S. cerevisiae* which seem to be bifunctional (Henstrand *et al*., 1995; Henstrand *et al*., 1996; Jones *et al*., 1991).

From chorismic acid, the final product of the shikimate pathway, several metabolic branches are initiated. Additionally, every intermediate of the main trunk is a potential branch point compound feeding other metabolic pathways (for review see Bentley, 1990).

1.2 Chorismate, the Central Intermediate

The existence of chorismic acid as the last common intermediate in the biosynthesis of tyrosine, phenylalanine, and tryptophan was uncovered in 1962 from an *Aerobacter aerogenes* strain blocked both in the tyrosine/phenylalanine and tryptophan branches (Gibson, 1964; Gibson and Gibson, 1964). NMR spectroscopy studies as well as UV spectrum analysis unravelled the structure of the accumulated intermediate and proved the chemical nature of this formerly unidentified branch point compound. With respect to the branch point concept linked to the compound, the name ‘chorismic’ acid (from Greek: *inter alia*, a being separated, parting etc.) was chosen (Gibson, 1999).

The intramolecular rearrangement of chorismic acid to prephenic acid (PA) initiates the tyrosine/phenylalanine-specific branch of aromatic amino acid biosynthesis. This [3,3] sigmatropic conversion, formally a Claisen rearrangement, is a rare example for a pericyclic reaction in primary metabolism and is catalysed by a unique enzymatic activity, the chorismate mutase (E.C. 5.4.99.5, see section 2.1). On the other hand, anthranilic acid (AA) is formed from chorismate by an anthranilate synthase complex (E.C. 4.1.3.27) to feed the tryptophan branch of the pathway (see section 2.2).

Besides its central position in aromatic amino acid biosynthesis, chorismate is the common precursor for a variety of other metabolites like folate (through 4-amino-benzoate), ubiquinone and menaquinone (through 4-hydroxybenzoate), or the iron-binding compound enterochelin (through 2,3-hydroxybenzoate) (Bentley and Meganathan, 1982; Liu *et al*., 1990). From this point of view it is obvious that the cellular chorismate pool requires strict regulation with respect to the catalytic activities depending on chorismic acid as substrate.

1.3 Biosynthesis of Tyrosine and Phenylalanine

After the formation of PA from chorismate the tyrosine/phenylalanine-specific part of the pathway branches again by two alternative routes to form the end products. One proceeds via phenylpyruvate (PPY) and 4-hydroxyphenylpyruvate (HPP), respectively, whereas the alternative one is constituted by the formation of *L*-arogenate (AGN) (for review see Jensen and Fischer, 1987). In plants the latter pathway is preferred, in contrast to the situation in *S. cerevisiae* or *E. coli* where only the PPY/HPP route is followed. Additionally, combinations of both alternatives are found for instance in cyanobacteria or *Pseudomonas aeruginosa*.

The oxidative decarboxylation and dehydratation of PA to yield 4-hydoxy-phenylpyruvate is catalysed by a prephenate dehydrogenase (E.C. 1.3.1.13). By final transamination of HPP by an aminotransferase (E.C. 2.6.1.57) the end product tyrosine is formed. Phenylalanine on the other hand is synthesised from PA by a dehydratase activity (E.C. 4.2.1.51) followed by transamination of PPY. Alternatively, transamination of prephenate yields arogenate which in turn can serve as common precursor for both amino acids.

1.4 Biosynthesis of Tryptophan

Tryptophan biosynthesis proceeds in five steps requiring seven enzyme activities after chorismate formation (Weiss and Edwards, 1980). As described before, the chorismate-to-anthranilate conversion initiates this pathway branch. The synthesis of anthranilate is a two-step process in which the reversible reaction of chorismate with ammonia to 2-amino-2-deoxyisochorismate (ADIC) is followed by the irreversible elimination of pyruvate from ADIC (Morollo and Bauerle, 1993). Ammonia is generated from a glutamine aminotransferase activity associated with the anthranilate synthase activity (E.C. 4.1.3.27) or can *in vitro* be added exogenously, but at unphysiologically high concentrations. The next step in tryptophan biosynthesis is the transfer of a 5-phosphorybosyl moiety to the amino group of AA to form phosphoribosylanthranilate (PRA). This reaction is accelerated by a phospho-ribosyltransferase activity (E.C. 2.4.2.18) that utilises 5-phosphoribosyl-pyrophosphate for transfer. Formation of the ketone carboxy-phenylamino-1-deoxyribulose-5-phosphate (CDRP), the next step in the reaction cascade, resembles a practically irreversible Amadori rearrangement and is catalysed by the PRA isomerase enzyme. From CDRP indoleglycerol phosphate (IGP) is formed by decarboxylation through the action of indoleglycerol phosphate synthase (E.C. 4.1.1.48). In the ultimate step of tryptophan biosynthesis IGP is cleaved to release glyceraldehyde-3-phosphate (G3P) and the resulting indole is condensed with serine to yield the end product. The corresponding enzyme catalysing this two-step process is the tryptophan synthase (E.C. 4.2.1.20), one of the best-studied enzymes of the pathway (Hyde *et al*., 1988; Miles *et al*., 1987; Yanofsky, 1987).

The tryptophan-specific branch is of special interest with respect to genetic organisation as considerable variations exist between different microorganisms (Crawford, 1987; Hütter *et al*., 1986). Some gene products are bi- or trifunctional, and some enzyme activities require two gene products. The number of genes necessary to constitute the metabolic branch ranges from four, as in *A. nidulans*, *N. crassa* or *S. pombe*, to seven, like in *Ps. putida*. In *S. cerevisiae* and *E. coli* five encoding genes exist for tryptophan synthesis from chorismate.

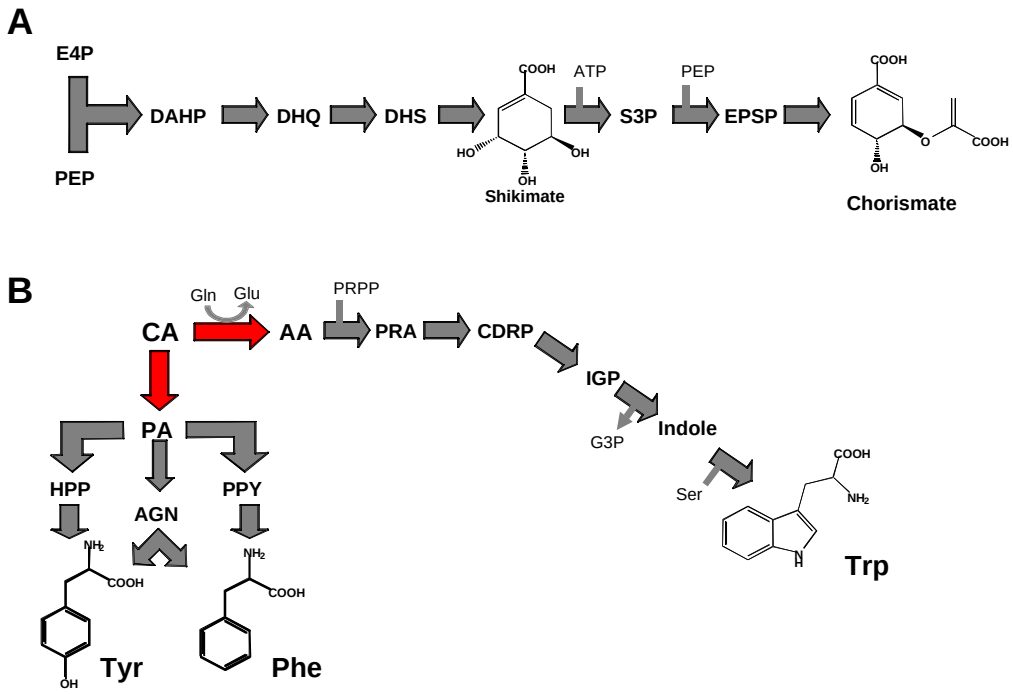

Figure 1: Schematic outline of the biosynthetic pathway resulting in aromatic amino acids. Enzymatic activities are indicated by arrows with the initiations of tyrosine/phenylalanine- and tryptophan-specific branches highlighted in red. See text for details concerning abbreviations of intermediate compounds as well as enzymatic activities. *A*, shikimate pathway converting erythrose-4-phosphate (E4P) and phosphoenolpyruvate (PEP) in seven steps to chorismic acid. *B*, main biosynthetic routes emerging from chorismate (CA) resulting in the end products tryptophan (Trp), phenylalanine (Phe), and tyrosine (Tyr).

2. The Branch Point Enzymes

2.1 Chorismate Mutase

Chorismate mutase (CM) activities (chorismate pyruvate mutase, E.C. 5.4.99.5) catalyse the intramolecular rearrangement of (-)chorismic acid to prephenic acid (Fig. 2) (Andrews *et al.*, 1973). In comparison to the uncatalysed, thermal [3,3] sigmatropic rearrangement, CMs can enhance the conversion of chorismate to prephenate by a factor of up to 10^6. A variety of CM enzymes have been described and characterised during the past three decades and also catalytic antibodies (‘abzymes’) accelerating the chorismate-to-prephenate rearrangement have been generated (Bowdish *et al.*, 1991). Prokaryotic CM activities are often found to be part of a bifunctional enzyme in which the CM domain is fused to a prephenate dehydratase (P-protein), a prephenate dehydrogenase (T-Protein), and a 3-deoxy-*D*-arabinoheptulosonate-7-phosphate synthase moiety, respectively (Romero *et al.*, 1995a). In contrast, all eukaryotic CMs characterised to date as well as the only known CM

from an archeon, the one of *Methanococcus jannaschii* (MacBeath *et al.*, 1998), are described to be monofunctional.

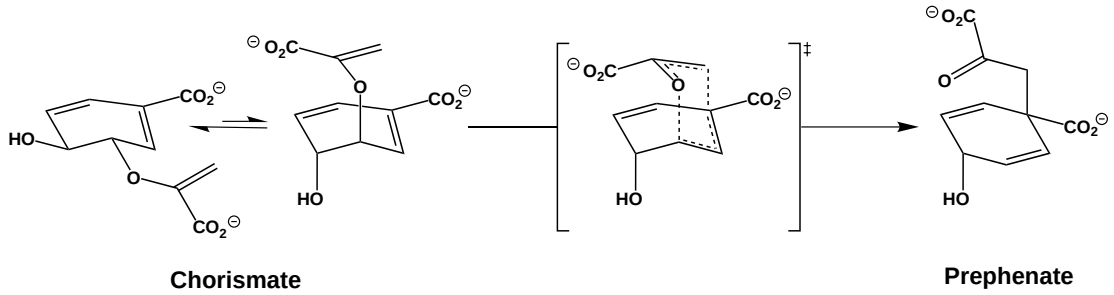

Figure 2: The Claisen rearrangement of chorismic acid resulting in prephenic acid. The two conformations of chorismate are shown as well as the proposed transition state finally leading to prephenate.

In most organisms CM activity is strictly regulated. Whereas both enzyme activities of bifunctional T-proteins are inhibited by tyrosine, phenylalanine inhibits the two activities of P-proteins. However, in Gram-negative bacteria as well as in Gram-positive *B. subtilis* and *S. aureofaciens* and in cyanobacteria, monofunctional CMs were found that lack regulatory properties. Eukaryotic CM enzymes are generally monofunctional and subject to allosteric inhibition and activation. Tyrosine and/or phenylalanine are negative effectors whereas tryptophan serves as positive regulator of enzyme activity. In plants different isoenzymes are often present which differ in their regulatory behaviour. Furthermore, some of them are regulated in their activity not only by end products of aromatic amino acid biosynthesis but alternatively by secondary metabolites (Romero *et al.*, 1995a).

The crystal structures of three natural CM enzymes have been determined. Based on these structural insights and on primary sequence information of the encoding genes cloned to date it has become evident that two completely different structural folds have evolved to contrive the enzymatic isomerization of chorismate to prephenate. One structural class, AroH, is represented by the monofunctional, homotrimeric enzyme of *Bacillus subtilis* the X-ray structure of which was determined at 1.9 Å resolution (Fig. 2A, B) (Chook *et al.*, 1993). The *aroH* gene product is a nonallosteric CM of 127 amino acids per monomer. Each monomer consists of a five-stranded mixed β-sheet packed against an 18-residue α-helix and a two-turn 3_{10} helix. The C-terminal part resembles one turn of a 3_{10} helix facing away from the β-sheet on the face opposite the helices into the solvent region. In the trimeric structure with pseudo-3-fold symmetry, large portions of each β-sheet form the sides of a prism. This structural core is surrounded by three α-helices and three 3_{10} helices

while the side chains looming into the core of the barrel structure being almost exclusively hydrophobic. Structural data of the trimer in complex with an *endo*-oxabicyclic transition state analogue have identified the enzymatically active sites. The interfaces between adjacent subunits form three equivalent clefts open and accessible to solvent where the structural analogue is bound.

Sequences of all CM domains from bifunctional enzymes characterized to date as well as most prokaryotic and eukaryotic monofunctional CMs match into the AroQ class of CM enzymes. These enzymes are, in contrast to the three-dimensional pseudo-α/β-barrel structure established by the AroH class, all-helical polypeptides and show similarity in sequence to the monofunctional CM of *Erwinia herbicola* encoded by the *aroQ* gene (Xia *et al.*, 1993). To indicate the origin of a particular CM activity, subclasses were defined by Jensen and co-workers: $AroQ_f$ enzymes are monofunctional, whereas $AroQ_p$ domains are fused to a prephenate dehydratase, $AroQ_t$ enzymes to a prephenate dehydrogenase, and $AroQ_d$ enzymes to a 3-deoxy-D-arabinoheptulosonate-7-phosphate synthase activity, respectively (Gu *et al.*, 1997). In contrast to the situation in prokaryotes, primary sequences of eukaryotic CM proteins are rare. Only a few encoding sequences have been determined to date like the genes from the yeasts *S. cerevisiae* and *S. pombe*, and those coding for three isoenzymes in *A. thaliana* (Schmidheini *et al.*, 1989; Oliver *et al.*, 1995; Eberhard *et al.*, 1993; Kuhn *et al.*, 1999; Mobley *et al.*, 1999). On the basis of the solved structure of the *S. cerevisiae* CM and on conserved primary structures among cloned eukaryotic CM-encoding genes, these chorismate mutases are included in the AroQ class. Nevertheless, as eukaryotic CMs additionally contain regulatory domains, they constitute the separate subclass of $AroQ_r$ enzymes (formerly AroR) (MacBeath *et al.*, 1998).

The structural prototype of the AroQ class is the CM domain of the bifunctional, homodimeric *Escherichia coli* CM-prephenate dehydratase enzyme. The N-terminal 109 residues of this P-protein constitute a functional CM and its X-ray structure was solved at 2.2 Å resolution (Fig. 3A, B) (Lee *et al.*, 1995). In the monomer, the polypeptide chain resembles the figure "4" by its unusual fold of three α-helices, two long and one short, connected by two loops. Upon dimer formation, an antiparallel four-helix-bundle, which is quite hydrophobic and well packed, is formed by three helices from one monomer and the first, long helix from the other. By interaction of other pairs of helices, two other relatively open helical bundles are formed which have been shown to bind the stable transition state analogue in the crystal structure. Therefore, two equivalent active sites with contributions from each monomer are present in the quaternary structure of this engineered CM from

E. coli. The only solved crystal structure of an eukaryotic CM enzyme, the 256 amino acid *ARO7* gene product of the baker's yeast *S. cerevisiae,* also is an all-helical polypeptide (Fig. 3A, B). Several X-ray structures have been determined to date, representing different allosteric states of this enzyme (Sträter *et al.*, 1996; Sträter *et al.*, 1997; Xue *et al.*, 1994). The basic topology of one monomeric subunit is that of a Greek key motif forming a four-helix bundle with essentially no β-sheet elements. The twelve helices of the polypeptide chain are arranged in a twisted two-layer structure with a packing angle between the helical axes from each layer of about 60°. The dimer has the shape of a bipyramid with four helices (H2, H4, H8, and H11) forming the hydrophobic interface between he protomers. The active site is part of the four-helix bundle set up by the helices H2, H8, H11, and H12 separately in each monomer whereas the binding site for both heterotropic effectors is a cleft in the dimer interface between the subunits. This regulatory site is formed by two helices (H4 and H5) of one monomer and the 80s loop and helix H8 of the other. The latter one is the longest helix in the molecule as it consists of 32 residues and spans the overall structure from the regulatory site to the catalytic domain. In addition, hydrophilic side chains of this helix and of helices H2, H4, H4 and of loop 80s form a hydrophilic channel through the centre of the enzyme.

The fact that the three-dimensional structure of the *E. coli* CM domain and its eukaryotic counterpart, both AroQ class enzymes, resemble similar folds has led to the speculation of a common evolutionary origin (Lee *et al.*, 1995; Xue and Lipscomb, 1995). In fact, the *E. coli* CM dimer can be superimposed onto a monomer of yeast CM. The topology of a four-helix bundle forming the active site is conserved in the two enzymes and also the binding mode of the *endo*-oxabicyclic inhibitor is similar. Modelling two *E. coli* CM dimers onto the *S. cerevisiae* dimer has led to further insights: two bacterial CM monomers superimpose well on the catalytic domains of the yeast CM whereas the other monomers and the other halves of the yeast monomers are more diverse due to the evolution of regulatory domains in this region of the molecules (Sträter *et al.*, 1997). In conclusion, it may be speculated that the yeast CM fold might have evolved from an ancestral protein similar to the bacterial CM by a gene duplication event followed by dimerization.

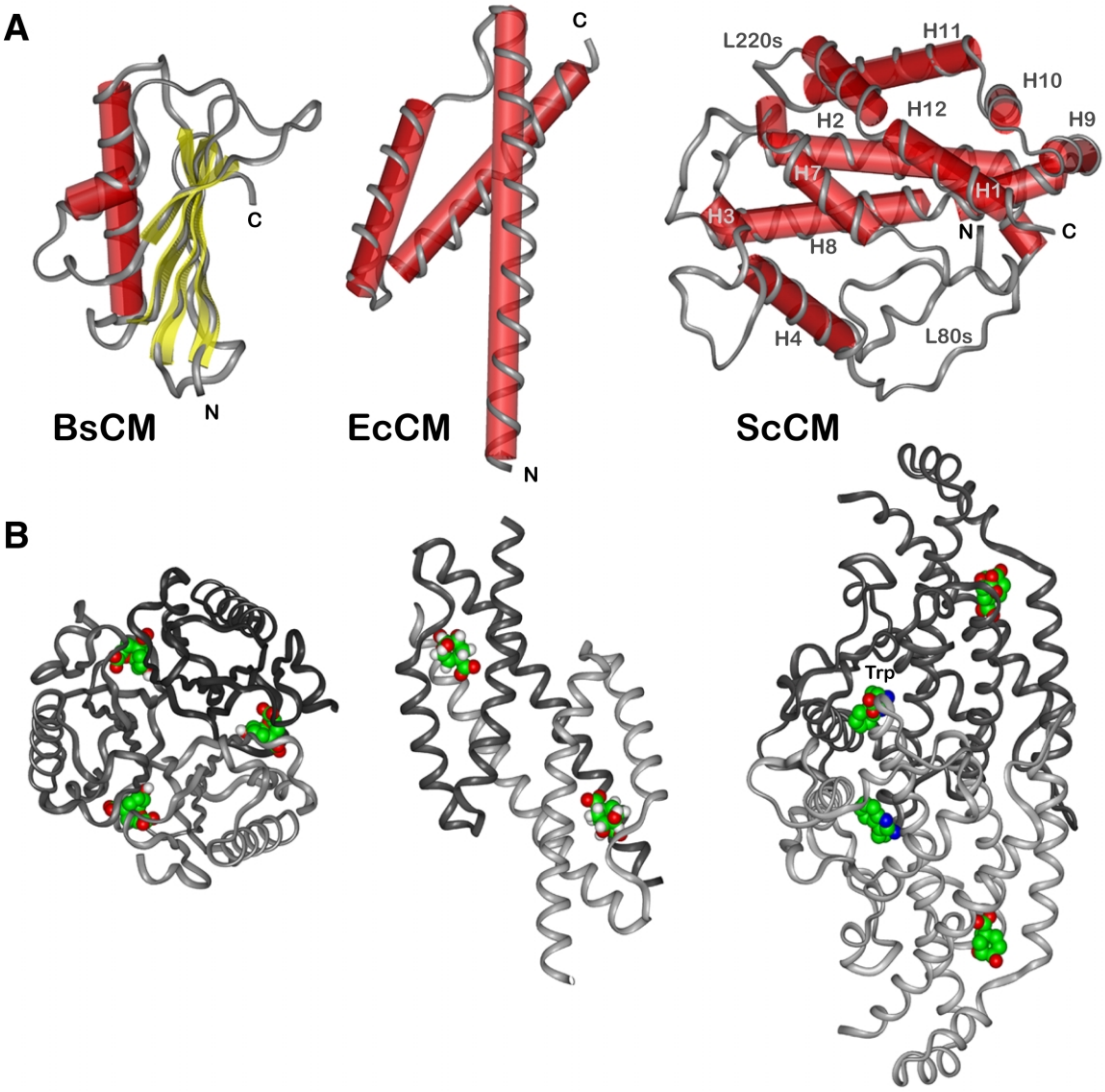

Figure 3: Structural properties of chorismate mutases. *A*, Schematic presentations of the structural fold displayed by chorismate mutase from *B. subtilis* (BsCM, left), *E. coli* (EcCM, middle), and *S. cerevisiae* (ScCM, right). The polypeptide backbone is displayed in ribbon style and secondary elements are labelled with red cylinders (helices) and yellow bars (sheets). N and C termini are indicated as well as structural elements of ScCM (see text for details). *B*, Oligomeric structure of BsCM (left), EcCM (middle), and ScCM (right) in complex with a stable transition state analogue. Monomeric subunits are indicated by different shades of grey. For ScCM also the binding position of the positive effector tryptophan is shown.

2.2 Anthranilate Synthase

Generally, glutamine-dependent amidotransferases accelerate the transfer of the amido nitrogen of glutamine to an acceptor substrate to produce one molecule of glutamate and one molecule of an aminated product. Therefore, they are organised in two separable domains bearing glutamine and substrate binding sites. The former is called the GAT (glutamine amide transfer) domain and bears glutaminase activity whereas the latter generally is designated as synthase domain.

Anthranilate synthase (AAS) enzymes (chorismate pyruvate-lyase (amino accepting), E.C. 4.1.3.27) catalyse the formation of anthranilate and pyruvic acid from chorismate and glutamine. This conversion requires three distinct steps: generation of ammonia from glutamine, addition of ammonia to chorismate to yield the diene intermediate 2-amino-2-deoxyisochorismate (ADIC), followed by elimination of pyruvate (Fig. 4).

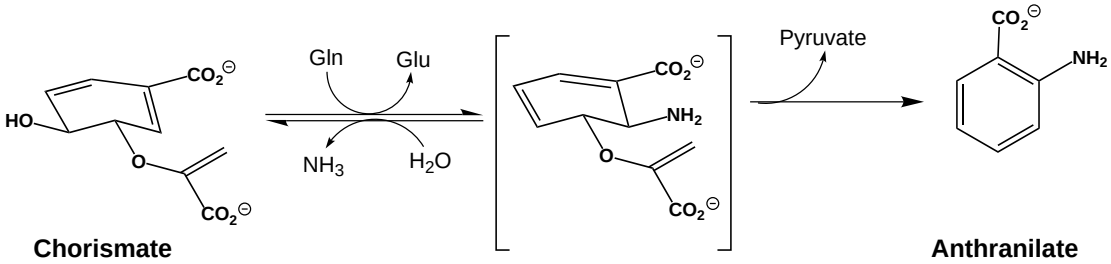

Figure 4: Formation of anthranilate from chorismic acid. The two-step reaction of the chorismate-to-anthranilate conversion is shown with the proposed reaction intermediate 2-amino-2-deoxyisochorismate in parentheses.

Anthranilate synthases have been characterized from a number of microbial species (Romero *et al.*, 1995b) and all of them are composed of two nonidentical subunits. Component I (AAS-I or α-subunit), the synthase domain, binds the substrate chorismate and catalyses its aromatisation, whereas component II (AAS-II or β-subunit), the GAT domain, binds glutamine and transfers its amino group to chorismate. AAS-I requires Mg^{2+} ions for activity and is capable of anthranilate synthesis when exogenous NH_3 is present making the glutamine amidotransferase activity of AAS-II dispensable. Nevertheless, this NH_3-dependent AAS activity is unlikely to be functional *in vivo* as deduced from the high K_m value of 22 mM determined for the baker's yeast enzyme (Prantl *et al.*, 1985). Furthermore, AAS-I contains the binding site for the heterotropic ligand tryptophan which serves as negative effector of catalytic activity. Kinetic studies implicate an ordered mechanism of anthranilate synthesis with the acceptor substrate chorismate bound before

glutamine (Zalkin, 1973). With respect to their modular structure, several arrangements are found for AAS complexes. Mostly, both activities are separated on distinct polypeptide chains within a heteromeric enzyme, but also fusion of both modules has been reported as for the eukaryote *Euglena gracilis* (Lara and Mills, 1973). Furthermore, the AAS-II subunit is often found to be associated with additional catalytic activities. For instance, in most bacteria the GAT domain is fused to anthranilate phosphoribosyltransferase (Romero *et al.*, 1995b and references therein), in yeast to IGP synthase (Prantl *et al*., 1985). In other fungi like *N. crassa, A. nidulans* or *S. pombe* a trifunctional polypeptide containing additional IGP synthase and PRA isomerase activity is found (Walker and DeMoss, 1986; Roberts, 1967; Thuriaux *et al.*, 1982). Monofunctional AAS complexes have been described for species of the genera Pseudomonas, Erwinia, and Bacillus.

GAT domains of AAS complexes match into the class I subfamily (formerly G-type or trpG) (Massière and Badet-Denisot, 1998). For this class three conserved regions that contain an invariant glycine residue each have been deduced from primary sequence alignments (Zalkin, 1993). The glutamine binding site has been identified by using reactive analogues like azaserine or 6-diazo-5-oxo-*L*-norleucine (DON) as affinity label that block the active site (Zalkin, 1973). Target of these reagents is a cysteine residue that has been shown to be essential for catalytic activity and that is conserved in the AAS-II subunits of all anthranilate synthase complexes characterized to date (Zalkin *et al*., 1984). In addition, a catalytic triad was suggested and an invariant lysyl residue associated with the active site was found to be important for catalytic activity (Bower and Zalkin, 1982; Mei and Zalkin, 1989). In conclusion, the formation of a covalent γ-glutaminyl-S-cysteinyl enzyme intermediate is proposed as a current mechanistic model for glutaminase reaction (Walsh, 1990) with the lysine residue acting as general acid-base to promote ionisation of the cysteinyl residue.

Once native ammonia is formed by the glutaminase activity it remains trapped in the polypeptide structure as protonation in neutral medium would abolish its nucleophilic character. Transfer to the acceptor substrate may then occur in a concerted way or alternatively through channelling. Amination of the acceptor substrate chorismate occurs in the synthase domain of AAS-I. Formally this is a *syn*-1,5 displacement of hydroxide by ammonia to form the intermediate ADIC, the existence of which was proven by a block mutant form of AAS from *Salmonella typhimurium* (Morollo and Bauerle, 1993). Subsequent *cis* elimination/aromatisation yields the product anthranilic acid. In conclusion,

anthranilate synthase activity is made up by a composite ADIC synthase as well as ADIC lyase activity which both require Mg^{2+} for catalytic turnover.

Almost all known microbial anthranilate synthases are subject to feedback inhibition by the end product of the pathway, tryptophan. The only exception reported to date is that of an AAS isoenzyme in *Ps. aeruginosa* which contributes to the biosynthesis of the secondary metabolite pyocyanin, a blue-green phenazine pigment, and is not inhibited by tryptophan (Essar *et al*., 1990; Shinomiya *et al*., 1983). By the isolation of mutant enzymes insensitive to the structural analogue 5-methyl-tryptophan crucial residues for allosteric inhibition have been identified. Detailed analysis from *S. typhimurium* and *S. cerevisiae* suggest that a conserved $LLESX_{10}S$ element in the variable N-terminal part of AAS-I domains accounts for a tryptophan binding site (Caligiuri and Bauerle, 1991; Graf *et al*., 1993).

Although crystallization of AAS from *S. typhimurium* has been reported (Tolbert *et al*., 1999), the only solved X-ray structure of an AAS complex was determined from the hyperthermophile *Sulfolobus solfataricus* (Knöchel *et al*., 1999). The holoenzyme of *S. solfataricus* consists of two AAS-I:AAS-II protomers that associate mainly via the glutaminotransferase subunits. The structure of the small AAS-II subunit (195 residues) is that of a compact, spherical-shaped polypeptide with an open, seven-stranded, mixed β-sheet constituting the structural core. The active site containing the catalytic triade appears to be closed and does not allow glutamine to enter. The AAS-I subunit (421 residues) displays a complicated α/β folding pattern of novel topology with two domains and a cleft. Domain I is set up by an 11-stranded, antiparallel β-sheet and four helices, whereas domain II is formed by a nine-stranded antiparallel β-sheet and six helices. Four β-sheet strands of both domains form an orthogonal β-sandwich with an hydrophobic interface. By comparison with reported residues important for catalysis, the active domain of AAS-I was localised in-between the cleft. All feedback-sensitive residues cluster on one side of the orthogonal β-sandwich constituting a putative tryptophan binding site.

In summary, functional implications concerning catalysis and allosteric regulation can be drawn from this solved structure of a microbial anthranilate synthase complex. After conversion of chorismate, ADIC might remain bound to the original chorismate binding site before the ADIC lyase reaction takes place. Alternatively, both, chorismate and ADIC, can bind simultaneously to the active site. As chorismate has to be bound before glutamine, conformational changes accompanying chorismate binding are likely. As a result, the AAS-II subunit switches to a functional conformation and a channel for transfer of nascent

ammonia is formed. Tryptophan as heterotropic, negative-acting ligand might stabilise a protein conformation to which chorismate has reduced affinity and therefore prevents the suggested structural rearrangements caused by chorismate binding.

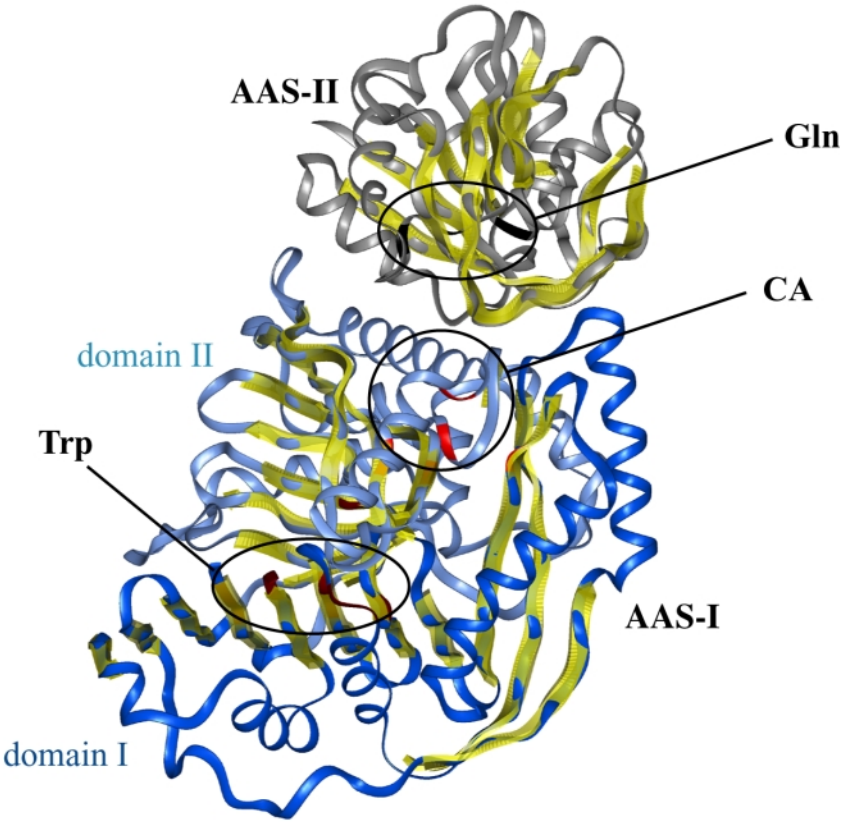

Figure 5: Three-dimensional structure of anthranilate synthase from *S. solfataricus*. One TrpG:TrpE protomer is shown in ribbon style with the AAS-I subunit (TrpE) in blue and AAS-II (TrpG) in grey. β-sheet elements of subunit AAS-I are highlighted in yellow, domains I and II of AAS-I are indicated by different shades of blue. Binding regions for glutamine (Gln), chorismate (CA), and the effector tryptophan (Trp) are indicated by black ovals. Residues important for binding of chorismate and glutamine are highlighted in red and black, respectively (modified from Knöchel *et al.*, 1999).

In summary, both branch point enzymes, chorismate mutase and the anthranilate synthase complex, compete for their common substrate chorismic acid. The regulatory mechanisms controlling the distribution of substrates and fluxes through metabolic pathways will be briefly outlined next.

3. General Mechanisms Controlling the Flux through a Metabolic Branch Point

Supply of precursor metabolites and energy for anabolic pathways to synthesise cellular components is necessary for growth and maintenance of a living cell. Metabolic pathways, accomplished by a regulated, highly coupled network of about 1000 enzyme catalysed reactions and selective membrane transport systems, are numerous and extremely plastic. Often metabolic pathways are interdependent and the fluxes of compounds and intermediates have to be controlled and regulated. With the rise of recombinant DNA technology, metabolic engineering has gained increasing attention, especially for industrial purposes (Bailey, 1991; Ostergaard *et al*., 2000; Schuster *et al*., 2000). A variety of approaches and models have evolved from basic research on metabolic networks and special interest has always been set on the regulatory systems triggering the carbon flux through a pathway. Different modes of regulation are possible to channel intermediates from the input reactions to the formation of end products. With respect to enzymatic activities, two main mechanisms have to be taken into account: regulating catalytic turnover and regulating the amount of enzymes via protein expression. Additionally, distributions of branch point intermediates have to be controlled in branched systems as flux alterations often interfere with balanced growth conditions.

3.1 Metabolic Nodes and the Concept of Preferential Synthesis

Branched reaction cascades are of special interest, as most metabolic networks are constituted by such pathways. The regulatory mechanisms acting on intermediate branch points, also referred to as nodes, are often complex and complicated. Based on the branch split ratio, a general classification for metabolic branch points has been defined (Stephanopoulos and Vallino, 1991). In a flexible node, the reaction velocities and affinities of each branch are of similar magnitude and the flux through each branch is controlled by feedback inhibition (Fig. 6A). As a result, flexible nodes are most amenable to alterations in flux distributions. Weakly rigid nodes are characterised by the dominance of the kinetics of one of its branches. This is achieved by high catalytic activity or high affinity towards the branch point compound and lack of feedback inhibition in the dominant branch (Fig. 6B). Strong rigidity of a node is defined by the tightly controlled split ratio of one or more of its branches, based on combinations of feedback control and enzyme trans-activation by metabolites of the opposite branch (Fig. 6C). Positive control of the opposite branch often is achieved when an allosteric enzyme initiates this branch. As a result, flux partitioning at the node is effectively stabilised.

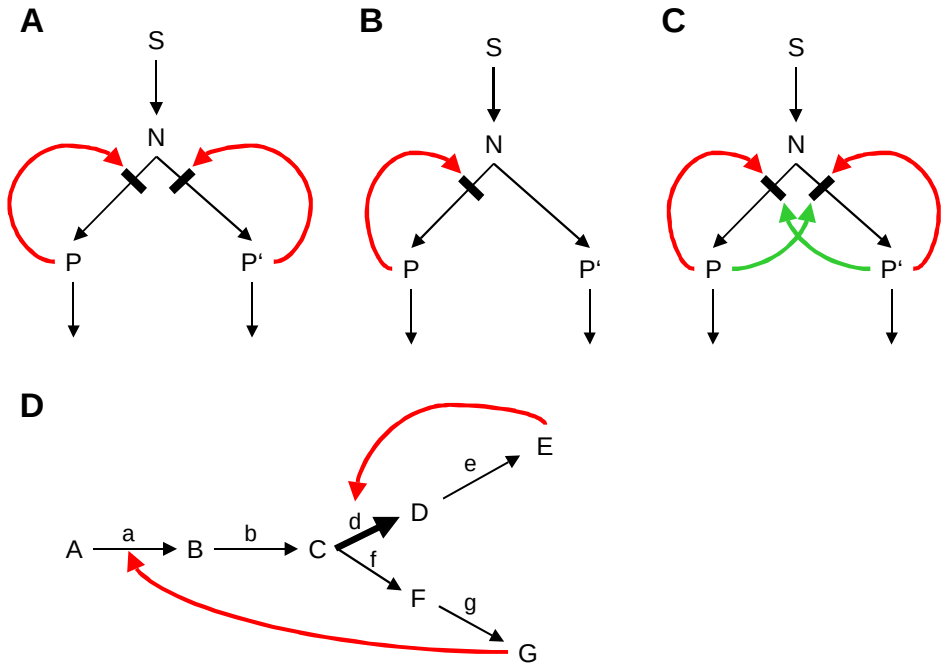

Figure 6: Branch point classifications and the concept of preferential synthesis. Schematic representation of a flexible (*A*), weakly rigid (*B*), and strongly rigid (*C*) node in a metabolic network. The substrate S is converted to the branch point intermediate N, from which end products P and P' are formed. Coloured arrows indicate negative (red) and positive (green) feedback from the corresponding metabolite (adapted from Stephanopoulos and Vallino, 1991). *D*, schematic outline of regulation by preferential synthesis in a branched pathway. Pathway 'd' (bold arrow) is favoured over pathway 'f' and the entire pathway is efficiently regulated by feedback inhibition of product 'E' acting on 'd' and inhibition of the input reaction 'a' by the end product of the less favoured pathway 'G' (red arrows) (modified from Shiio, 1982).

When the overall pathway is concerned, the regulatory pattern controlling the flux becomes more complex. The simplest mechanism for regulation of a branched pathway is modelled by the concept of preferential synthesis (Shiio, 1982) (Fig. 6D). Here, one branch is greatly favoured over the other due to very unbalanced enzyme activities at the branch point. The entire pathway is triggered efficiently if the end product of the favoured branch inhibits its own synthesis after the branch, combined with feedback inhibition of the first enzyme of the unbranched part of the pathway by the opposite end product(s). Regulating the enzymatic activities after the branch point can either be achieved by activation of the weaker enzyme or inhibition of the stronger one. As a general result, balanced synthesis of all end products of the branched pathway is ensured.

3.2 Allosteric Regulation of Catalytic Turnover

Control of protein function is a *sine qua non* requirement in a living system. Mechanisms for control are manifold including noncovalent interactions with regulatory factors, covalent modification, proteolytic cleavage, or conformational alterations. A widespread mechanism of direct control was first uncovered in 1954 by Abelson on the inhibition of isoleucine biosynthesis in *E. coli* by the end product (Abelson, 1954; Umbarger and Brown, 1958). This feedback inhibition turned out to act on the first enzymatic step of the pathway with the effector isoleucine binding at an effector site spatially separated from the catalytic site (Changeux, 1961).

Direct control of protein function via **allo**steric regulation is usually achieved through conformational changes of a given protein structure induced by effectors or ligands that bind to regulatory sites distinct (Greek: *allos* = other, *stereos* = rigid, solid or space) from the active site. In contrast to this, **intra**steric regulation occurs directly at the active site of a protein (Kobe and Kemp, 1999). Homotropic effects are defined concerning interactions between identical effectors, opposed to heterotropic effects between different ligands (Monod *et al.*, 1963). Several models have been established to date in order to describe allosteric effects. Generally, it is assumed that in an oligomeric protein each subunit exists in different allosteric states with different affinities towards a particular ligand and therefore different catalytic activities. Binding of an allosteric ligand to one subunit influences the properties of the remaining ones, therefore these effects were termed co-operative. In kinetical terms, cooperativity results in a sigmoid plot of velocities versus substrate concentrations. Quantitative aspects of cooperativity are addressed by the Hill equation, which defines the Hill coefficient n_H as degree of cooperativity. Furthermore, two quaternary conformations, termed ‘tense’ (T) and ‘relaxed’ (R) have been defined. The R state has higher affinity towards the substrate (K-systems) or increased catalytic turnover (V-systems) in comparison to the T state. The ratio between these two conformational states determines the allosteric equilibrium constant L. In the model of global allosteric transition, binding of an allosteric effector induces a concerted shift in the equilibrium between the two quaternary conformations of the oligomeric protein (Monod-Wyman-Changeux model, Monod *et al.*, 1965). One assumption of the MWC model, the maintenance of symmetry in the overall structure, was later challenged by the sequential model established by Koshland, Némethy, and Filmer (Koshland *et al.*, 1966). Here, binding of a ligand induces a conformational change in the subunit to which it is bound. This allosteric signal can be transduced to neighbouring subunits, sequentially altering the

allosteric state of the whole structure. Both the MWC and KNF extremes are combined in the general model for allostery by Eigen (1967).

3.3 Cross Pathway Control of Amino Acid Biosynthesis in Fungi

Direct control of enzymatic activities is a general feature in channelling the fluxes through biochemical pathways. An additional level of regulation is achieved by triggering the expression of specific genes required for metabolism. One of the best-understood examples for transcriptional regulation in prokaryotes is the *trp* operon of *E. coli* which acts by means of transcriptional repression and attenuation (Yanofsky, 1981).

In eukaryotes, additional mechanisms have evolved, linking different pathways by regulatory networks. As a result, changes in environmental conditions can be counteracted in flexible and instant responses. In fungi like *N. crassa*, *A. nidulans*, or *S. cerevisiae* biosynthesis of amino acids is subjected to a complex regulatory network, entitled 'cross pathway control' in filamentous fungi or 'general control' in yeast (Bode *et al*., 1990; Hinnebusch, 1988; Piotrowska, 1980). Unlike as in prokaryotes, fungi generally maintain high levels of amino acid biosynthetic proteins by relatively high levels of expression. As a consequence of this high basal level of transcription, intracellular amino acid pools are relatively large. Upon exposure to conditions of an amino acid imbalance or in the case of starvation for a single amino acid, the derepression of numerous genes involved in amino acid biosynthesis, purine biosynthesis, as well as synthesis of translational precursors is co-regulated by the cross pathway control. Due to the high basal level of expression of amino acid biosynthetic genes, starvation under laboratory conditions is usually generated by artificial means. False feedback inhibitors like the histidine analogue 3-amino-1,2,4-triazole (3AT) and 5-*DL*-methyltryptophan (5MT) have been shown to deplete histidine and tryptophan pools, respectively, in fungi, and therefore are common reagents to induce the derepression by the cross pathway control system (Hilton *et al*., 1965; Schürch *et al*., 1974). This system is best-understood for the baker's yeast *S. cerevisiae* and much insight has been gained concerning the molecular mechanisms constituting the genera control network (reviewed by Hinnebusch, 1992). There, the external signal 'amino acid starvation' is reflected by the intracellular accumulation of uncharged tRNA molecules. Binding of these to the sensor kinase Gcn2p is transmitted via a signal transduction cascade to the translational machinery. As a consequence, translation of a specific mRNA is drastically increased, resulting in elevated levels for the transcription factor Gcn4p which represents the final effector of the general control. Translational derepression of Gcn4p expression is

mediated by four short upstream open reading frames (uORFs) preceding the *GCN4* coding sequence. These uORFs act as translational barriers under non-starvation conditions but are omitted upon amino acid starvation. Gcn4p in turn binds to UAS elements within the promoter region of general control target genes to trigger transcriptional activation of those. The palindrome sequence 5'-ATGA(C/G)TCAT-3' has been mapped as optimal promoter-binding site for the regulator protein and therefore was termed general control responsive element (GCRE). Homologues for Gcn4p have been identified in other fungi like *Cryphonectria parasitica, N. crassa,* and *A. niger*, and all share homology to the *jun* oncoprotein (Bohmann *et al*., 1987; Paluh *et al*., 1988; Wang *et al*., 1998; Wanke *et al*., 1997).

In summary, a variety of mechanisms exist in a living cell to regulate the fluxes through metabolic pathways. In combination with the general modes of regulation described before, pathway-specific regulatory systems are always present, resulting in finely tuned outputs upon environmental stimuli.

4. Biosynthesis of Aromatic Amino Acids as a Model System for a Branched, Strictly Regulated Metabolic Pathway

Biosynthesis of aromatic amino acids has been studied in a variety of organisms and plants. Very comprehensive studies have been done on the pathway of the baker's yeast *S. cerevisiae* (for review see Braus, 1991, and references therein). 14 genes have been identified in this yeast that code for enzymes accelerating the 17 reactions of the entire pathway.

The first reaction of the shikimate pathway is catalysed by the *ARO3* and *ARO4* gene products. Each gene encodes a DAHP synthase isoenzyme, both differing in their regulatory properties (Schnappauf *et al*., 1998a). The next five reactions from DAHP to EPSP are carried out by a pentafunctional enzyme encoded by the *ARO1* locus. The last common intermediate of the pathway, chorismic acid, is formed by the Aro2 protein, a bifunctional chorismate synthase/diaphorase activity. From chorismate the pathway is split into two main branches. By the *ARO7*-encoded chorismate mutase the phenylalanine/tyrosine-specific branch is initiated, followed by the PPY/HPP route. The *PHA2* gene was identified to encode the prephenate dehydratase activity, the *TYR1* gene encodes the respective dehydrogenase enzyme. The *ARO8* and *ARO9* gene products were identified to be redundant for the terminal aminotransferase activities catalysing the final steps of phenylalanine and tyrosine biosynthesis (Urrestarazu *et al.*, 1998).

The tryptophan branch is initiated by the formation of anthranilate. The corresponding anthranilate synthase activity is constituted by the Trp2p/Trp3p heterodimer, in which the glutamineamidotransferase activity is located in the *TRP3*-encoded subunit and the synthase activity in the *TRP2* gene product. The bifunctional Trp3p additionally carries the IGP synthase activity catalysing the fourth step in the tryptophan-specific branch. Anthranilic acid is transformed by the action of the Trp4p phosphoribosyl transferase activity, followed by the PRA isomerase reaction accelerated by the *TRP1* gene product. The last step in the reaction cascade, the formation of tryptophan, is finally catalyzed by the tryptophan synthase enzyme which is encoded by the *TRP5* gene.

In contrast to numerous prokaryotes like *E. coli,* all enzymatic activities are expressed from independent genes scattered over seven chromosomes. Due to this genetic organisation transcription of each gene is regulated individually by specific factors binding to their promoter elements. Most of the genes constituting the yeast pathway are subjected to the general control of amino acid biosynthesis.

4.1 Regulation of Enzyme Levels

The amount of a given protein in a cellular compartment is determined by protein synthesis and degradation as well as transport phenomenons. Gene expression is the major determinant for protein synthesis and includes various parameters. The general control system which acts on the initiation of transcription contributes mainly to the regulation of enzyme synthesis in the aromatic amino acid pathway (see section 3.3). Almost all encoding genes of the pathway (*ARO*3, *ARO4*, *ARO1*, *ARO2*, and four of the five *TRP* genes) are derepressed under amino acid conditions (Duncan *et al.*, 1987; Jones *et al.*, 1991; Miozzari *et al.*, 1978; Teshiba *et al.*, 1986). The only exceptions are *ARO7*, *TYR1*, and *TRP1* which have been shown not to be derepressible by this system (Braus *et al.*, 1988; Mannhaupt *et al.*, 1989; Schmidheini *et al.*, 1990b). Especially for the chorismate mutase-encoding gene *ARO7* this is of special interest as a general control responsive element with two mismatches to the consensus has been identified in reverse orientation (position –496 relative to the translational start codon) in the *ARO7* promoter region that is able to bind Gcn4p *in vitro* but that is not functional *in vivo*. In contrast, the genes encoding the anthranilate synthase complex in *S. cerevisiae*, *TRP2* and *TRP3*, are both targets of the general control system. Both promoters contain a GCRE with a single mismatch (position –162 for *TRP2* and –124 for *TRP3*, respectively) and amino acid starvation derepresses transcription of both up to 3-fold (Hinnebusch, 1992).

4.2 Triggering Catalytic Turnover

The aromatic amino acid biosynthesis in *S. cerevisiae* is a model system for a branched metabolic pathway. In addition to the regulation of enzyme levels by the general control, specific regulatory points of attack acting on catalytic turnover rates have been identified. The main control points are at the pathway input reaction catalysed by the DAHP isoenzymes and at the first branch point emerging from chorismate.

The DAHP synthase activity is feedback inhibited by two end products of the pathway. As two isoenzymes contribute to this catalytic activity, different modes of inhibition have evolved. The *ARO3*-encoded DAHP synthase is strongly inhibited by phenylalanine with a K_i of 75 µM (Paravicini *et al.*, 1989). Phenylalanine acts as competitive inhibitor with respect to E4P but is non-competitive with respect to PEP. This situation is opposite to the inhibition mode for the *ARO4*-encoded enzyme. Here, tyrosine acts as feedback inhibitor competitive to PEP with a K_i of 0.9 µM and is non-competitive with respect to E4P (Schnappauf *et al.*, 1998a). For both enzymes similar rate constants have been determined, 10 s^{-1} for Aro3p and 6 s^{-1} for Aro4p, respectively. The difference in sensitivity for each inhibitor indicates a major flux towards phenylalanine in the aromatic amino acid pathway.

The branch point enzyme initiating the biosynthesis of phenylalanine and tyrosine serves as a model enzyme for allostery. The homodimeric chorismate mutase, encoded by the *ARO7* gene, is regulated in its activity by homotropic as well as heterotropic effectors (Schmidheini *et al.*, 1990a). Chorismate serves as positive allosteric ligand resulting in a sigmoid saturation curve of catalytic velocities ($[S]_{0.5}$ of 4.0 mM) with a k_{cat} of 176 s^{-1}. A deduced Hill coefficient of 1.71 reflects this positive cooperativity. Tryptophan, the end product of the opposite branch, strongly activates chorismate mutase activity with a K_a of 1.5 µM resulting in Michaelis-Menten substrate saturation kinetic. In the presence of this positive effector, cooperativity is lost and the k_{cat} value is increased to 264 s^{-1}. Tyrosine on the other hand is a negative effector of enzymatic activity. The k_{cat} value is reduced to 129 s^{-1} when tyrosine is bound with a K_i value of 50 µM at the allosteric site, which is identical for both heterotropic effectors (Schnappauf *et al.*, 1998b), but cooperativity is retained. The regulatory properties of yeast chorismate mutase fits well in the allosteric model proposed by Monod (see section 3.2). Increasing concentrations of the substrate shift the T/R equilibrium to the R state resulting in higher affinity towards chorismate. Binding of tryptophan stabilises the R state, in contrast to tyrosine which stabilises the T state. The T/R

equilibrium is modulated by different concentrations of activator and inhibitor leading to a finely tuned level of catalytic activity.

Tryptophan not only acts as positive effector of chorismate mutase but additionally is a feedback inhibitor for the anthranilate synthase activity. For the unliganded AAS complex, the K_m values have been determined as 0.0017 mM for chorismate, 0.74 mM for glutamine, and 0.57 mM for Mg^{2+} (Prantl *et al.*, 1985). Tryptophan acts as competitive inhibitor (K_i of 56 µM) with respect to chorismate. This feedback inhibition of AAS activity by the end product can be mimicked by structural analogues like 5-methyltryptophan.

The overall pattern of regulation of this branched pathway fits into the concept of preferential synthesis (section 3.1). As deduced from different K_m values for chorismate mutase and anthranilate synthase towards chorismate, the tryptophan-specific branch is favoured. The resulting end product inhibits its own biosynthetic branch, whereas the end products of the opposite branch inhibit the input reaction of the entire pathway. Due to the trans-activation of the chorismate mutase enzyme by tryptophan, the metabolic node emerging from chorismate has to be classified as strongly rigid. Complexity of the situation is further increased by the action of the general control of amino acid biosynthesis. This regulatory systems acts on expression of almost every enzyme of the pathway but not on *ARO7* expression. Therefore, chorismate mutase activity is solely but effectively triggered by allosteric means.

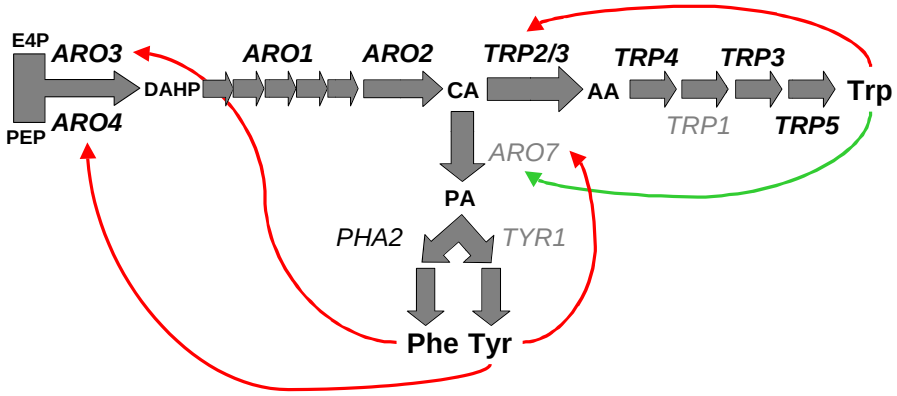

Figure 7: Modes of regulation of aromatic amino acid biosynthesis in *S. cerevisiae*. The pathway and corresponding genes are schematically shown. Genes under general control of amino acid biosynthesis are shown in bold type, genes not derepressed under amino acid starvation conditions in grey. Positive feedbacks of the encoded enzymes are indicated by green arrows, feedback inhibition by red arrows.

Aim of this Work

In this work, the mechanisms that control the flux of chorismate through the first metabolic node of aromatic amino acid biosynthesis as it exists in fungi were investigated. As known for the baker's yeast *S. cerevisiae*, two main regulatory levels contribute to the regulation of catalytic actvities of the branch point enzymes, namely allostery and transcriptional regulation of protein levels. By introduction of an allosterically unregulated, constitutively active chorismate mutase in *S. cerevisiae* cells, the interplay of the regulatory mechanisms should be investigated. As only a few eukaryotic chorismate mutase enzymes are charcterized to date, additional CM-encoding genes of fungal sources have to be cloned and analysed in order to gain further insight into the regulatory properties of fungal chorismate mutases. For that purpose, the chorismate mutase of a related species, the one of the methylotrophic yeast *Hansenula polymorpha,* was chosen. Furthermore, we were interested in the properties of a chorismate mutase enzyme derived from a filamentous fungus. Therefore, the *aroC* gene of *A. nidulans* had to be cloned and its gene product had to be analysed with respect to catalytic properties, quaternary structure, and regulatory behavior.

References

Abelson, P.H. (1954) Amino acid biosynthesis in *Escherichia coli*: isotopic competition with ^{14}C glucose. *J. Biol. Chem.* **206:** 335-343.

Andrews, P.R., G.D. Smith, and I.G. Young (1973) Transition-state stabilization and enzymic catalysis. Kinetic and molecular orbital studies of the rearrangement of chorismate to prephenate. *Biochemistry* **12:** 3492-3498.

Bailey, J.E. (1991) Toward a science of metabolic engineering. *Science* **252:** 1668-1675.

Bentley, R. (1990) The shikimate pathway - a metabolic tree with many branches. *Crit. Rev. Biochem. Mol. Biol.* **25:** 307-384.

Bentley, R., and R. Meganathan (1982) Biosynthesis of vitamin K (menaquinone) in bacteria. *Microbiol. Rev.* **46:** 241-280.

Bode, R., K. Schüssler, H. Schmidt, T. Hammer, and D. Birnbaum (1990) Occurrence of the general control of amino acid biosynthesis in yeasts. *J. Basic Microbiol.* **30:** 31-35.

Bohmann, D., T.J. Bos, A. Admon, T. Nishimura, P.K. Vogt, and R. Tijan (1987) Human proto-oncogene *c-Jun* encodes a DNA binding protein with structural and functional properties of transcription factor AP-1. *Science* **238:** 1386-1392.

Bowdish, K., Y. Tang, J.B. Hicks, and D. Hilvert (1991) Yeast expression of a catalytic antibody with chorismate mutase activity. *J. Biol. Chem.* **266:** 11901-11908.

Bower, S., and H. Zalkin (1982) Modification of *Serratia marcescens* anthranilate synthase with pyridoxal 5'-phosphate. *Arch. Biochem. Biophys.* **219:** 121-127.

Braus, G.H. (1991) Aromatic amino acid biosynthesis in the yeast *Saccharomyces cerevisiae*: a model system for the regulation of a eukaryotic biosynthetic pathway. *Microbiol. Rev.* **55:** 349-370.

Braus, G.H., K. Luger, G. Paravicini, T. Schmidheini, K. Kirschner, and R. Hütter, (1988) The role of the *TRP1* gene in yeast tryptophan biosynthesis. *J. Biol. Chem.* **263:** 7868-7875.

Caligiuri, M.G., and R. Bauerle (1991) Identification of amino acid residues involved in feedback regulation of the anthranilate synthase complex from *Salmonella typhimurium.* Evidence for an amino-terminal regulatory site. *J. Biol. Chem.* **266:** 8328-8335.

Catcheside, D.E., P.J. Storer, and B. Klein (1985) Cloning of the *ARO* cluster gene of *Neurospora crassa* and its expression in *Escherichia coli*. *Mol. Gen. Genet.* **199:** 446-451.

Changeux, J.P. (1961) The feedback mechanism of biosynthetic *L*-threonine deaminase by *L*-isoleucine. *Cold Spring Harb. Symp. quant. Biol.* **26:** 313-318.

Charles, I.G., J.W. Keyte, W.J. Brammar, M. Smith, and A.R. Hawkins (1986) The isolation and nucleotide sequence of the complex AROM locus of *Aspergillus nidulans*. *Nucleic Acids Res.* **14:** 2201-2213.

Chook, Y.M., H. Ke, and W.N. Lipscomb (1993) Crystal structures of the monofunctional chorismate mutase from *Bacillus subtilis* and its complex with a transition state analog. *Proc. Natl. Acad. Sci. USA* **90:** 8600-8603.

Coggins, J.R., M.R. Boocock, M.S. Campbell, S. Chaudhuri, J.M. Lambert, A. Lewendon, D.M. Mousdale, and D.D. Smith (1985) Functional domains involved in aromatic amino acid biosynthesis. *Biochem. Soc. Trans.* **13:** 299-303.

Crawford, I.P. (1987) Synthesis of tryptophan from chorismate: comparative aspects. *Methods Enzymol.* **142:** 293-300.

Duncan, K., R.M. Edwards, and J.R. Coggins (1987) The pentafunctional arom enzyme of *Saccharomyces cerevisiae* is a mosaic of monofunctional domains. *Biochem. J.* **246:** 375-386.

Eberhard, J., H.-R. Raesecke, J. Schmid, and N. Amrhein (1993) Cloning and expression in yeast of a higher plant chorismate mutase. *FEBS Lett.* **334:** 233-236.

Eigen, M. (1967) Kinetics of reaction control and information transfer in enzymes and nucleic acids. In *Fast Reactions and Primary Processes in Chemical Kinetics*. Claesson, S. (ed.), *Nobel Symposium* **5:** 333-369.

Essar, D.W., L. Eberly, A. Hadero, and I.P. Crawford (1990) Identification and characterization of genes for a second anthranilate synthase in *Pseudomonas aeruginosa*: interchangeability of the two anthranilate synthases and evolutionary implications. *J. Bacteriol.* **172:** 884-900.

Gibson, F. (1964) Chorismic acid: purification and some chemical and physical studies. *Biochem. J.* **90:** 256-261.

Gibson, F. (1999) The elusive branch-point compound of aromatic amino acid biosynthesis. *Trends Biochem. Sci.* **24:** 36-38.

Gibson, M.I., and F. Gibson (1964) Preliminary studies on the isolation and metabolism of an intermediate in aromatic biosynthesis: chorismic acid. *Biochem. J.* **90**: 248-256.

Graf, R., B. Mehmann, and G.H. Braus (1993) Analysis of feedback-resistant anthranilate synthases from *Saccharomyces cerevisiae*. *J. Bacteriol.* **175:** 1061-1068.

Gu, W., D.S. Williams, H.C. Aldrich, G. Xie, D.W. Gabriel, and R.A. Jensen (1997) The *aroQ* and *pheA* domains of the bifunctional P-protein from *Xanthomonas campestris* in a context of genomic comparison. *Microb. Comp. Genomics* **2:** 141-158.

Hasan, N., and E.W. Nester (1978) Purification and properties of chorismate synthase from *Bacillus subtilis*. *J. Biol. Chem.* **253:** 4993-4998.

Henstrand, J.M., N. Amrhein, and J. Schmid (1995) Cloning and characterization of a heterologously expressed bifunctional chorismate synthase/flavin reductase from *Neurospora crassa*. *J. Biol. Chem.* **270:** 20447-20452.

Henstrand, J.M., A. Schaller, M. Braun, N. Amrhein, and J. Schmid (1996) *Saccharomyces cerevisiae* chorismate synthase has a flavin reductase activity. *Mol. Microbiol.* **22:** 859-866.

Hilton, J.L., P.C. Kearney, and B.N. Ames (1965) Mode of action of the herbicide 3-amino-1,2,4-triazole(amitrole): inhibition of an enzyme of histidine biosynthesis. *Arch. Biochem. Biophys.* **112:** 544-547.

Hinnebusch, A.G. (1988) Mechanisms of gene regulation in the general control of amino acid biosynthesis in *Saccharomyces cerevisiae*. *Microbiol. Rev.* **52:** 248-273.

Hinnebusch, A. (1992) General and pathway-specific regulatory mechanisms controlling the synthesis of amino acid biosynthetic genes in *Saccharomyces cerevisiae*. In *The Molecular and Cellular Biology of the Yeast Saccharomyces*. Vol. 2: Gene expression. E.W. Jones, J.R. Pringle, J.R. and Broach (eds.), pp. 319-414, Cold Spring Harbor Laboratory Press, Cold Spring Harbor, New York.

Hütter, R., P. Niederberger, and J.A. DeMoss (1986) Tryptophan biosynthetic genes in eukaryotic microorganisms. *Annu. Rev. Microbiol.* **40:** 55-77.

Hyde, C.C., S.A. Ahmed, E.A. Padlan, E.W. Miles, and D.R. Davies (1988) Three-dimensional structure of the tryptophan synthase $\alpha_2\beta_2$ multienzyme complex from *Salmonella typhimurium*. *J. Biol. Chem* **263**: 17857-17871.

Jensen, R., and R. Fischer (1987) The postprephenate biochemical pathways to phenylalanine and tyrosine: an overview. *Methods Enzymol.* **142:** 472-478.

Jones, D.G., U. Reusser, and G.H. Braus (1991) Molecular cloning, characterization and analysis of the regulation of the *ARO2* gene, encoding chorismate synthase, of *Saccharomyces cerevisiae*. *Mol. Microbiol.* **5:** 2143-2152.

Knöchel, T., A. Ivens, G. Hester, A. Gonzalez, R. Bauerle, M. Wilmanns, K. Kirschner, and J.N. Jansonius, (1999) The crystal structure of anthranilate synthase from *Sulfolobus solfataricus*: functional implications. *Proc. Natl. Acad. Sci. USA* **96:** 9479-9484.

Kobe, B., and B.E. Kemp (1999) Active site-directed protein regulation. *Nature* **402:** 373-376.

Koshland, D.E., Jr., G. Nemethy, and D. Filmer (1966) Comparison of experimental binding data and theoretical models in proteins containing subunits. *Biochemistry* **5:** 365-385.

Kuhn, R., E. Vogt, J. Schmid, N. Amrhein, and A. Schaller (1999) Expression analysis of *Arabidopsis thaliana* genes for plastidic (CM1) and cytosolic (CM2) chorismate mutases. Direct submission to GenBank, Acc. No. AJ242647 and AJ242648.

Lara, J.C., and S.E. Mills (1972) Tryptophan synthetase in *Euglena gracilis* strain G. *J. Bacteriol.* **110:** 1100-1106.

Liu, J., N. Quinn, G.A. Berchtold, and C.T. Walsh (1990) Overexpression, purification, and characterization of isochorismate synthase (EntC), the first enzyme involved in the biosynthesis of enterobactin from chorismate. *Biochemistry* **29:** 1417-1425.

MacBeath, G., P. Kast, and D. Hilvert (1998) A small, thermostable, and monofunctional chorismate mutase from the archaeon *Methanococcus jannaschii*. *Biochemistry* **37:** 10062-10073.

Mannhaupt, G., R. Stucka, U. Pilz, C. Schwarzlose, and H. Feldmann (1989) Characterization of the prephenate dehydrogenase-encoding gene, *TYR1*, from *Saccharomyces cerevisiae*. *Gene* **85:** 303-311.

Massière, F., and M.-A. Badet-Denisot (1998) The mechanism of glutamine-dependent amidotransferases. *Cell. Mol. Life Sci.* **54:** 205-222.

Mei, B., and H. Zalkin (1989) A cysteine-histidine-aspartate catalytic triad is involved in glutamine amide transfer function in *purF*-type glutamine amidotransferases. *J. Biol. Chem* **264:** 16613-16619.

Miles, E. W., R. Bauerle, and S.A. Ahmed (1987) Tryptophan synthase from *Escherichia coli* and *Salmonella typhimurium*. *Methods Enzymol.* **142:** 398-414.

Miozzari, G., P. Niederberger, and R. Hütter (1978) Tryptophan biosynthesis in *Saccharomyces cerevisiae*: control of the flux through the pathway. *J. Bacteriol.* **134:** 48-59.

Mobley, E., B. Kunkel, and B. Keith (1999) CM-3, a novel Arabidopsis gene encoding chorismate mutase. Direct submission to GenBank, Acc. No. AF131219.

Monod, J., J.-P. Changeux, and F. Jacob (1963) Allosteric proteins and molecular control systems. *J. Mol. Biol.* **6:** 306-329.

Monod, J., J. Wyman, and J.-P. Changeux (1965) On the nature of allosteric transition: a plausible model. *J. Mol. Biol.* **12:** 88-118.

Morollo, A.A., and R. Bauerle (1993) Characterization of composite aminodeoxyisochorismate synthase and aminodeoxyisochorismate lyase activities of anthranilate synthase. *Proc. Natl. Acad. Sci. USA* **90:** 9983-9987.

Oliver, K., D. Harris, B.G. Barrell, M.A. Rajandream, and V. Wood (1995) *Schizosaccharomyces pombe* chromosome I sequencing project. Direct submission to GenBank, Acc. No. Z98529.

Ostergaard, S., L. Olsson, and J. Nielsen (2000) Metabolic engineering of *Saccharomyces cerevisiae*. *Microbiol. Mol. Biol. Rev.* **64:** 34-50.

Paluh, J.L., M.J. Orbach, T.L. Legerton, and C. Yanofsky (1988) The cross-pathway control gene of *Neurospora crassa, cpc-1*, encodes a protein similar to *GCN4* of yeast and the DNA-binding domain of the oncogene *v-jun*-encoded protein. *Proc. Natl. Acad. Sci. USA* **85:** 3728-3732.

Paravicini, G., T. Schmidheini, and G. Braus (1989) Purification and properties of the 3-deoxy-D-arabino-heptulosonate-7-phosphate synthase (phenylalanine-inhibitable) of *Saccharomyces cerevisiae*. *Eur. J. Biochem.* **186:** 361-366.

Piotrowska, M. (1980) Cross-pathway regulation of ornithine carbamoyltransferase synthesis in *Aspergillus nidulans*. *J. Gen. Microbiol.* **116:** 336-339.

Pittard, A.J. (1996) Biosynthesis of the aromatic amino acids. In *Escherichia coli and Salmonella*. F.C. Neidhardt, R. Curtiss, J.L. Ingraham, E.C.C. Lin, K.B. Low, B. Magasanik, W.S. Reznikoff, M. Riley, M. Schaechter, and H.B. Umbarger (eds.) pp. 458-484, American Society for Microbiology, Washington, D.C..

Prantl, F., A. Strasser, M. Aebi, R. Furter, P. Niederberger, K. Kirschner, and R. Hütter (1985) Purification and characterization of the indole-3-glycerolphosphate synthase/anthranilate synthase complex of *Saccharomyces cerevisiae*. *Eur. J. Biochem.* **146:** 95-100.

Roberts, C.A. (1967) Complementation analysis of the tryptophan pathway in *Aspergillus nidulans*. *Genetics* **55:** 233-239.

Roberts, F., C.W. Roberts, J.J. Johnson, D.E. Kyle, T. Krell, J.R. Coggins, G.H. Coombs, W.K. Milhous, S. Tzipori, D.J. Ferguson, D. Chakrabarti, and R. McLeod (1998) Evidence for the shikimate pathway in apicomplexan parasites. *Nature* **393:** 801-805.

Romero, R.M., M.F. Roberts, and J.D. Phillipson (1995a) Chorismate mutase in microorganisms and plants. *Phytochemistry* **40:** 1015-1025.

Romero, R.M., M.F. Roberts, and J.D. Phillipson (1995b) Anthranilate synthase in microorganisms and plants. *Phytochemistry* **39:** 263-276.

Schmidheini, T., P. Sperisen, G. Paravicini, R. Hütter, and G. Braus (1989) A single point mutation results in a constitutively activated and feedback-resistant chorismate mutase of *Saccharomyces cerevisiae*. *J. Bacteriol.* **171:** 1245-1253.

Schmidheini, T., H.-U. Mösch, J.N.Evans, and G. Braus (1990a) Yeast allosteric chorismate mutase is locked in the activated state by a single amino acid substitution. *Biochemistry* **29:** 3660-3668.

Schmidheini, T., H.-U. Mösch, R. Graf, and G.H. Braus (1990b) A GCN4 protein recognition element is not sufficient for GCN4-dependent regulation of transcription in the *ARO7* promoter of *Saccharomyces cerevisiae*. *Mol. Gen. Genet.* **224:** 57-64.

Schnappauf, G., M. Hartmann, M. Künzler, and G.H. Braus (1998a) The two 3-deoxy-D-arabino-heptulosonate-7-phosphate synthase isoenzymes from *Saccharomyces cerevisiae* show different kinetic modes of inhibition. *Arch. Microbiol.* **169:** 517-524.

Schnappauf, G., S. Krappmann, and G.H. Braus (1998b) Tyrosine and tryptophan act through the same binding site at the dimer interface of yeast chorismate mutase. *J. Biol. Chem.* **273:** 17012-17017.

Schürch, A., J. Miozzari, and R. Hütter (1974) Regulation of tryptophan biosynthesis in *Saccharomyces cerevisiae*: mode of action of 5-methyl-tryptophan and 5-methyl-tryptophan-sensitive mutants. *J. Bacteriol.* **117:** 1131-1140.

Schuster, S., D.A. Fell, and T. Dandekar (2000) A general definition of metabolic pathways useful for systematic organization and analysis of complex metabolic networks. *Nat. Biotechnol.* **18:** 326-332.

Shiio, I. (1982) In *Overproduction of Microbial Products*. K. Krumphanzl, B. Sikytaand, Z. Vanek (eds.), pp. 463-472, Academic Press,

Shinomiya, T., S. Shiga, A. Kikuchi, and M. Kageyama (1983) Genetic determinant of pyocin R2 in *Pseudomonas aeruginosa* PAO. II. Physical characterization of pyocin R2 genes using R-prime plasmids constructed from R68.45. *Mol. Gen. Genet.* **189:** 382-389.

Stephanopoulos, G., and J.J. Vallino (1991) Network rigidity and metabolic engineering in metabolite overproduction. *Science* **252:** 1675-1681.

Sträter, N., K. Håkansson, G. Schnappauf, G. Braus, and W.N. Lipscomb (1996) Crystal structure of the T state of allosteric yeast chorismate mutase and comparison with the R state. *Proc. Natl. Acad. Sci. USA* **93:** 3330-3334.

Sträter, N., G. Schnappauf, G. Braus, and W.N. Lipscomb (1997) Mechanisms of catalysis and allosteric regulation of yeast chorismate mutase from crystal structures. *Structure* **5:** 1437-1452.

Teshiba, S., R. Furter, P. Niederberger, G. Braus, G. Paravicini, and R. Hütter (1986) Cloning of the *ARO3* gene of *Saccharomyces cerevisiae* and its regulation. *Mol. Gen. Genet.* **205:** 353-357.

Tolbert, W.D., S. Chatterji, R. Bauerle, and R. Kretsinger (1999) Crystallization and preliminary crystallographic studies of the anthranilate synthase partial complex from *Salmonella typhimurium*. *Acta Crystallogr. D Biol. Crystallogr.* **55:** 305-306.

Umbarger, E., and B. Brown (1958) Isoleucine and valine metabolism in *Escherichia coli*. VII. The negative feedback mechanism controlling isoleucine synthesis. *J. Biol. Chem.* **233:** 415-420.

Urrestarazu, A., S. Vissers, I. Iraqui, and M. Grenson (1998) Phenylalanine- and tyrosine-auxotrophic mutants of *Saccharomyces cerevisiae* impaired in transamination. *Mol. Gen. Genet.* **257:** 230-237.

Walker, M.S., and J.A. DeMoss (1986) Organization of the functional domains of anthranilate synthase from *Neurospora crassa*. Limited proteolysis studies. *J. Biol. Chem.* **261:** 16073-16077.

Walsh, C. (1979) *Enzymatic Reaction Mechanisms*. p. 555, W. H. Freeman, San Francisco.

Wang, P., T.G. Larson, C.H. Chen, D.M. Pawlyk, J.A. Clark, and D.L. Nuss (1998) Cloning and characterization of a general amino acid control transcriptional activator from the chestnut blight fungus *Cryphonectria parasitica*. *Fungal Genet. Biol.* **23:** 81-94.

Wanke, C., S. Eckert, G. Albrecht, W. van Hartingsveldt, P. J. Punt, C.A. van den Hondel, and G.H. Braus (1997) The *Aspergillus niger GCN4* homologue, *cpcA,* is transcriptionally regulated and encodes an unusual leucine zipper. *Mol. Microbiol.* **23:** 23-33.

Weiss, U., and J.M. Edwards (1980) *The Biosynthesis of Aromatic Amino Acids*. John Wiley & Sons Inc., New York, USA.

White, P.J., G. Millar, and J.R. Coggins (1988) The overexpression, purification and complete amino acid sequence of chorismate synthase from *Escherichia coli* K12 and its comparison with the enzyme from *Neurospora crassa*. *Biochem. J.* **251:** 313-322.

Xia, T., J. Song, G. Zhao, H. Aldrich, and R.A. Jensen (1993) The *aroQ*-encoded monofunctional chorismate mutase (CM-F) protein is a periplasmic enzyme in *Erwinia herbicola*. *J. Bacteriol.* **175:** 4729-4737.

Xue, Y., and W.N. Lipscomb (1995) Location of the active site of allosteric chorismate mutase from *Saccharomyces cerevisiae*, and comments on the catalytic and regulatory mechanisms. *Proc. Natl. Acad. Sci. USA* **92:** 10595-10598.

Xue, Y., W.N. Lipscomb, R. Graf, G. Schnappauf, and G. Braus (1994) The crystal structure of allosteric chorismate mutase at 2.2 Å resolution. *Proc. Natl. Acad. Sci. USA* **91:** 10814-10818.

Yanofsky, C. (1981) Attenuation in the control of expression of bacterial operons. *Nature* **289:** 751-758.

Yanofsky, C. (1987) Tryptophan synthetase: its charmed history. *Bioessays* **6:** 133-137.

Zalkin, H. (1973) Anthranilate synthetase. *Adv. Enzymol. Relat. Areas Mol. Biol.* **38:** 1-39.

Zalkin, H. (1993) The amidotransferases. *Adv. Enzymol. Relat. Areas Mol. Biol.* **66:** 203-309.

Zalkin, H., J.L. Paluh, M. van Cleemput, W.S. Moye, and C. Yanofsky (1984) Nucleotide sequence of *Saccharomyces cerevisiae* genes *TRP2* and *TRP3* encoding bifunctional anthranilate synthase: indole-3-glycerol phosphate synthase. *J. Biol. Chem.* **259:** 3985-3992.

Chapter 2

Engineering a Metabolic Branch Point in *Saccharomyces cerevisiae*

Abstract

Saccharomyces cerevisiae strains were constructed by recombinant DNA technology that differed in their regulation of enzymatic activities at the first branch point of aromatic amino acid biosynthesis. When the *ARO7*-encoded, allosterically regulated chorismate mutase was expressed in a Gcn4p-dependent manner, no obvious growth defect was present, emphasising the large reserve capacity of the pathway. Expression of an unregulated, constitutively activated chorismate mutase did not sufficiently deplete the chorismate pool, even when expression of this allele is subjected to the general control of amino acid biosynthesis. Exogenous phenylalanine in combination with the unregulated chorismate mutase reduced the input into the pathway and resulted in tryptophan auxotrophy but expression of the transcriptional activator Gcn4p suppressed this starvation situation. Reducing the metabolic flux into the tryptophan-specific branch led to severe growth defects when an unregulated chorismate mutase was expressed in a Gcn4p-dependent manner. We therefore conclude that the specific regulatory pattern acting on the first metabolic node of aromatic amino acid biosynthesis is necessary to maintain proper flux distribution and that allosteric regulation of chorismate mutase activity has evolved after the encoding gene was removed from the general control system.

Introduction

The field of metabolic engineering with its aim to restructure metabolic networks has become of increasing interest in the last decade. Especially for biotechnological as well as industrial purposes, a lot of research and engagement is spent to modify specific reactions cascades of primary and secondary metabolism within a living organism (Bailey, 1991; Ostergaard *et al*., 2000). Metabolic pathways are often found to be very plastic and strictly regulated with respect to environmental conditions, and flux alterations to achieve higher yields of a desired metabolite are often counteracted by the system. To circumvent general problems in enhancing yield and productivity of a biotechnological process, detailed analysis of the given pathway and its regulatory peculiarities is strictly required. Generally, metabolic pathways are interdependent due to interlocks, couplings, feedbacks and other mechanisms. Often, metabolic cascades split into different branches to feed other pathways by common compounds. These branched pathways have gained increasing attention in metabolic engineering because flux control is complicated by the existence of different sinks for a common intermediate. The metabolic flux through a branch point determines the rates of productivity for end products and by-products and therefore is a valuable point of attack to regulate or alter metabolic fluxes. Branch points, also referred to as nodes, have been classified with respect to their regulatory patterns (Stephanopoulos and Vallino, 1991). Flexible nodes display flexible and ready changes in branch partitioning due to metabolic demands. Both enzymes of a flexible branch have similar affinities for the common substrate and reaction velocities are of similar magnitude. Both routes are controlled by feedback inhibition of the corresponding end product resulting in varying split ratios. In contrast to this situation, highly rigidity of a node is characterized by strictly controlled split ratios of one or more of its branches. This is based on the combination of feedback control and enzyme trans-activation by metabolites of competing branches. In conclusion, flux partitioning at the rigid branch is highly stabilised. Nevertheless, for flux control often the entire pathway and its regulatory systems has to be considered.

In eukaryotes, additional mechanisms contribute to regulatory networks acting on metabolic fluxes. As a model pathway for a branched metabolic reaction cascade, the biosynthesis of aromatic amino acids in the baker's yeast *Saccharomyces cerevisiae* has been studied intensively in the past (reviewed by Braus, 1991), especially with concern to metabolic flux of tryptophan synthesis (Miozzari *et al*., 1978; Niederberger *et al*., 1992; Small and Kacser, 1994). Two DAHP synthase isoenzymes (E.C. 4.1.2.15) encoded by the *ARO3* and *ARO4* genes, respectively, catalyse the first step of the pathway (Künzler *et al*.,

1992; Teshiba *et al.*, 1986). In six invariable steps the last common intermediate of the pathway, chorismic acid, is formed to constitute the shikimate pathway. The chorismate pool feeds two main branches emerging from the main trunk. Either it is converted to anthranilate to initiate the tryptophan-specific branch, or its isomerisation to prephenate is catalysed to set up the tyrosine/phenylalanine-specific part of the pathway. The former reaction is carried out by the anthranilate synthase complex (E.C. 4.1.3.27), a heterodimeric enzyme constituted by the *TRP2* and *TRP3* gene products (Zalkin *et al.*, 1984; Aebi *et al.*, 1982). The two-step process of anthranilate formation requires two distinct enzymatic activities (Morollo and Bauerle, 1993). Ammonia is formed from glutamine by the action of a glutamineamidotransferase activity resting on the Trp3p polypeptide, and the actual anthranilate synthase activity is constituted by the Trp2p subunit. Formation of prephenate from chorismate, formally a Claisen rearrangement, is accelerated by the homodimeric chorismate mutase enzyme (E.C. 5.4.99.5) which is encoded by *ARO7* (Ball *et al.*, 1986). With respect to catalytic turnover, three major targets of regulation within the pathway are evident. Both DAHP synthase activities are feedback inhibited by the end products of the phenylalanine/tyrosine branch. Phenylalanine acts as competitive inhibitor for the *ARO3*-encoded DAHP synthase, whereas tyrosine is a competitive inhibitor of the *ARO4* gene product (Schnappauf *et al.*, 1998). Tyrosine additionally acts on the first enzyme of its biosynthetic branch where it serves as heterotropic negative effector of chorismate mutase activity. On the other hand, the chorismate mutase enzyme is strongly activated by the end product of the opposite branch, tryptophan. As a result, both heterotropic effectors of chorismate mutase finely trigger catalytic turnover at this allosteric enzyme (Sprossler *et al.*, 1970; Schmidheini *et al.*, 1989). Tryptophan itself regulates the flux through its own biosynthetic branch via feedback inhibition of anthranilate synthase activity (Prantl *et al.*, 1985). Regulatory mutants have been characterized in detail for both allosteric enzymes constituting the first branch point of this pathway. A single site mutation in a flexible loop (loop220s) of the *ARO7*-encoded chorismate mutase results in an unregulated enzyme (Schmidheini *et al.*, 1990a). In the wild-type enzyme, a threonine residue is displayed at this position 226, whereas substitution for isoleucine locks the enzyme in its activated allosteric R state with no response to both effectors. The effect of this $ARO7^{T226I}$ mutant allele, here referred to as $ARO7^{c}$, and other alleles of residue 226 has been investigated in detail but its precise role in allosteric transition remains unclear (Graf *et al.*, 1995). On the other hand a particular anthranilate synthase mutant enzyme which is unresponsive to feedback inhibition has been characterized (Graf *et al.*, 1993). This $TRP2^{S76L}$ allele, here

referred to as *TRP2*^{fbr}, leads to insensitivity towards tryptophan as well as the structural analogue 5-methyltryptophan (Miozzari *et al*., 1977) due to reduced affinity towards the allosteric binding site. In *S. cerevisiae*, one specialised regulatory network acting on enzyme expression additionally triggers the flux through the pathway. The general control of amino acids counteracts imbalances in amino acid availability as well as environmental starvation conditions (reviewed by Hinnebusch, 1992). The final effector of this cross-pathway control system is constituted by the transcriptional activator Gcn4p that binds to conserved promoter elements of target genes to elevate their transcription. Expression of Gcn4p itself is regulated by the translational machinery mediated by four short upstream open reading frames in the *GCN4* mRNA leader region (Müller and Hinnebusch, 1986). When the aromatic amino acid biosynthesis pathway is concerned, a strong imbalance with respect to the general control system is evident. All genes coding for the enzymes of the shikimate pathway are derepressed upon amino acid starvation conditions (Jones *et al*., 1991; Teshiba *et al*., 1986). Furthermore, four of the five genes necessary for the tryptophan-specific branch are target genes of transcriptional activation by Gcn4p, among them *TRP2* (Miozzari *et al*., 1978). In contrast, the gene coding for the first enzyme of the opposite branch, *ARO7*, is not under general control despite an inverted binding site for Gcn4p in its 5' region that is able to bind the transcription factor *in vitro* (Schmidheini *et al*., 1990b).

Here, a detailed analysis of the regulatory interplay between the two mechanisms, general control and allosteric regulation, acting on the biosynthesis of aromatic amino acids in yeast is presented. With the focus on the first branch point emerging from chorismate, several alleles of *ARO7* and *TRP2* with altered regulatory properties were introduced in different combinations and systemic parameters were determined. By altering the expression level of Gcn4p, the impact of the general control system on flux control was monitored. The fact that tryptophan biosynthesis is characterized by a large reserve capacity is supported and that both regulatory systems are interdependent to contribute proper regulation of the entire pathway under conditions of amino acid imbalance.

Experimental Procedures

Materials

Chorismic acid as barium salt and 5-*DL*-methyltryptophan were purchased from SIGMA (St. Louis, MO, USA). 5-Fluoroorotic acid was obtained from TORONTO RESEARCH CHEMICALS INC. (Toronto, Canada). PLATINUM *Pfx* DNA polymerase from LIFE TECHNOLOGIES GmbH (Karlsruhe, Germany) was used for PCR reactions. All other chemicals were supplied by FLUKA (Neu-Ulm, Germany) or SIGMA-ALDRICH Chemie GmbH (Steinheim, Germany).

Yeast Strains and Growth Conditions

All yeast strains in this study are congenic to the S288C genetic background and are listed in Table I. The *aro7::hisG* and *trp2::hisG* mutations were introduced in the progenitor strain RH1408 using deletion plasmids pME1901 and pME1902, respectively, followed by counterselection on 5FOA-supplemented medium (Boeke *et al*., 1987). The *aro3::loxP-kanMX* deletion strains were obtained by transformation with plasmid pME1756. All mutant alleles of *ARO7* and *TRP2* were re-introduced at the homologous loci in single copy as verified by Southern analyses.

Complex medium for growth of *S. cerevisiae* was YEPD (1% yeast extract, 2% peptone, 2% glucose). Minimal MV medium contained 0.14% yeast nitrogen base (w/o amino acids and w/o ammonium sulphate), 0.5% ammonium sulfate, 2% glucose, and was buffered to acidic pH with succinic acid and KOH as described previously by Miozzari *et al.* (1977). As cells harbouring no functional Gcn4p starve for arginine, this amino acid was supplemented in all minimal growth media. Supplements were added according to Guthrie and Fink (1991). Growth rates were determined turbidimetrically at 595 nm and the specific growth rate is given as μ defined by $(\ln x_2 - \ln x_1)/(t_2 - t_1)$ where x stands for OD at the corresponding time t.

Plasmids

Plasmid DNAs generally were propagated in *E. coli* strain DH5α (Woodcock *et al*., 1989). Plasmids used in this study are listed in Table II. Deletion cassettes for *ARO7* and *TRP2* were created by replacement of coding sequences by the *hisG::URA3::hisG* marker (Schneider *et al*., 1996). The *loxP-kanMX* module used for deletion of the *ARO3* gene has been described by Güldener *et al*. (1996). Plasmid pME1905, carrying the *ARO7* gene

under the control of the *TRP2* promoter, was constructed by separate amplification of the *TRP2* promoter region from pME1903 and the *ARO7* coding sequence from pME1187 via PCR using oligonucleotide combinations OLSK24 (5'-GGCAAAAAATGGATTT CACAAAACCAGAAAC-3') / OLSK15 (5'-TCCTATA GAATTTATGAGCCATCG-3') and T7 (5'-GTAATACGACTCACTATAGGGC-3') / OLSK25 (5'-GTGAAATCCATTTT TTGCCTTTTTTCCAATC-3'), respectively, and a second PCR using both products as template in combination with T7/OLSK15. The amplified DNA was ligated as *Xba*I fragment to a *Aat*II/*Xba*I DNA fragment comprising part of the 5' region of *ARO7* (position – 1482 to – 652 relative to the translational start codon) and cloned in the plasmid pGEM7(+) (PROMEGA Corp., Madison, WI, USA). Plasmid pME1907 was constructed as described for pME1905 using oligonucleotide combinations T7 / OLSK27 (5'-GCGGTC ATATCTTATACCAATTTTATGCAG-3') and OLSK26 (5'-GGTATAAGATATG ACCGCTTCCATCAAAATTC-3') / OLSK17 (5'-ACAGAGAATGCCCTTTTTAAGC-3'). The resulting ^{p}*ARO7::trp2 Eco*RI/*Eco*72I fragment was ligated in pME1903 together with a *Aat*II/*Eco*RI fragment comprising part of the *TRP2* 5' region (position –1505 to –735). Plasmid pME1906 with the *ARO7*^{c} allele driven by the *TRP2* promoter was constructed by combination of a *Aat*II/*Hin*dIII fragment from pME1905 and a *Hin*dIII/*Eco*RI fragment from pME606. For construction of pME1908 with the *TRP2*^{fbr} allele under the control of the *ARO7* promoter, a *Aat*II/*Eco*72I fragment from pME1907 was fused to a *Eco*72I/*Bam*HI fragment of pME1904. Gcn4p was expressed either at low levels from plasmid p164 which carries the wt-*GCN4* gene in the low-copy vector YCp50 (Rose *et al.*, 1987) or at high levels from p238 which carries a mutant allele of *GCN4* in YCp50 with mutated upstream open reading frames (Müller and Hinnebusch, 1986). Plasmid pME1909 was used for probe preparation in Southern analyses and Northern experiments.

Transformation Procedures

Transformation of *E. coli* was performed as described by Inoue *et al*. (1990) and *S. cerevisiae* strains were transformed following a modified protocol of Elble (1992).

Nucleic Acids Preparation and Analyses

For isolation of plasmid DNA from bacterial strains the plasmid purification system from QIAGEN (Hilden, Germany) was used. Genomic DNA from yeast was isolated according to Hoffman and Winston (1987) and analysed by Southern blot (Southern, 1975) or diagnostic PCR (Saiki *et al*., 1992). Total RNA from *S. cerevisiae* cultures was prepared according to Cross and Tinkelenberg (1991) and transcript levels were determined by

Northern hybridisation (Rave *et al*., 1979) using a Bio-Imaging Analyzer from Fuji Photo Film Co. Ltd. (Tokyo, Japan). Sequencing reactions were carried out using a BigDye™ sequencing kit and analysed on an ABI PRISM® 310 Genetic Analyzer (PE BIOSYSTEMS, Foster City, CA, USA).

Enzyme assays

Enzymatic assays were performed at 37°C with TritonX-100-treated cell suspensions prepared by the method of Miozzari *et al*. (1977). Glutamine-dependent anthranilate synthase activities were determined according to Egan and Gibson (1972) at 0.5 mM substrate concentration. Chorismate mutase activity was measured spectro-photometrically as described by Schmidheini *et al*. (1989) with the modification that permeabilized cells were spun down and resuspended in cold buffer containing 125 mM potassium phosphate (pH 7.6), 25 mM *DL*-dithiotreitol, 2.5 mM EDTA, and 0.125 mM phenylmethylsulfonyl fluoride before chorismate was added to 1 mM final concentration. The concentration of phenylpyruvate was determined after cells had been removed from the assay mixture by brief centrifugation. Since absorbance of phenylpyruvate is temperature-dependent due to a keto-enol equilibrium, the assay was standardised by keeping the spectrophotometer cell at 30°C and a molar extinction coefficient of 13095 M^{-1} cm^{-1} was used. Specific activities are quantified in Units (U) equalling 1 nmole product formed in 1 min turnover by 1 mg total protein. Protein contents of the detergent-treated cell suspensions were measured by the method of Herbert *et al*. (1971) using the Bradford assay (Bradford, 1976).

***Table I: S. cerevisiae* strains used in this study**

Strain	Genotype	Source
RH1408	*MAT***a**, *ura3-52, gcn4-103*	Hinnebusch, 1985
RH2457	*MAT***a**, *ura3-52, gcn4-103, aro7::hisG-URA3-hisG*	This study
RH2458	*MAT***a**, *ura3-52, gcn4-103, aro7::hisG*	This study
RH2459	*MAT***a**, *ura3-52, gcn4-103, trp2::hisG-URA3-hisG*	This study
RH2460	*MAT***a**, *ura3-52, gcn4-103, trp2::hisG*	This study
RH2461	*MAT***a**, *ura3-52, gcn4-103, aro7::hisG, trp2::hisG-URA3-hisG*	This study
RH2462	*MAT***a**, *ura3-52, gcn4-103, aro7::hisG, trp2::hisG*	This study
RH2463	*MAT***a**, *ura3-52, gcn4-103, ARO7^{c}*	This study
RH2464	*MAT***a**, *ura3-52, gcn4-103, TRP2^{fbr}*	This study
RH2465	*MAT***a**, *ura3-52, gcn4-103, ARO7^{c}, TRP2^{fbr}*	This study
RH2466	*MAT***a**, *ura3-52, gcn4-103, ^{p}TRP2::ARO7*	This study
RH2467	*MAT***a**, *ura3-52, gcn4-103, ^{p}ARO7::TRP2*	This study
RH2468	*MAT***a**, *ura3-52, gcn4-103, ^{p}TRP2::ARO7, ^{p}ARO7::TRP2*	This study
RH2469	*MAT***a**, *ura3-52, gcn4-103, ^{p}TRP2::ARO7^{c}*	This study
RH2470	*MAT***a**, *ura3-52, gcn4-103, ARO7^{c}, ^{p}ARO7::TRP2*	This study
RH2471	*MAT***a**, *ura3-52, gcn4-103, ^{p}TRP2::ARO7^{c}, TRP2^{fbr}*	This study
RH2472	*MAT***a**, *ura3-52, gcn4-103, ARO7^{c}, ^{p}ARO7::TRP2^{fbr}*	This study
RH2473	*MAT***a**, *ura3-52, gcn4-103, ^{p}TRP2::ARO7^{c}, ^{p}ARO7::TRP2*	This study
RH2474	*MAT***a**, *ura3-52, gcn4-103, ^{p}TRP2::ARO7^{c}, ^{p}ARO7::TRP2^{fbr}*	This study
RH2475	*MAT***a**, *ura3-52, gcn4-103, aro3::kanMX*	This study
RH2476	*MAT***a**, *ura3-52, gcn4-103, aro3::kanMX, ARO7^{c}*	This study
RH2477	*MAT***a**, *ura3-52, gcn4-103, aro3::kanMX, ARO7^{c}, ^{p}ARO7::TRP2*	This study
RH2478	*MAT***a**, *ura3-52, gcn4-103, aro3::kanMX, ^{p}TRP2::ARO7^{c}*	This study
RH2479	*MAT***a**, *ura3-52, gcn4-103, aro3::kanMX, ^{p}TRP2::ARO7^{c}, ^{p}ARO7::TRP2*	This study

Table II: **Plasmids used in this study**

Plasmid	Description	Source
pME1756	*aro3::loxP-kanMX-loxP* cassette for deletion of *ARO3* open reading frame	O. Grundmann, pers. comm.
pME1901	3.3 kb *aro7::hisG-URA3-hisG* cassette for deletion of *ARO7* open reading frame	This study
pME1902	3.1 kb *trp2::hisG-URA3-hisG* cassette for deletion of *TRP2* open reading frame	This study
pME1187	2 kb *Eco*RI fragment containing *ARO7* in pGEM7(+)	Graf *et al*., 1995
pME606	2 kb *Eco*RI fragment containing $ARO7^{c}$ in pJDB207	Schmidheini *et al*., 1989
pME1903	2.3 kb *Xba*I/*Bam*HI fragment containing *TRP2* in pGEM7(+)	This study
pME1904	2.3 kb *Xba*I/*Bam*HI fragment containing $TRP2^{fbr}$ in pGEM7(+)	This study
pME1905	3 kb *Aat*II/*Eco*RI fragment containing *5'-ARO7::*^{p}*TRP2::ARO7* replacement cassette in pGEM7(+)	This study
pME1906	3 kb *Aat*II/*Eco*RI fragment containing *5'-ARO7::*^{p}*TRP2::*$ARO7^{c}$ replacement cassette in pUC19	This study
pME1907	3 kb *Aat*II/*Bam*HI fragment containing *5'-TRP2::*^{p}*ARO7::TRP2* replacement cassette in pGEM7(+)	This study
pME1908	3 kb *Aat*II/*Bam*HI fragment containing *5'-TRP2::*^{p}*ARO7::*$TRP2^{fbr}$ replacement cassette in pUC19	This study
p164	2.8 kb *Sal*I/*Eco*RI fragment containing *GCN4* in YCp50	Müller and Hinnebusch, 1986
p238	2.8 kb *Sal*I/*Eco*RI fragment containing *GCN4* with all four uORFs mutated in YCp50	Müller and Hinnebusch, 1986
pME1909	470 bp *Ssp*I/*Eco*RV fragment of *ARO7* open reading frame and 465 bp *Eco*72I/*Eco*RV fragment of *TRP2* open reading frame in pBluescript II KS	This study

Results

Directing the flux of chorismate by genetic engineering

The chorismate mutase-encoding gene *ARO7* of *Saccharomyces cerevisiae* is an amino acid biosynthetic gene which is not transcriptionally regulated by the general control activator Gcn4p (Schmidheini *et al.*, 1990b). To characterize the physiological effects of regulated *ARO7* expression, the *ARO7* coding sequence was fused to a Gcn4p-regulated promoter and integrated in an *aro7Δ* deletion strain. The promoter of the anthranilate synthase-encoding gene *TRP2* was chosen which encodes the competing enzyme of the chorismate branch point of aromatic amino acid biosynthesis. Furthermore, constructs were generated in which *TRP2* expression is driven by the *ARO7* promoter and therefore is no more regulated by the general control. Theses alleles were combined with the wt-*ARO7* allele and the promoter fusion, respectively. To monitor the effects of Gcn4p-dependent and -independent *ARO7* and *TRP2* expression in the resulting strains, the allelic combinations were introduced into a *gcn4-101* background. Strains were transformed with plasmids expressing either no, low, or high levels of functional Gcn4p. To quantify expression of *ARO7* and *TRP2*, steady state transcript levels were determined by Northern analyses in the resulting four strains grown in minimal medium (Fig. 8A). To assess steady state levels of *ARO7* and *TRP2* transcripts simultaneously, total RNAs were hybridized to a probe that is specific for both genes prepared from plasmid pME1909. Transcript levels of the actin-encoding gene *ACT1* were used as internal standard. In the wild-type situation of strain RH1408, transcript levels of *ARO7* and *TRR2* were comparable in the absence of Gcn4p. Low levels of this transcription factor induced *TRP2* expression slightly whereas *ARO7* expression remained almost unchanged. High levels of Gcn4p induced *TRP2* transcription by a factor of 1.6 and did not substantially affect *ARO7* expression. The ratio between *TRP2/ARO7* transcript levels decreased from 0.72 over 0.67 to 0.54. Accordingly, *ARO7* transcription driven by the *TRP2* promoter resulted in an 1.7-fold induction by Gcn4p. The co-expression of ^{p}*TRP2::ARO7* and the wt-*TRP2* allele (strain RH2466), had a mirror image effect on regulation and therefore the transcript level ratio between both genes was never significantly changed. Vice versa, when both genes were expressed from the general control-insensitive *ARO7* promoter (strain RH2467), no induction with respect to Gcn4p levels was present and *ARO7*/*TRP2* transcript ratios also remained constant at 0.56. In strain RH2468, the transcriptional regulation pattern with respect to the general control is

inverted for both genes. As a consequence, transcript level ratios changed from 0.65 to 1.2 when Gcn4p was expressed at high levels.

A

strain	RH1408			RH2466			RH2467			RH2468		
genotype	*ARO7*, *TRP2*			^{p}*T::ARO7*, *TRP2*			*ARO7*, ^{p}*A::TRP2*			^{p}*T::ARO7*, ^{p}*A::TRP2*		
Gcn4p	-	+	+++	-	+	+++	-	+	+++	-	+	+++
TRP2	11.6	12.9	18.0	12.5	12.1	18.6	12.1	11.7	10.1	11.1	13.0	10.5
ARO7	8.4	8.7	9.8	6.5	6.5	10.4	6.9	6.5	5.7	7.2	6.7	12.5
ratio	**0.72**	**0.67**	**0.54**	**0.52**	**0.54**	**0.56**	**0.57**	**0.56**	**0.56**	**0.65**	**0.52**	**1.2**

B

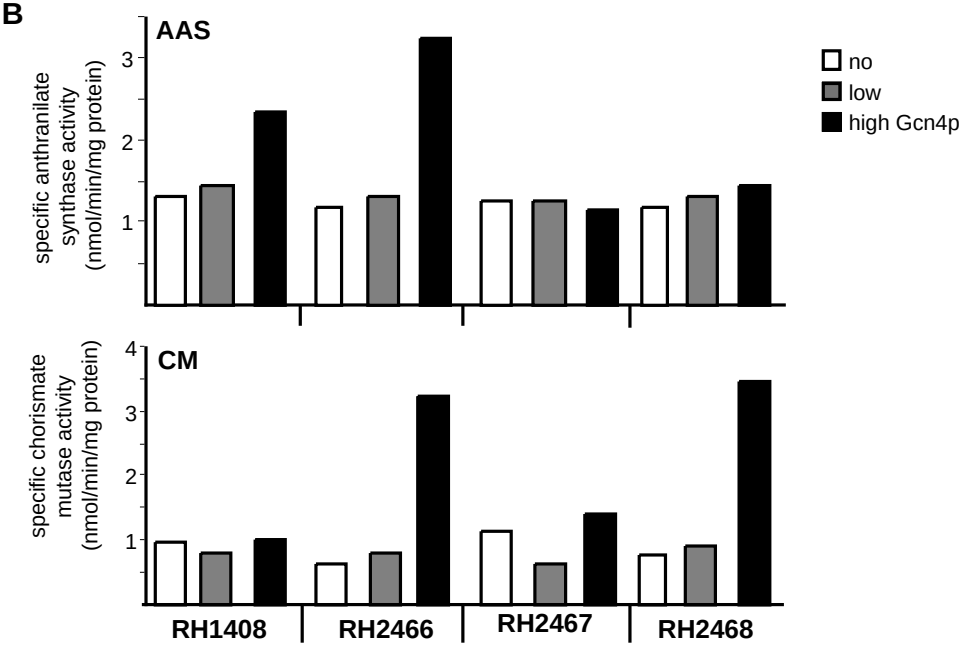

C

	RH1408			RH2466			RH2467			RH2468		
Gcn4p	-	+	+++	-	+	+++	-	+	+++	-	+	+++
μ	0.21	0.21	0.17	0.20	0.20	0.17	0.21	0.21	0.16	0.21	0.21	0.15

Figure 8: Properties of yeast strains expressing *ARO7* and *TRP2* with altered dependency on the general control activator Gcn4p. *A*, Northern analysis of strains RH1408, RH2466, RH2467, and RH2468. The specific genotype is indicated with the *TRP2* promoter abbreviated by ^{p}*T* and the *ARO7* promoter by ^{p}*A*, as well as the levels of Gcn4p expressed from plasmids YCp50 (-, no Gcn4p), p164 (+, low levels), and p238 (+++, high levels), respectively. Transcript levels are given in arbitrary units after standardization to transcript levels of the *ACT1* gene. The ratio between

TRP2 and *ARO7* steady state mRNA amounts is given in the last row. *B*, specific glutamine-dependent anthranilate synthase activities (AAS, upper panel) and specific chorismate mutase activities (CM, lower panel) as determined from permeabilized cells of strains described in *A*. Levels of functional Gcn4p are indicated in the histograms by white (no Gcn4p), gray (low levels), and black (high levels) bars, respectively. *C*, growth rates of strains RH1408, RH2466, RH2467, and RH2468 determined in minimal medium. Gcn4p levels are indicated as described in *A*.
All values are the mean of two independent measurements with a standard deviation not exceeding 20%.

The different transcriptional expression patterns were properly reflected by specific chorismate mutase (CM) and glutamine-dependent anthranilate synthase (AAS) activities determined from permeabilized cells (Fig. 8B). In wild-type strain RH1408 the basal levels were determined as 1.3 U for specific AAS activity and 1 U for specific CM activity, respectively. When Gcn4p was expressed at high levels, AAS activity was raised to 2.4 U whereas CM activity was not affected. In strain RH2466 both activities were induced in a Gcn4p-dependent manner with AAS activity ranging from 1.2 U to 3.3 U and CM activity increasing from 0.7 U to 3.3 U. In strain RH2467 no induction of both activities was determined when Gcn4p was expressed at high levels. Strain RH2468 displayed a constitutively basal level of AAS activity with an average value of 1.3 U whereas CM activity was elevated from 0.8 U to 3.5 U when the transcription factor was present in high amounts.

No obvious growth phenotype for any of the strains was observed in minimal medium. Growth rates μ, which reflect the flux through the pathway, of RH2468, RH2466, and RH2467 were not significantly altered in minimal medium in comparison to the wild-type strain (Fig. 8C). Nevertheless, growth rates decreased when the transcriptional activator was expressed in high amounts. Growth tests on various solid media supplemented with combinations of aromatic amino acids did not reveal any nutritional requirements upon amino acid imbalance (not shown). In conclusion, altered expression of *ARO7* and *TRP2* with respect to the general control of amino acid biosynthesis does not severely alter the flux through the first branch point of aromatic amino biosynthesis and indicates a high reserve capacity of this metabolic pathway.

The impact of a constitutively active chorismate mutase encoded by *ARO7^c*

The *ARO7^c* allele encoding an unregulated chorismate mutase is reported to display high enzymatic activity which leads to depletion of the chorismate pool in *S. cerevisiae*. To modulate distribution of this intermediate in aromatic amino acid biosynthesis more stringently, we replaced the wt-*ARO7* gene in strain RH1408 by the *ARO7^c* allele resulting in strain RH2463. Alternatively, the *ARO7^c* allele was introduced under the control of the *TRP2* promoter to yield strain RH2469. Additionally, combinations of these two *ARO7^c* alleles with *TRP2* expressed from the *ARO7* promoter yielded strains RH2470 and RH2473, respectively. In all genetic backgrounds both genes were expressed properly and in accordance to their promoters as determined by Northern analysis (not shown). Enzymatic activities of both branch point enzymes reflected the altered flux at the metabolic node (Fig. 9A). For strain RH2463 carrying the constitutively active chorismate mutase, a specific CM activity of 12.2 was determined and specific anthranilate synthase activity was at a basal level of 1.4 U when no Gcn4p was expressed. High levels of Gcn4p increased AAS activity to 2.6 U, whereas CM activity was unaffected at 11.9 U. When both genes, *ARO7^c* as well as *TRP2*, were expressed from the *ARO7* promoter (strain RH2470), both enzymatic activities were not significantly changed at different Gcn4p levels with CM activity ranging from 12.2 U to 10.4 U and AAS activity from 1.2 U to 1.7 U. When gene expression was driven from the *TRP2* promoter (strain RH2469), both enzymatic activities increased upon high levels of Gcn4p. CM activity was elevated from 9.5 U to 26.4 U, and specific AAS activity from 1.2 U to 3.1 U. In the reversed promoter combination of strain RH2473, AAS activity was almost unaffected with respect to Gcn4p levels at a basal level of 1.2 U but specific chorismate mutase activity was shifted from 9.4 U to 19.6 U when the level of the transcriptional activator was increased. The *in vivo* effect of the different allelic combinations was monitored by determination of the growth rate constants μ (Fig. 9B). For all strains expressing the *ARO7^c* allele no significant reduction in growth rates was detected in comparison to the wild-type strain, indicating that no internal amino acid pool was sufficiently depleted and no starvation situation was present in these strains.

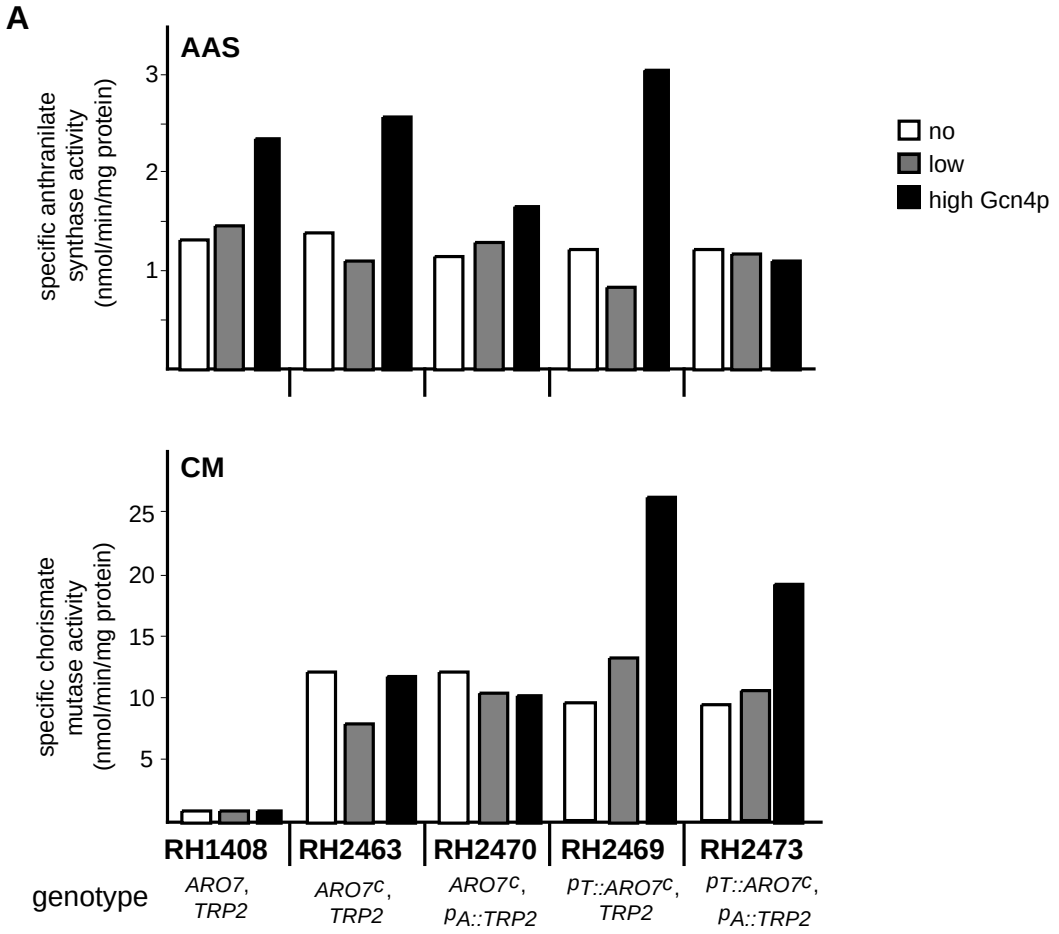

B

	RH1408			RH2463			RH2470			RH2469			RH2473		
Gcn4p	-	+	+++	-	+	+++	-	+	+++	-	+	+++	-	+	+++
μ	0.21	0.21	0.17	0.21	0.20	0.17	0.20	0.20	0.16	0.20	0.20	0.17	0.19	0.21	0.17

Figure 9: Enzymatic activities and growth rates of yeast strains expressing a constitutively active and unregulated chorismate mutase encoded by the *ARO7*^{c} allele. *A*, specific glutamine-dependent anthranilate synthase activities (AAS, upper panel) and specific chorismate mutase activities (CM, lower panel) as determined from permeabilized cells of strains RH1408, RH2463, RH2470, RH2469, and RH2473. The corresponding genotype is indicated as well as the amount of functional Gcn4p expressed from plasmids (see Fig. 8). *B*, growth rates of strains described in *A* determined in minimal medium.

All values are the mean of two independent measurements with a standard deviation not exceeding 20%.

ARO7^c expression requires Gcn4p in the presence of exogenous phenylalanine

The strains expressing the unregulated and constitutivley activated chorismate mutase were tested for growth on different media supplemented with aromatic amino acids. When phenylalanine was present in the minimal medium at a standard concentration of 50 mg·ml^{-1}, cells expressing no Gcn4p were not viable. Expression of the transcription factor Gcn4p either at low or high levels restored growth. So did supplementation of tryptophan (not shown) as well as anthranilic acid (Fig. 10A). Even when *ARO7*^{c} expression was driven by the *TRP2* promoter in combination with *TRP2* expression not under general control (strain RH2473), cells expressing high levels of Gcn4p grew in the presence of phenylalanine. The fact that the tryptophan precursor anthranilic acid suppresses lethality of exogenous phenylalanine in a *ARO7*^{c}, *gcn4Δ* background indicates that cells starve severely for tryptophan due to the redirected flux of chorismate into the tyrosine/phenylalanine-specific branch.

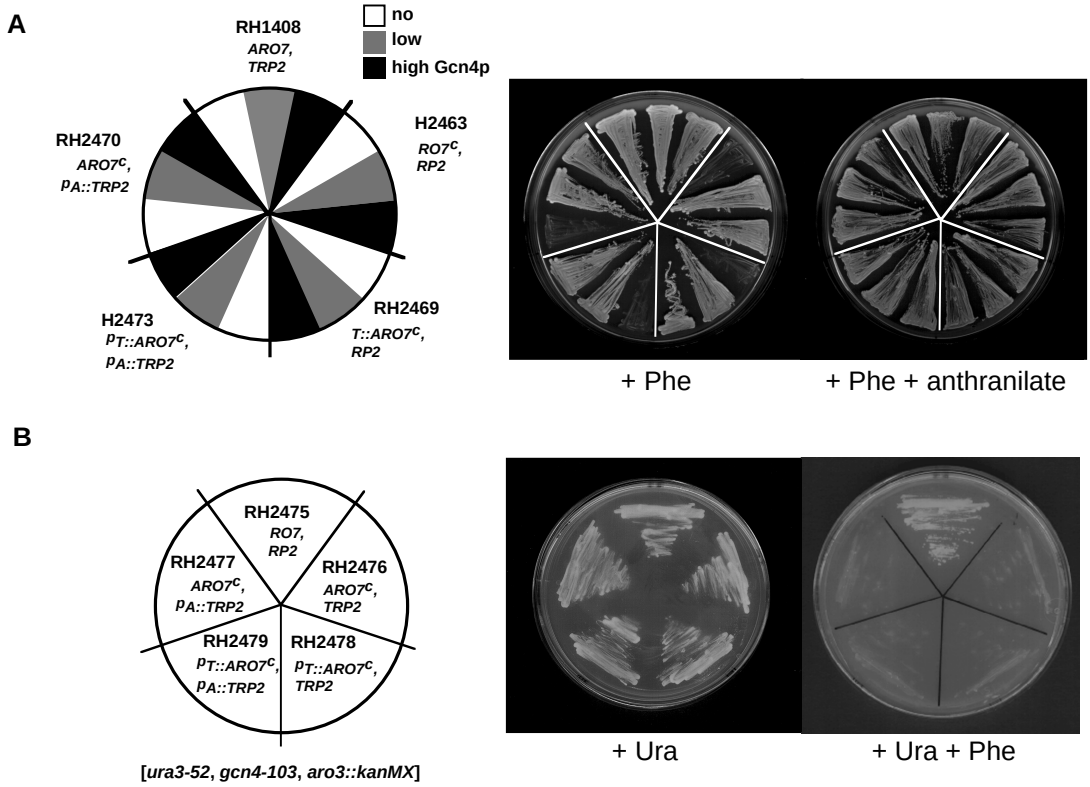

Figure 10: Growth behavior of *ARO7*^{c} strains in the presence of phenylalanine. *A*, cells were streaked out on minimal medium supplemented with phenylalanine or phenylalanine and anthranilic acid, respectively, and growth was monitored after three days. See Fig. 8 for legends on genotypes and levels of Gcn4p. *B*, growth of strains expressing *ARO7*^{c} in a *gcn4-101*, *aro3Δ* background on minimal medium.

Three modes of action for phenylalanine are possible. Either repression of the tryptophan biosynthetic branch, or activation of the opposite branch, or repression of the entire pathway. The only characterized target in the pathway for phenylalanine is the *ARO3*-encoded DAHP synthase contributing to the input reaction of the shikimate pathway. Therefore, we deleted the *ARO3* gene in the strains expressing the *ARO7*^{c} allele and monitored growth on minimal medium without exogenous phenylalanine (Fig. 10B). Interestingly, these *gcn4* strains (RH2476, RH2477, RH2478, RH2479) grew well on minimal medium at a rate comparable to a strain expressing the wild-type *ARO7* gene in a *aro3Δ, gcn4-103* background (RH2475). Nevertheless, addition of phenylalanine inhibited growth indicating that exogenous phenylalanine not solely acts of the Aro3p gene product but triggers the flux of chorismate at an additional point of attack.

Tryptophan starvation is not suppressed by the general control when an unregulated chorismate mutase is expressed in a Gcn4p-dependent manner

To characterize the impact of the general control system on expression of the *ARO7*^{c} allele in more detail, growth of all strains expressing *ARO7*^{c} under tryptophan-limiting conditions was monitored. This was induced by the addition of the tryptophan analogue 5-*DL*-methyltryptophan (5MT) (Fig. 11A). This compound inhibits the anthranilate synthase activity in yeast due to binding to the allosteric site of Trp2p and therefore limits the flux of chorismate into the tryptophan-specific branch (Miozzari *et al.*, 1977). When *ARO7*^{c} was expressed from its native promoter in combination with the wt-*TRP2* gene in strain RH2463, cell growth on solid minimal medium supplemented with 10 mM 5MT was strongly reduced in the *gcn4* null background but expression of Gcn4p restored growth. Expression of *ARO7*^{c} combined with expression of *TRP2* driven by the *ARO7* promoter resulted in almost the same growth phenotype but growth was delayed. Making *ARO7*^{c} a target of the general control lead to a more drastic effect. Even when *GCN4* was expressed in high amounts, no growth was observed in the presence of 5MT and this was independent with respect to the transcriptional regulation of the *TRP2* gene, either Gcn4p-dependent or –independent (strains RH2469 or RH2473, respectively). All effects observed in the presence of 5MT were suppressed by the *TRP2*^{fbr} allele (not shown), indicating that the growth defects were solely based on tryptophan limitation due to a reduced anthranilate synthase activity. By monitoring the growth rates of the *ARO7*^{c} strains in liquid cultures, the effect of 5MT was determined more precisely (Fig. 11B). As concentration for this drug 10^{-4} M was chosen. The wild-type strain grew even in the absence of functional Gcn4p at a decreased rate of 0.18 that was altered to 0.20 and 0.16, respectively, when the transcription

factor was expressed at low and high levels. All *ARO7*^{c} strains showed no growth when no Gcn4p was expressed, indicating the super-sensitivity towards 5MT. RH2463 expressing *TRP2* in a Gcn4p-dependent manner grew at a rate of 0.094 when carrying the plasmid-encoded wt-*GCN4* gene. This growth rate increased to 0.127 by high levels of Gcn4p present in the cell. For strain RH2470 which expresses *ARO7*^{c} and *TRP2* from the *ARO7* promoter, similar growth rates of 0.094 and 0.096 were determined when Gcn4p was present at low or high levels, respectively. Growth rates of strain RH2469 were influenced by the levels of Gcn4p. When low levels of Gcn4p were expressed, growth was monitored with a μ of 0.081. This value increased slightly to 0.091 when Gcn4p was expressed at high levels. In strain RH2473 with its inverse expression pattern for *ARO7*^{c} and *TRP2*, very slow growth was detected in the presence of 5MT. Growth rates were determined to be 0.045 and 0.039, respectively, in the presence of Gcn4p in low and high amounts.

A

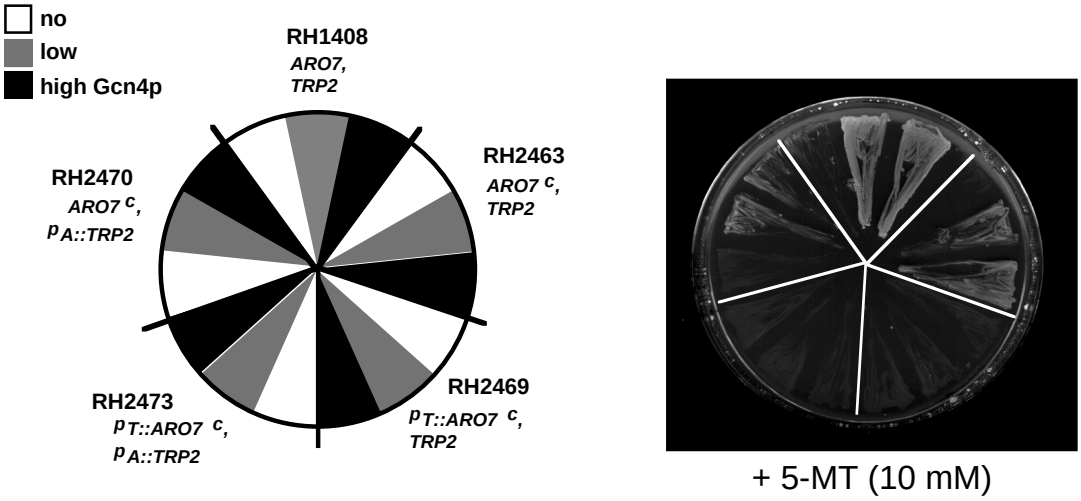

B

	RH1408			RH2463			RH2470			RH2469			RH2473		
Gcn4p	-	+	+++	-	+	+++	-	+	+++	-	+	+++	-	+	+++
μ	0.18	0.20	0.16	/	0.094	0.13	/	0.094	0.096	/	0.081	0.091	/	0.045	0.039

Figure 11: Growth behavior of strains expressing *ARO7*^{c} in the presence of 5-methyltryptophan. *A*, growth after three days on solid medium. *B*, growth rates in minimal medium in the presence of 10^{-4} M 5MT. Values are the mean of two independent measurements with a standard deviation not exceeding 20%. See Fig. 8 for legends on genotypes and levels of Gcn4p.

Taken together, these data indicate that a Gcn4p-independent expression of an unregulated, constitutively active chorismate mutase is necessary for survival under conditions where the flux into the tryptophan specific branch of aromatic amino acid biosynthesis is limited. Additionally, the severe growth defects induced by *ARO7*^{c} upon tryptophan limitation were suppressed by the wild-type *ARO7* allele that restores allosteric regulation of chorismate mutase activity at the branch point.

Discussion

Biosynthesis of aromatic amino acids in the yeast *Saccharomyces cerevisiae* is a model system for a branched, strictly regulated metabolic reaction cascade. Different modes of regulation acting on catalytic turnover as well as enzyme synthesis are present to trigger the flux through the pathway. Focussing on the first branch point, this metabolic node has to be classified as strictly rigid. With respect to the allosteric regulation of the key enzymes, the pathway fits quite well into the model of preferential synthesis set up by Shiio for branched reaction cascades (Shiio, 1982). There, one pathway emerging from a branch is favoured over the other, and efficient regulation is achieved by feedback inhibition of this branch by its own end product and by the end product(s) of the less favoured branch inhibiting the input reaction of the entire pathway. The data determined for enzymatic activities of anthranilate synthase and chorismate mutase suggest a preference of the tryptophan-specific branch emerging from chorismate and the end product tryptophan serves as negative allosteric effector of anthranilate synthase activity. The observed preference is in agreement with catalytic data determined before (Braus, 1991 and references therein). Given a percentage for total cellular protein of 0.01 % for chorismate mutase and 0.05 % for the anthranilate synthase complex and considering the different molecular masses of both enzymes, it is deduced that both proteins are present in roughly the same number of molecules per cell. In the unliganded state, for chorismate mutase a $[S]_{0.5}$ value of 4.0 mM for the substrate chorismate is reported, whereas the anthranilate synthase complex has a higher affinity towards chorismate with a K_m value of 0.017 mM. The most crucial parameter of the pathway for cell survival is the tryptophan pool and previous studies have mainly focused on this branch (Miozzari *et al*., 1978; Niederberger *et al*., 1992; Small and Kascer, 1994). The free tryptophan pool was determined to be relatively small with a concentration of 0.07 nmol per mg dry weight (Fantes *et al*., 1976). Given a basal level of 1.3 nmol per minute and mg protein of AAS activity, a three-fold excess to maintain growth can be calculated (Miozzari *et al*., 1978). This buffer capacity of the pathway is strongly supported by our findings that growth was maintained under all conditions tested when the competing enzyme, chorismate mutase, was expressed in a Gcn4p-dependent manner. Even a derepressed CM activity of 3.6 U did not alter AAS activity sufficiently and therefore no growth defect was present. Expression of an unregulated, constitutively active chorismate mutase had no effect either under non-starvation and balanced conditions. Somehow, this allele reflects the normal situation as chorismate mutase is fully activated 10-fold at a tryptophan concentration of 10 µM (Schmidheini *et al*., 1990a) and cellular concentration

of tryptophan is reported to be of the order of 20 μM (Braus, 1991). By making the *ARO7*^{c} allele a target of the general control, further increase in CM activity was achieved. The fact that anthranilate synthase activity was not reduced below 1 U even when chorismate mutase activity was elevated to 20 U implies that the cellular chorismate pool is sufficiently high enough to maintain the flux into the tryptophan-specific branch, even when the flux to the opposite sink is strongly favoured.

Nevertheless, the chorismate pool turned out to be crucial in the presence of an amino acid imbalance. Exogenous phenylalanine was lethal due to tryptophan starvation in a *gcn4* null background when chorismate was channelled into the tyrosine/phenylalanine-specific branch by expression of the *ARO7*^{c} allele. In conclusion, the internal level of tyrosine is sufficiently high enough to repress the *ARO4*-encoded DAHP synthase contributing to the pathway input. The presence of phenylalanine decreases the input flux furthermore as this amino acid acts negatively on the DAHPS isoenzyme encoded by *ARO3*. As strains deleted for *ARO3* were viable on minimal medium, an additional target of phenylalanine must exist. Either this amino acid inhibits an enzymatic activity of the main trunk or, alternatively, activates catalytic turnover in the tyrosine/phenylalanine branch. To date, no such additional target has been characterized. Additionally, the growth of the *aro3Δ, ARO7*^{c} strains indicates that the internal tyrosine pool not completely inhibits the *ARO4* gene product but that enzymatic activity of this DAHPS isoenzyme is not sufficiently high enough to maintain the basal chorismate level in the presence of phenylalanine. The general control of amino acid biosynthesis counteracts this starvation situation by derepressing the enzymatic activities contributing to chorismate synthesis. This is of special importance for *ARO3* expression as the basal level for *ARO3* transcription was reported to be dependent on the general control activator Gcn4p (Paravicini *et al*., 1989). In conclusion, we refer to the general control as a backup system providing sufficient levels of chorismate to feed both branches of aromatic amino acid biosynthesis.

Expression of the *ARO7*^{c} allele had severe effects when the flux into the tryptophan branch was reduced by the action of 5-methyltryptophan. No growth was observed in the absence of the general control backup system. This is in agreement with the reported super-sensitivity towards the drug of strains expressing the unregulated and constitutively active chorismate mutase enzyme (Schmidheini *et al*., 1989). Placing the *ARO7*^{c} allele behind a general control-dependent promoter abolished the rescue of high levels of the transcriptional activator Gcn4p. This allelic situation with an allosterically unregulated chorismate mutase expressed in a Gcn4p-dependent manner might reflect an early

evolutionary situation. The existence of a Gcn4p recognition element in the *ARO7* promoter region that is able to bind the transcriptional activator *in vitro* implies that this gene formerly was subjected to the general control system (Schmidheini *et al*., 1990b). From structural studies it has been deduced that the dimeric, allosterically regulated chorismate mutase might have evolved from a monomeric, unregulated ancestor by a gene duplication/gene fusion event (Sträter *et al*., 1997). Given the drastic effects observed for the *ARO7*^{c} allele when being subjected to the general control, we speculate that chorismate mutase expression was removed from the general control system before this gene duplication and fusion. As a result, the different regulation of both branch point enzymes with respect to the general control provides that flux imbalances can be counteracted in an asymmetric manner.

In summary, the interplay of two modes of regulation acting on the first metabolic node of aromatic amino acid biosynthesis was investigated. Under laboratory conditions with balanced availability of amino acids, no drastic effects were monitored. Nevertheless, by manipulating the enzymatic activities at the branch point, the different impacts of the general control system and allostery could be monitored. Based on these studies, further research concerning the evolutionary formation of the regulatory pattern at the metabolic node will be stimulated as well as implications for biotechnological purposes.

References

Aebi, M., P. Niederberger, and R. Hütter (1982) Isolation of the *TRP2* and *TRP3* genes of *Saccharomyces cerevisiae* by functional complementation. *Curr. Genet.* **5:** 39-46.

Bailey, J.E. (1991) Toward a science of metabolic engineering. *Science* **252:** 1668-1675.

Ball, S.G., R.B. Wickner, G. Cottarel, M. Schaus, and C. Tirtiaux (1986) Molecular cloning and characterization of *ARO7-OSM2*, a single yeast gene necessary for chorismate mutase activity and growth in hypertonic medium. *Mol. Gen. Genet.* **205:** 326-330.

Boeke, J.D., J. Trueheart, G. Natsoulis, and G.R. Fink (1987) 5-Fluoroorotic acid as a selective agent in yeast molecular genetics. *Methods Enzymol.* **154:** 164-175.

Bradford, M.M. (1976) A rapid and sensitive method for the quantitation of microgram quantities of protein utilizing the principle of protein-dye binding. *Anal. Biochem.* **72:** 248-254.

Braus, G.H. (1991) Aromatic amino acid biosynthesis in the yeast *Saccharomyces cerevisiae*: a model system for the regulation of a eukaryotic biosynthetic pathway. *Microbiol. Rev.* **55:** 349-370.

Cross, F.R., and A.H.Tinkelenberg (1991) A potential positive feedback loop controlling *CLN1* and *CLN2* gene expression at the start of the yeast cell cycle. *Cell* **65:** 875-883.

Egan, A.F., and F. Gibson (1972) Anthranilate synthase-anthranilate 5-phosphoribosyl 1-pyrophosphate phosphoribosyltransferase from *Aerobacter aerogenes*. *Biochem. J.* **130:** 847-859.

Elble, R. (1992) A simple and efficient procedure for transformation of yeasts. *BioTechniques* **13:** 18-20.

Graf, R., Y. Dubaquie, and G.H. Braus (1995) Modulation of the allosteric equilibrium of yeast chorismate mutase by variation of a single amino acid residue. *J. Bacteriol.* **177:** 1645-1648.

Graf, R., B. Mehmann, and G.H. Braus (1993) Analysis of feedback-resistant anthranilate synthases from *Saccharomyces cerevisiae*. *J. Bacteriol.* **175:** 1061-1068.

Güldener, U., S. Heck, T. Fielder, J. Beinhauer, and J.H. Hegemann (1996) A new efficient gene disruption cassette for repeated use in budding yeast. *Nucleic Acids Res.* **24:** 2519-2524.

Guthrie, C., and G.R. Fink (1991) Guide to yeast genetics and molecular biology. *Methods Enzymol.* **194:** 15.

Herbert, D., P.J. Phipps, and R.E. Strange (1971) Chemical analysis of microbial cells. In *Methods of Microbiology* 5B (Norris, J. R. and Ribbons, D. W., eds), pp. 209-344. Academic Press Inc., New York.

Hinnebusch, A.G. (1985) A hierarchy of trans-acting factors modulates translation of the activator of general amino acid control in *Saccharomyces cerevisiae*. *Mol. Cell. Biol.* **5:** 2349-2360.

Hinnebusch, A. (1992) General and pathway-specific regulatory mechanisms controlling the synthesis of amino acid biosynthetic genes in Saccharomyces cerevisiae. In *The Molecular and Cellular Biology of the Yeast Saccharomyces.* Vol. 2: Gene expression. (E.W.Jones, J.R. Pringle, and J.R. Broach, eds), pp. 319-414. Cold Spring Harbor Laboratory Press, Cold Spring Harbor, New York.

Hoffman, C.S., and F. Winston (1987) A ten-minute DNA preparation from yeast efficiently releases autonomous plasmids for transformation of *Escherichia coli*. *Gene* **57:** 267-272.

Inoue, H., H. Nojima, and H. Okayama (1990) High efficiency transformation of *Escherichia coli* with plasmids. *Gene* **96:** 23-28.

Jones, D.G., U. Reusser, and G.H. Braus (1991) Molecular cloning, characterization and analysis of the regulation of the *ARO2* gene, encoding chorismate synthase, of *Saccharomyces cerevisiae*. *Mol. Microbiol.* **5:** 2143-2152.

Künzler, M., G. Paravicini, C.M. Egli, S. Irniger, and G.H. Braus (1992) Cloning, primary structure and regulation of the *ARO4* gene, encoding the tyrosine-inhibited 3-deoxy-D-arabino-heptulosonate-7-phosphate synthase from *Saccharomyces cerevisiae*. *Gene* **113:** 67-74.

Miozzari, G., P. Niederberger, and R. Hütter (1977) Action of tryptophan analogues in *Saccharomyces cerevisiae*. *Arch. Microbiol.* **115:** 307-316.

Miozzari, G., P. Niederberger, and R. Hütter (1978) Tryptophan biosynthesis in *Saccharomyces cerevisiae*: control of the flux through the pathway. *J. Bacteriol.* **134:** 48-59.

Morollo, A.A., and R. Bauerle (1993) Characterization of composite aminodeoxy-isochorismate synthase and aminodeoxyisochorismate lyase activities of anthranilate synthase. *Proc. Natl. Acad. Sci. USA* **90:** 9983-9987.

Müller, P.P., and A.G. Hinnebusch (1986) Multiple upstream AUG codons mediate translational control of *GCN4*. *Cell* **45:** 201-207.

Niederberger, P., R. Prasad, G. Miozzari, and H. Kacser (1992) A strategy for increasing an in vivo flux by genetic manipulations. The tryptophan system of yeast. *Biochem. J.* **287:** 473-479.

Ostergaard, S., L. Olsson, and J. Nielsen (2000) Metabolic engineering in *Saccharomyces cerevisiae*. *Microbiol. Mol. Biol. Rev.* **64:** 34-50.

Paravicini, G., H.-U. Mösch, T. Schmidheini, and G. Braus (1989) The general control activator protein GCN4 is essential for a basal level of *ARO3* gene expression in *Saccharomyces cerevisiae*. *Mol. Cell. Biol.* **9:** 144-151.

Prantl, F., A. Strasser, M. Aebi, R. Furter, P. Niederberger, K. Kirschner, and R. Hütter (1985) Purification and characterization of the indole-3-glycerolphosphate synthase/anthranilate synthase complex of *Saccharomyces cerevisiae*. *Eur. J. Biochem.* **146:** 95-100.

Rave, N., R. Crkvenjakov, and H. Boedtker (1979) Identification of procollagen mRNAs transferred to diazobenzyloxymethyl paper from formaldehyde agarose gels. *Nucleic Acids Res.* **6:** 3559-3567.

Rose, M.D., P. Novick, J.H. Thomas, D. Botstein, and G.R. Fink (1987) A *Saccharomyces cerevisiae* genomic plasmid bank based on a centromere-containing shuttle vector. *Gene* **60:** 237-243.

Saiki, R.K., S. Scharf, F. Faloona, K.B. Mullis, G.T. Horn, H.A. Erlich, and N. Arnheim (1992) Enzymatic amplification of beta-globin genomic sequences and restriction site analysis for diagnosis of sickle cell anemia. *Biotechnology* **24:** 476-480.

Schmidheini, T., P. Sperisen, G. Paravicini, R. Hütter, and G. Braus (1989) A single point mutation results in a constitutively activated and feedback-resistant chorismate mutase of *Saccharomyces cerevisiae*. *J. Bacteriol.* **171:** 1245-1253.

Schmidheini, T., H.-U. Mösch, J.N. Evans, and G. Braus (1990a) Yeast allosteric chorismate mutase is locked in the activated state by a single amino acid substitution. *Biochemistry* **29:** 3660-3668.

Schmidheini, T., H.-U. Mösch, R. Graf, and G.H. Braus (1990b) A GCN4 protein recognition element is not sufficient for GCN4-dependent regulation of transcription in the *ARO7* promoter of *Saccharomyces cerevisiae*. *Mol. Gen. Genet.* **224:** 57-64.

Schnappauf, G., M. Hartmann, M. Künzler, and G.H. Braus (1998) The two 3-deoxy-D-arabino-heptulosonate-7-phosphate synthase isoenzymes from *Saccharomyces cerevisiae* show different kinetic modes of inhibition. *Arch. Microbiol.* **169:** 517-524.

Schneider, B.L., B. Steiner, W. Seufert, and A.B. Futcher (1996) pMPY-ZAP: a reusable polymerase chain reaction-directed gene disruption cassette for *Saccharomyces cerevisiae*. *Yeast* **12:** 129-134.

Shiio, I. (1982) in *Overproduction of Microbial Products* (K. Krumphanzl, B. Sikyta, and Z. Vanek, eds), pp. 463-472. Academic Press, New York.

Small, J.R., and H. Kacser (1994) A method for increasing the concentration of a specific internal metabolite in steady-state systems. *Eur. J. Biochem.* **226:** 649-656.

Southern, E.M. (1975) Detection of specific sequences among DNA fragments separated by gel electrophoresis. *J. Mol. Biol.* **98:** 503-517.

Sprossler, B., U. Lenssen, and F. Lingens (1970) Properties of chorismate mutase from *Saccharomyces cerevisiae* S288C. *Hoppe Seylers Z. Physiol. Chem.* **351:** 1178-1190.

Stephanopoulos, G., and J.J. Vallino (1991) Network rigidity and metabolic engineering in metabolite overproduction. *Science* **252:** 1675-1681.

Sträter, N., G. Schnappauf, G. Braus, and W.N. Lipscomb (1997) Mechanisms of catalysis and allosteric regulation of yeast chorismate mutase from crystal structures. *Structure* **5:** 1437-1452.

Teshiba, S., R. Furter, P. Niederberger, G. Braus, G. Paravicini, and R. Hütter (1986) Cloning of the *ARO3* gene of *Saccharomyces cerevisiae* and its regulation. *Mol. Gen. Genet.* **205:** 353-357.

Woodcock, D.M., P.J. Crowther, J. Doherty, S. Jefferson, E. DeCruz, M. Noyer-Weidner, S.S. Smith, M.Z. Michael, and M.W. Graham (1989) Quantitative evaluation of *Escherichia coli* host strains for tolerance to cytosine methylation in plasmid and phage recombinants. *Nucleic Acids Res.* **17:** 3469-3478.

Zalkin, H., J.L. Paluh, M. van Cleemput, W.S. Moye, and C. Yanofsky (1984) Nucleotide sequence of *Saccharomyces cerevisiae* genes *TRP2* and *TRP3* encoding bifunctional anthranilate synthase: indole-3-glycerol phosphate synthase. *J. Biol. Chem.* **259:** 3985-3992.

Chapter 3

HARO7 Encodes Chorismate Mutase of the Methylotrophic Yeast *Hansenula polymorpha* and is Derepressed upon Methanol Utilization

Abstract

The *HARO7* gene of the methylotrophic, thermotolerant yeast *Hansenula polymorpha* was cloned by functional complementation. *HARO7* encodes a monofunctional 280 amino acid protein with chorismate mutase (E.C. 5.4.99.5) activity that catalyzes the conversion of chorismate to prephenate, a key step in the biosynthesis of aromatic amino acids. The *HARO7* gene product shows strong similarities to primary sequences of known eukaryotic chorismate mutase enzymes. After homologous overexpression and purification of the 32 kDa protein, its kinetic parameters (k_{cat}=319.1 s^{-1}, n_H=1.56, $[S]_{0.5}$ =16.7 mM) as well as its allosteric regulatory properties were determined. Tryptophan acts as heterotropic positive effector, tyrosine is a negative acting, heterotropic feedback-inhibitor of enzyme activity. The influence of temperature on catalytic turnover and the thermal stability of the enzyme were determined and compared to the chorismate mutase enzyme of *Saccharomyces cerevisiae*. Using the Cre-*loxP* recombination system, mutant strains carrying a disrupted *HARO7* gene were constructed that showed tyrosine auxotrophy and severe growth defects. The amount of the 0.9 kb *HARO7* mRNA is independent of amino acid starvation conditions but increases twofold in the presence of methanol as the sole carbon source implying a catabolite repression system acting on *HARO7* expression.

Introduction

Methylotrophic yeasts have gained increasing recognition in basic research as well as in applied biotechnology in the last few years. Most of them are ascomycetes of the genera *Hansenula*, *Pichia*, and *Candida* (Lee and Komagata, 1980), with *Hansenula polymorpha* (syn. *Pichia angusta*) representing the most prominent member (for review see Hansen and Hollenberg, 1996). Utilization of methanol as sole source of carbon and energy by *H. polymorpha* is generally accompanied by strong proliferation of microbodies, so called peroxisomes, and high-level induction of peroxisomal matrix enzymes required for the C_1 metabolism (Veehuis *et al.*, 1978; Roggenkamp *et al.*, 1984). The first step in the methanol-utilizing pathway is the oxidation of methanol to formaldehyde and H_2O_2, catalyzed by the *MOX*-encoded methanol oxidase (E.C. 1.1.3.13) (Ledeboer *et al.*, 1985). Additional important gene products involved in methanol assimilation are a dihydroxyacetone synthase (E.C. 2.2.1.3) encoded by the *DAS* gene, a catalase (E.C. 1.11.1.6) encoded by the *CAT1* gene, and a formate dehydrogenase activity (E.C. 1.2.1.2) which is the *FMD* gene product (Janowicz *et al.*, 1985; Didion and Roggenkamp, 1992; Hollenberg and Janowicz, 1989). In the presence of glucose, expression of these genes is subject to a repression system, whereas upon methanol utilization the promoters of these genes are strongly induced (Egli *et al.*, 1980). The tightly regulated strength of genes involved in methanol metabolism forms the basis for the biotechnological and commercial use of *H. polymorpha* in recombinant gene expression systems. In recent years, a tractable vector-host-system has been developed using either homologous or heterologous metabolic genes as selectable markers in combination with defined mutant strains and making advantage of the strong promoters of genes being part of the methanol-utilizing machinery (Gellissen *et al.*, 1994; Faber *et al.*, 1995). Integration of autonomously replicating plasmids into the chromosomal DNA can be achieved, yielding up to 100 tandemly repeated copies of the transforming DNA that are mitotically stable in the *H. polymorpha* genome (Janowicz *et al.*, 1991; Gatzke *et al.*, 1995). Additionally, *H. polymorpha* is able to grow at temperatures of up to 48°C, with an optimal temperature for growth of 37°C, which is unusual for methylotrophic yeasts (Levine and Cooney, 1973).

In contrast to the specialized methanol-utilizing pathway of methylotrophic yeasts, biosynthesis of aromatic amino acids is a common feature of most living organisms. Chorismic acid, the end product of the shikimate pathway, is formed in seven invariable enzyme-catalyzed reactions starting with compounds of primary metabolism, erythrose-4-phosphate and phosphoenolpyruvate (Haslam, 1974). Conversion of chorismate to

anthranilate initiates the biosynthetic branch resulting in *L*-tryptophan, whereas intramolecular rearrangement of the enolpyruvyl side chain of chorismate to yield prephenate is the initial step in the synthesis of L-tyrosine and *L*-phenylalanine (Weiss and Edwards, 1980). The latter reaction is unique as it is the only Claisen rearrangement identified so far in primary metabolism (Ganem, 1996). Generally, the conversion of chorismate to prephenate is catalyzed by chorismate mutases (E.C. 5.4.99.5) which have been identified and characterized in archea, bacteria, fungi, and plants (for review see Romero *et al.*, 1995). Crystallographic data of three natural enzymes have led to a classification based on structural elements as well as primary sequence information. AroH class chorismate mutases are α/β-barrel proteins as the trimeric *Bacillus subtilis* enzyme (Chook *et al.*, 1993), whereas the AroQ class comprises all-helix bundle polypeptides that are often part of a bifunctional enzyme like the chorismate mutase domain of the *Escherichia coli* chorismate mutase-prephenate dehydratase activity (Lee *et al.*, 1995). Eukaryotic chorismate mutases are also classified in the latter class on the basis of conservation of crucial catalytic residues and related tertiary structure (Xue *et al.*, 1994; MacBeath *et al.*, 1998). Whereas a number of prokaryotic genes encoding chorismate mutase activities have been cloned to date, only few sequences are available that originate from eukaryotic organisms and code for chorismate mutase enzymes. The best-studied eukaryotic enzyme with respect to structure, allosteric regulation, and mechanism of catalytic turnover is that of the baker's yeast *Saccharomyces cerevisiae* (Schmidheini *et al.*, 1989; Sträter *et al.*, 1997; Schnappauf *et al.*, 1998a; Ma *et al.*, 1998). Recently, additional data for the chorismate mutase enzyme of the filamentous fungus *Aspergillus nidulans* which is encoded by the *aroC* gene have been made available (Krappmann *et al.*, 1999). In comparison with the well-characterized enzyme of *S. cerevisiae*, the *A. nidulans* chorismate mutase was found to be similar in catalytic and structural properties. Nevertheless, different mechanisms for allosteric regulation upon effector binding have been proposed for these two chorismate mutases.

To extend the eukaryotic subclass of AroQ enzymes we here present the cloning and characterization of the *HARO7* gene coding for a chorismate mutase activity of the methylotrophic yeast *H. polymorpha*, an organism quite related to the baker's yeast. *haro7Δ* disruption strains were constructed by establishing the Cre-*loxP* recombination system of bacteriophage P1 (Sternberg and Hamilton, 1981) in this yeast to constitute *HARO7* as a new marker gene to the vector-host expression system of *H. polymorpha* for biotechnological applications (Gellissen *et al.*, 1999). Transcriptional expression patterns of

HARO7 were monitored with respect to different environmental stimuli like amino acid starvation conditions or alternative carbon sources indicating that *HARO7* expression is the target of a catabolite repression system but not of the general control of amino acid biosynthesis. Additionally, the enzyme was overexpressed and purified to homogeneity taking advantage of a *H. polymorpha* expression system. Kinetic assays as well as regulatory analyses of the chorismate mutase indicated that catalytic activity is tightly regulated in an allosterical manner and that this enzyme of *H. polymorpha* has a higher optimal temperature for catalytic turnover than its counterpart from *S. cerevisiae* despite of lower thermal stability.

Experimental procedures

Materials

Chorismic acid and prephenic acid as barium salts were purchased from SIGMA (St. Louis, MO, USA). 5-Fluoroorotic acid was obtained from TORONTO RESEARCH CHEMICALS INC. (Toronto, Canada). *L*-Tyrosine for supplementation was obtained as free base (SigmaUltra, >99% (TLC)) from SIGMA-ALDRICH Chemie GmbH (Steinheim, Germany) and alternatively from FLUKA (Neu-Ulm, Germany) in BioChemika grade (>99% (NT), foreign amino acids <0.3%). Protein solutions were concentrated by using stirred cells (volumes of 180 ml and 10 ml) with PM-10 ultrafiltration membranes from MILLIPORE (Eschborn, Germany). The Mini 2D SDS-polyacrylamide gel electrophoresis system and the Bradford protein assay solution for determination of protein concentrations originated from BIO-RAD LABORATORIES (Hercules, CA, USA). PLATINUM *Pfx* DNA polymerase from LIFE TECHNOLOGIES GmbH (Karlruhe, Germany) was used for PCR reactions.
All other chemicals were supplied by FLUKA or SIGMA-ALDRICH Chemie GmbH.

Strains, media, growth conditions, and transformation procedures

Plasmid DNA was propagated in *E. coli* strain DH5α (Woodcock *et al.*, 1989). The *S. cerevisiae* strain RH2185 (*MATa, suc2-Δ9, ura3-52, leu2-3, leu2-112, his4-519, aro7::LEU2, GAL2*) (Schnappauf *et al.*, 1997) with the genetic background of the laboratory strain X2180-1A (*MATa, gal2, SUC2, mal, CUP1*) was used as recipient for cloning of a DNA fragment containing the *HARO7* gene of *H. polymorpha* from a genomic library. The uracil-auxotrophic *H. polymorpha* strain RB11 (*odc1*) was obtained from RHEIN BIOTECH GMBH (Düsseldorf, Germany) and has been described by Weydemann *et al.* (1995). *H. polymorpha* strain RH2408 (*odc1*, ^{p}*FMD::HARO7*, *URA3*) was used for homologous overexpession and purification of the *HARO7* gene product. Mutant strains RH2409 (*odc1*, *haro7::loxP-ODC1MX-loxP*) and RH2410 (*odc1*, *haro7::loxP*) are derivatives of *H. polymorpha* strain RB11 carrying a disrupted *HARO7* gene. *E. coli* cells were grown in LB medium (Maniatis *et al.*, 1982) supplemented with 100 $\mu g \cdot ml^{-1}$ ampicillin at 37°C. Complex medium for growth of yeasts was YEPD (1% yeast extract, 2% peptone, 2% glucose). Selective medium contained 0.14% yeast nitrogen base (w/o amino acids and w/o ammonium sulphate) and 0.5% ammonium sulfate. Carbon sources were either 2% glucose, 1% glycerol or 0.7% methanol. Supplements were added according to Guthrie and Fink (1991). In contrast to *S. cerevisiae*, which was cultivated at 30°C,

H. polymorpha strains were propagated at 37°C which is the optimal temperature for growth of this yeast. Transformation of *E. coli* was performed as described by Inoue *et al.* (1990). *S. cerevisiae* was transformed following a modified protocol of Elble (1992). For transformation of *H. polymorpha* an electroporation procedure was used (Faber *et al.*, 1994).

Isolation and analyses of nucleic acids

For isolation of plasmid DNA from bacterial strains the plasmid purification system from QIAGEN (Hilden, Germany) was used. Genomic DNA from yeasts was isolated according to Hoffmann and Winston (1987) and analyzed by Southern blot (Southern, 1975) or diagnostic PCR (Saiki *et al.*, 1985) using oligonucleotides OLSK57 (5´-CAATGCCAGCAATATGGAGACG-3´) and RP1 (5´-GAACTAGAATTCGAG AATAATTAAAG-3´). Total RNA from *H. polymorpha* cultures was prepared according to Cross and Tinkelenberg (1991) and transcript levels were determined by Northern hybridization (Rave *et al.*, 1979) using a Bio-Imaging Analyzer from Fuji Photo Film Co. Ltd. (Tokyo, Japan). Transcript length was determined using the 0.16-1.77-kb RNA ladder from LIFE TECHNOLOGIES, INC.. Sequencing reactions were carried out using a BigDye™ sequencing kit (Heiner *et al.*, 1998) and analyzed on an ABI PRISM® 310 Genetic Analyzer (PE BIOSYSTEMS, Foster City, CA, USA).

Cloning techniques, construction of genomic library and plasmids

Standard techniques for cloning and manipulation of recombinant DNA were applied (Maniatis *et al.*, 1982). For identification of the *HARO7* gene, a genomic library was constructed by ligating partially *Sau*3A-digested DNA of *H. polymorpha* strain RB11 in the *Bam*HI restriction site of shuttle vector pRS426 (Sikorski and Hieter, 1989). The ligation products were transformed in *E. coli* to yield a library pool of approximately 100 000 independend clones from which plasmid DNA was isolated. Plasmid pME1524 contains a 5 kb genomic *Sau3*A fragment containing the *HARO7* gene of *H. polymorpha* strain RB11 in pRS426. By subcloning, plasmid pME1525 was generated which carries a 1.8 kb *Apa*I/*Hin*dIII fragment, originating from pME1524, in pRS426. For working purposes, plasmid pME1526 was constructed which carries the 1.8 kb *Apa*I/*Hin*dIII fragment of pME1524 in the bacterial plasmid pBluescript II KS from STRATAGENE (La Jolla, CA, USA). Overexpression of the *HARO7* gene product in RB11 was achieved using plasmid pME1686. This plasmid carries the entire open reading frame of *HARO7* amplified from pME1525 using oligonucleotides OLSK50 (5´-TATAGAATTCATGGACTTTATGA

AGCC-3´, *Eco*RI site underlined) and RP1 in a polymerase chain reaction; the resulting *Eco*RI fragment was cloned in the expression vector pFPMT121 obtained from RHEIN BIOTECH GMBH to yield a ^{p}*FMD::HARO7::MOX*^{t} expression cassette in a plasmid autonomously replicating in *H. polymorpha*. For characterization of a *haro7Δ* mutant strain, a disruption cassette was constructed. Therefore, the 5‘ flanking sequence of *HARO7* was amplified from pME1524 using OLSK34 (5´-ATATAGATCT ACAAAAACTAAACAGG-3´, *Bgl*II site underlined) as reverse primer and cloned as 2 kb *Sal*I/*Bgl*II fragment. The 3‘ region flanking *HARO7* was cloned as 2.5 kb *Bgl*II/*Not*I fragment amplified in a polymerase chain reaction with OLSK35 (5´-ATATAGATCTGATGCGACGCAGAAAAGC-3´, *Bgl*II site underlined) as forward primer using a partial *Bgl*II genomic sublibrary of RB11 cloned in pBluescript II KS (*Bam*HI) as template. Both flanking regions were cloned in the plasmid pBluescript II KS (*Sal*I/*Not*I) to yield vector pME1687. A *loxP-ODC1MX-loxP* cassette as 1.6 kb *Bam*HI fragment was cloned in the *Bgl*II site of this disruption vector. This cassette was constructed from plasmid pUG-ODC1 and is a derivative of the *loxP-kanMX-loxP* module (Güldener *et al.*, 1996) where the *kan*^{r} gene was replaced by the *ODC1* gene of *H. polymorpha*. The resulting vector from which a 6 kb disruption cassette was released by *Kpn*I digestion is pME1688. For forcing recombination between the *loxP* sites in strain RH2409, plasmid pME1690 was used which carries the coding sequence of the Cre recombinase (Sternberg *et al.*, 1986) as PCR fragment fused to the *FMD* promoter as well as the *HARO7* gene as *Eco*72I/*Ssp*I fragment cloned in the *Sma*I site of pFPMT121. Plasmid pME1689 carries part of the coding region (exon III) of the *ACT* gene from *H. polymorpha* DL1-L (Hong *et al.*, 1998) as *Bam*HI/*Sca*I fragment.

Overexpression and purification of *H. polymorpha* chorismate mutase

H. polymorpha strain RH2408 (*odc1*, ^{p}*FMD::HARO7*, *URA3*) generally was grown at 37°C as shake flask (750 ml) culture in YNB supplemented with 3% glycerol as sole carbon source for *FMD* promoter derepression. Cells were harvested at an OD_{546nm} of 7-8, washed twice with 50 mM K-phosphate buffer, pH 7.6 and stored in 1 ml buffer per g wet cells at -20°C in the presence of protease inhibitors (0.1 mM phenylmethyl-sulfonylfluoride (PMSF), 0.2 mM ethylenediaminetetraacetate (EDTA) and 1 mM DL-dithiothreitol (DTT)). For purification, 20-30 g of cells were thawed and run three times through a French Pressure Cell (18,000 psi). Cell debris was sedimented by centrifugation at 30,000xg for 20 min. The chorismate mutase enzyme was purified as described by Schmidheini *et al.* (1990a) with the modification that for buffer changing or desalting pooled fractions after

the first anion exchange run, gelfitration on a Superdex 75pg column was applied. Chorismate mutase was detected by SDS-PAGE (Lämmli, 1970) and by enzymatic activity assays. Native PAGE was performed as described by Anderson *et al.* (1972) using a gradient of 4 to 15% polyacrylamide. Measurements of protein concentrations were performed applying the Bradford assay (Bradford, 1976).

Enzyme assays and data evaluation

Chorismate mutase activity was measured as described previously (Schmidheini *et al.*, 1990a). Enzymatic reactions were carried out at 37°C, as effector concentrations in substrate saturation assays 100 μM tyrosine or 10 μM tryptophan were chosen. Enzymatic activity was measured spectrophotometrically determining the concentration of phenylpyruvate. Since absorbance of phenylpyruvate is temperature-dependent due to a keto-enol equilibrium, the assay was standardized by keeping the spectrophotometer cell at 30°C. Evaluation of kinetic data was performed as described before (Krappmann *et al.*, 1999, and references therein). Thermal stabilities were determined according to Segel (1975) and DAHP synthase activities were measured as described by Teshiba *et al.* (1986).

Sequence alignments

Sequence analyses were performed using the LASERGENE Biocomputing software from DNASTAR (Madison, WC, USA). Alignments were created based on the Lipman-Pearson method (Lipman and Pearson, 1985).

Results

The *HARO7* gene of *Hansenula polymorpha* codes for a chorismate mutase enzyme

The *HARO7* gene from the methylotrophic yeast *H. polymorpha* was cloned by functional complementation of a *Saccharomyces cerevisiae aro7Δ* mutant strain. Strains of *S. cerevisiae* with a deleted *ARO7* gene are devoid of endogenous chorismate mutase activity and generally are unable to grow on medium lacking tyrosine or phenylalanine. The baker's yeast strain RH2185 (*aro7::LEU2*, *ura3-52*) (Schnappauf *et al.*, 1997) was transformed with genomic DNA of *H. polymorpha* strain RB11 (*odc1*) (Weydemann *et al.*, 1995) cloned into the high copy plasmid pRS426 (Sikorski and Hieter, 1989). Transformants were selected for viability on minimal medium YNB lacking tyrosine and phenylalanine. One colony appeared after 5 days of growth. A plasmid (pME1524) isolated from this clone was able to complement the auxotrophy of the recipient *aro7Δ S. cerevisiae* strain. Growth of the recipient strain harboring this plasmid was retarded compared to the positive control. Restriction analysis of this plasmid indicated that it contained a genomic DNA insert of 5 kb in length. Subcloning of this fragment revealed a 1.7 kb *Apa*I/*Sau*3A fragment that was able to complement the Tyr/Phe auxotrophy of *S. cerevisiae* strain RH2185 when recloned into pRS426. The recipient strain transformed with this subclone plasmid (pME1525) grew at a rate similar to that of a *S. cerevisiae* wild-type strain. The DNA insert of pME1525 was subject to sequence analyses. The genomic sequence is 1648 bp in length and includes an open reading frame of 843 bp with 281 codons with the capacity to encode a polypeptide with a calculated M_r of 32067. The 5´ flanking region of the genomic fragment spans 342 nucleotides whereas the 3´ region is 467 bp in length. The GenBank accession number for this sequence is AF204738. Conserved splicing motifs described for yeast (Rymond and Rosbach, 1992) are not present within the coding region of the identified gene, indicating the absence of any intron sequences. Upon alignment the deduced amino acid sequence of the gene indicated homology to genes of known chorismate mutases of other eukaryotic organisms by the high rate of similarities of amino acid residues (Fig. 12).

The best alignment was to the enzyme of the baker's yeast *S. cerevisiae* with 54% identity and 70% similarity when conservative changes are taken into account. With the described primary sequence of chorismate mutase from *Schizosaccharomyces pombe* 43% identities are shared and 63% similar residues including conservative replacements. Comparison to chorismate mutase of the filamentous fungus *Aspergillus nidulans* revealed

43% identity and 65% similarity. The plastidic chorismate mutase of *Arabidopsis thaliana* is less related. The deduced amino acid sequence is 35% identical to the mature plant enzyme and 58% similar when conservative exchanges are included. Due to this strong similarities to described chorismate mutases and the functional complementation of a chorismate mutase-deficient *S. cerevisiae* strain, the isolated gene from *H. polymorpha* was named *HARO7* with respect to the homologous *ARO7* gene of *S. cerevisiae*.

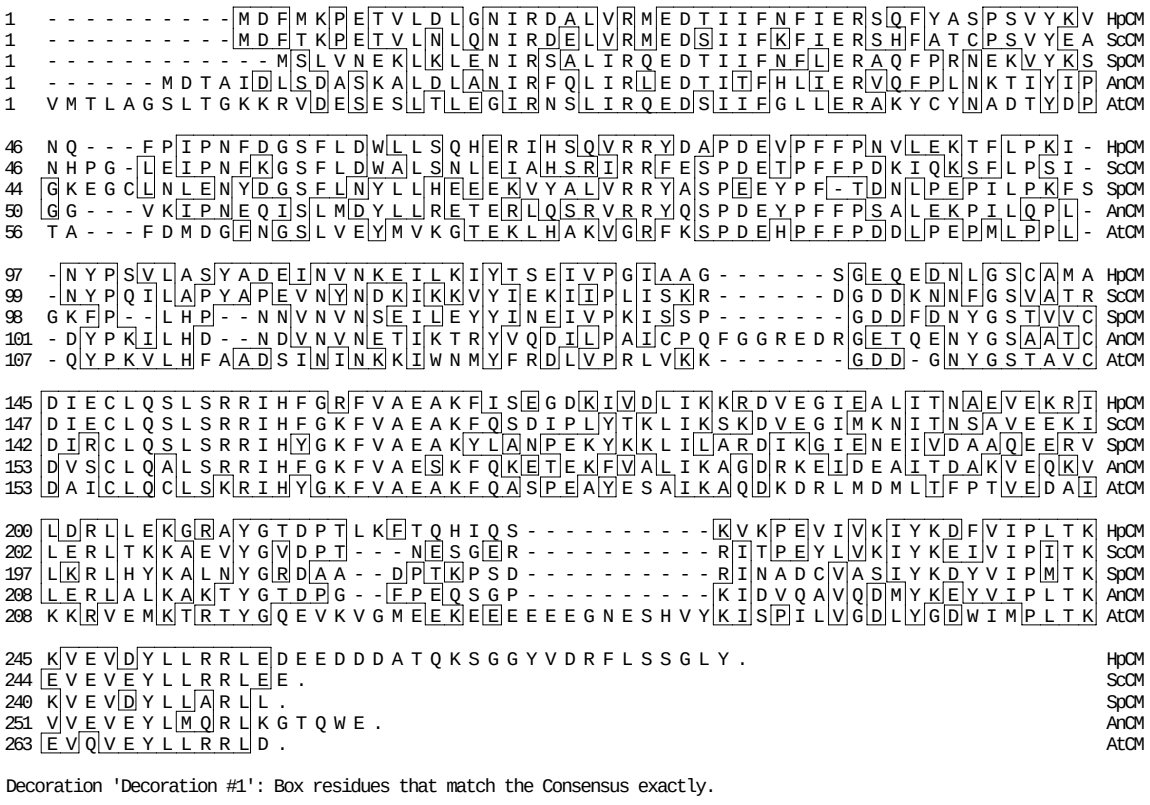

Figure 12: Multiple sequence alignment of deduced eukaryotic chorismate mutases including the amino acid sequence of *Hansenula polymorpha* chorismate mutase. The source of each sequence is as follows: HpCM, *Hansenula polymorpha* (Acc. No. AF204738); ScCM, *Saccharomyces cerevisiae* (Acc. No. M24517) (Schmidheini *et al.*, 1989); SpCM, *Schizosaccharomyces pombe* (Acc. No. Z98529) (Oliver *et al.*, 1995); AnCM, *Aspergillus nidulans* (Acc. No. AF133241) (Krappmann *et al.*, 1999); AtCM, *Arabidopsis thaliana*, mature plastidic enzyme (Acc. No. Z26519) (Eberhard *et al.*, 1993). Conserved residues are boxed.

Disruption of *HARO7* in *H. polymorpha* results in tyrosine auxotrophy

Gene replacement mutant strains were constructed via homologous integration to characterize the *HARO7* gene in more detail (Fig. 13A). Therefore, *H. polymorpha* strain RB11 was transformed with a disruption cassette consisting of a *loxP-ODC1MX-loxP* module flanked by 5´ and 3´ homologous sequences of the *HARO7* locus. In this construct, 93% of the *HARO7* coding sequence is replaced by the marker cassette expressing orotidine-5´-phosphate decarboxylase which is encoded by the *ODC1* gene (Merckelbach *et al.*, 1993). Transformants were selected on minimal medium supplemented with tyrosine and phenylalanine but lacking uracil. Auxotrophic mutants were identified by replica plating on minimal medium without supplements. Out of approximately 1000 Ura^+ transformants, five independent, auxotrophic clones were isolated, in line with the low frequency of homologous recombination reported previously for *H. polymorpha* (Faber *et al.*, 1992). Retransformation with a DNA fragment comprising the *HARO7* coding sequence restored prototrophy of these strains whereas in negative control experiments no transformants were able to grow. A descendant without the *ODC1* expression cassette was obtained from one of these clones (RH2409) taking advantage of the *loxP* recombination sites in the disruption construct (Sauer, 1987). For this purpose, *H. polymorpha* strain RH2409 was transformed with the autonomously replicating plasmid pME1690 carrying the *cre* coding sequence inserted between the inducible *FMD* promoter and the *MOX* termination region and the *HARO7* coding sequence as a marker gene in addition to the *S. cerevisiae URA3* gene. Transformants were selected on minimal medium and propagated for 24 hours on glycerol-containing medium to derepress expression of the Cre recombinase driven by the *FMD* promoter. Cured clones in which the *ODC1* cassette had been removed by forced homologous recombination between the flanking *loxP* sites were counterselected on supplemented medium in the presence of 5-fluoroorotic acid (Boeke *et al.*, 1987). One strain (RH2410) isolated by this procedure showed uracil auxotrophy.

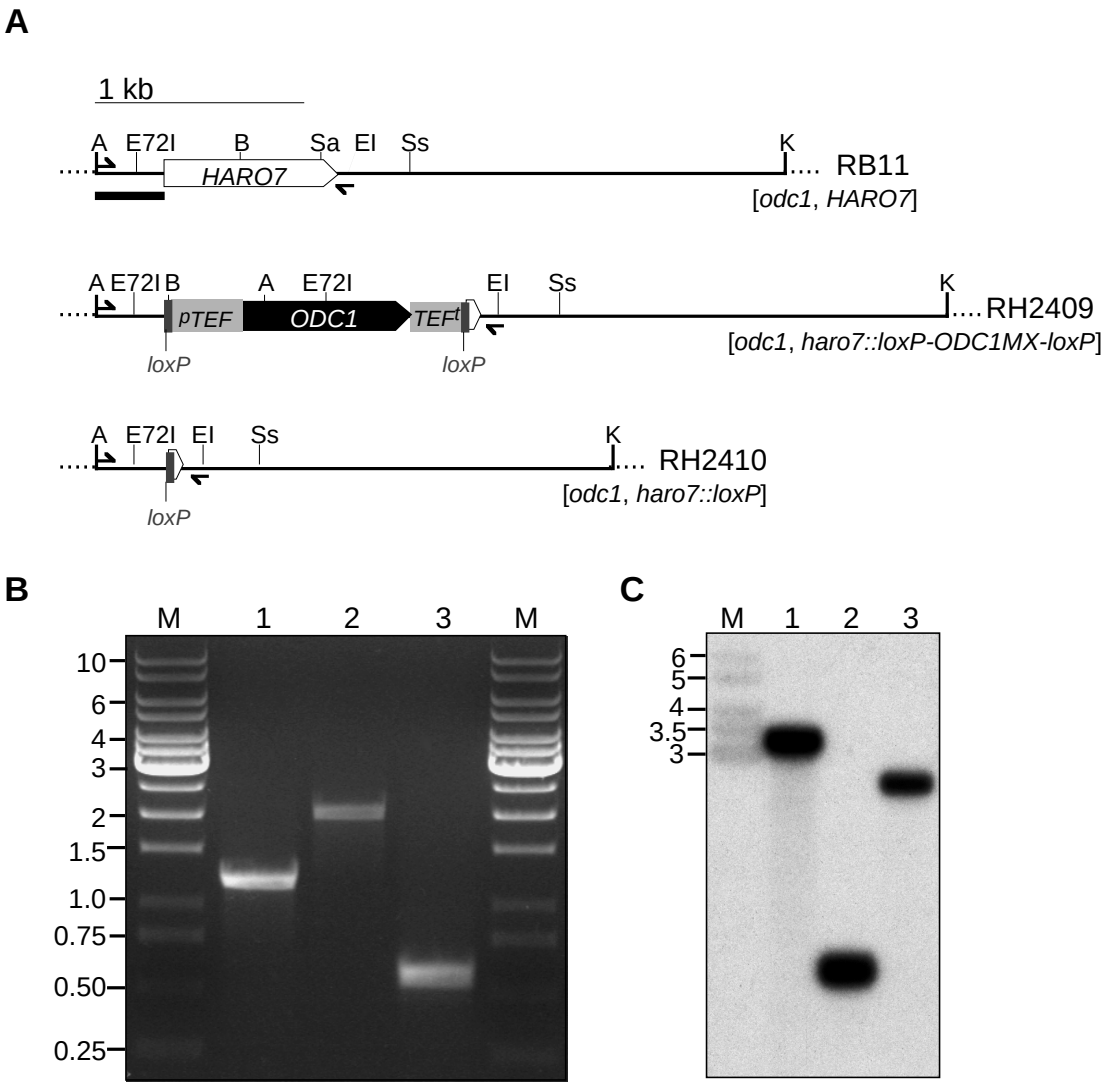

Figure 13: Construction of *haro7Δ* mutant strains of *H. polymorpha* using the Cre-*loxP* recombination system. *A*, Physical maps of the *HARO7* locus and of the *haro7::loxP-ODC1MX-loxP* and *haro7::loxP* loci. Coding sequences of *HARO7* and *ODC1*, respectively, are schematically drawn as tipped boxes, promoter and termination sequences of the *TEF2* gene from Ashbya gossypii as light gray boxes, and *loxP* sites are marked in dark gray. Primer positions chosen for diagnostic PCR are indicated by half arrows. The horizontal bar represents the *HARO7* promoter-specific probe used in Southern analysis. A, *Apa*I; B, *Bgl*II; E, *Eco*RI; E72I, *Eco*72I; K, *Kpn*I; Sa, *Sal*I; Ss, *Ssp*I. *B*, Diagnostic PCR on genomic DNA of H. polymorpha wt-*HARO7* strain RB11 (lane 1) and *haro7Δ* mutant strains RH2409 (lane 2) and RH2410 (lane 3) with *HARO7*-specific 5´ and 3´ oligonucleotides. M, marker DNA fragments of the indicated size in kilobases. *C*, Southern hybridization of a specific *HARO7* promoter probe on *Apa*I/*Kpn*I-digested genomic DNA of strains RB11 (lane 1), RH2409 (lane 2), and RH2410 (lane 3). M, Unspecifically hybridizing DNA marker fragments with the indicated length in kilobases.

The correct genotype of both *haro7Δ* mutant strains was confirmed by diagnostic PCR with oligonucleotides specific for *HARO7* 5´ and 3´ flanking regions (Fig. 13B). Whereas in the *H. polymorpha* wt-*HARO7* strain RB11 a 1.2 kb fragment was amplified from genomic DNA, insertion of the *loxP-ODC1MX-loxP* cassette resulted in a 2 kb amplicon. Removal of the *ODC1* expression cassette in strain RH2410 was indicated in the PCR approach by amplification of a 0.5 kb DNA fragment. In Southern analysis a *HARO7* promoter-specific probe was hybridized to *Apa*I/*Kpn*I-digested genomic DNA of the *H. polymorpha* strains RB11, RH2409, or RH2410 (Fig. 13C). For RB11 a 3.2 kb signal corresponding to the wild-type *HARO7* locus was observed. Insertion of the marker module introduced an additional *Apa*I site in RH2409, therefore the hybridizing signal was shortened to a size of 0.8 kb. Due to the removal of this *Apa*I site within in the *ODC1* gene, a 1.6 kb signal was detected in Southern analysis of RH2410. As expected, the *haro7Δ* strains showed no growth on solid, non-supplemented medium but grew on minimal medium supplemented with standard concentrations of tyrosine, phenylalanine, and uracil. No growth was observed on complex medium YEPD even in the presence of tyrosine and phenylalanine or on synthetic complete medium. Surprisingly, both strains grew slowly but reproducibly on minimal medium containing tyrosine as sole amino acid. Therefore, the *haro7Δ* mutant strains of *H. polymorpha* are auxotrophic for the aromatic amino acid tyrosine but bradytrophic for phenylalanine. In liquid cultures of minimal medium, retarded growth was only observed when tyrosine was added at 5 times the concentration used for supplementation in solid medium. In summary, both mutant strains showed growth defects that depended on the composition of the growth medium, indicating the importance of chorismate mutase activity for growth of *H. polymorpha*. This is supported by the fact that strains retransformed with the *HARO7* coding sequence, either as a linear DNA fragment or on a plasmid, did not show any of the growth defects described above and were able to grow on complex medium.

HARO7 expression is regulated transcriptionally upon methanol utilization but not upon amino acid starvation

In silico analysis of the flanking 5´ region of *HARO7* identified two sequence elements that resemble conserved binding sites for yeast transcription factors. One motif (5´-CACGTG-3´, position -140 to -135 relative to the translational start codon AUG) matches a binding site for Pho4p (5´-CANNTG-3´) (Fisher and Golding, 1992), the ultimate effector for phosphate utilization in *S. cerevisiae*. Additionally, an upstream regulatory sequence specific for *H. polymorpha* was identified in the *HARO7* promoter region. This sequence

element (5´-TTGCCACCGGAA-3´, position -275 to -264) is similar to the core region of a binding site for Mbf1p (5´-TTGCACCGCAA-3´) within the promoter of the *MOX* gene encoding the peroxisomal methanol oxidase of this methylotrophic yeast (Ledeboer *et al.*, 1985; Gödecke *et al.*, 1994). A similar motif is also found in the promoter of the *H. polymorpha CAT1* gene which codes for a peroxisomal catalase (5´-TCGCACCGCAA-3´) (Didion and Roggenkamp, 1992). In contrast, no conserved sequence elements directing 3´ end formation were identified in the *HARO7* gene fragment of pME1525. The putative Mbp1p-binding element in the *HARO7* promoter region implies a transcriptional regulation of *HARO7* expression upon methanol utilization. To monitor transcription of the *HARO7* gene, steady-state transcript levels were quantified in Northern hybridization analyses. The length of the *HARO7*-encoded mRNA was determined using an RNA size standard as approximately 0.9 kb (not shown). *HARO7* transcription was monitored with respect to availability of different carbon sources using expression of the *ACT* gene of *H. polymorpha* as internal standard (Fig. 14). Therefore, RB11 was cultured in minimal medium containing glycerol as a non-fermentable carbon source or methanol as inducer of the methanol-utilizing metabolic pathway in *H. polymorpha* (Eggeling and Sahm, 1981). Cells were harvested at mid-exponential phase of growth and 4 or 8 hours later for total RNA preparation. In addition, glucose was added to identical cultures grown in the presence of glycerol or methanol, respectively, and cultivation was continued for 4 and 8 hours prior to RNA preparation. Northern analysis using *ACT* transcript levels as internal standard revealed different expression patterns of *HARO7* transcription. Transcript levels increased slightly but reproducibly when cells were grown in glycerol-containing medium. Furthermore, methanol as carbon source had a more pronounced effect on *HARO7* transcription with transcript levels increasing by a factor of two compared to glucose-grown cells. These effects induced by the non-optimal carbon sources were diminished when glucose was added to the medium, implying repression of *HARO7* transcription.

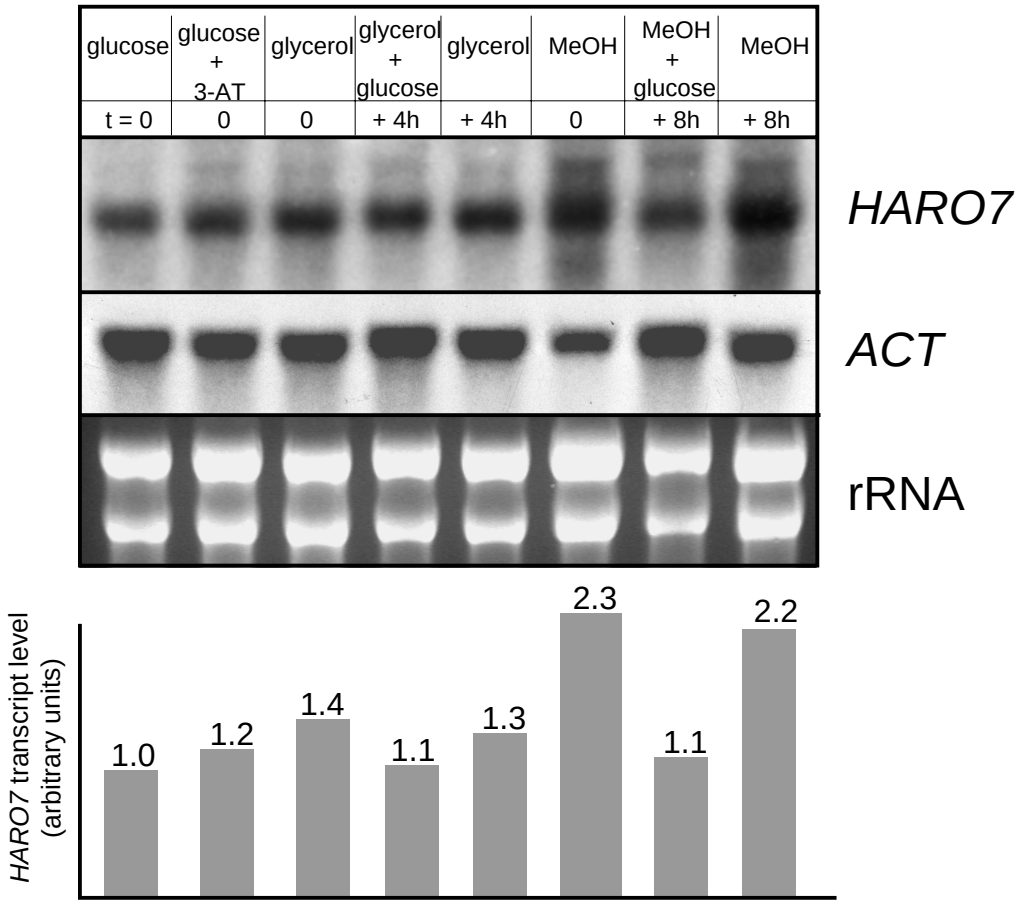

Figure 14: Expression pattern of *HARO7* under amino acid starvation conditions or in the presence of different carbon sources. *H. polymorpha* strain RB11 was grown in minimal medium containing glucose (lane1), glucose and 1 mM 3-amino-1,2,4-triazole (3-AT, lane 2), glycerol (lane 3), or methanol (MeOH, lane 6) to mid-log phase (OD_{546nm} ≈ 1.2, t=0) and total RNA was prepared. Additionally, glucose was added to cultures of RB11 grown in glycerol and methanol medium, respectively, and incubation was continued for 4 or 8 hours (lanes 4 and 7) before RNA preparation. As control, RNA was prepared from cultures after prolonged cultivation in the absence of additional glucose (lanes 5 and 8). For Northern analysis 20 µg total RNA each was loaded and probed successively with probes specific for *HARO7* and *ACT* of *H. polymorpha.* Ethidium bromide-stained total RNA is included as control. Quantified steady state levels of *HARO7* transcripts are shown in the histogram after standardization with respect to *ACT* transcript levels. The values are averages of two independent experiments with a standard deviation not exceeding 20%.

Chorismate mutase is a key enzyme in aromatic amino acid biosynthesis. Therefore transcript levels of *HARO7* mRNA were quantified under conditions of amino acid starvation. *H. polymorpha* strain RB11 was grown in minimal medium supplemented with the false feedback-inhibitor 3-amino-1,2,4-triazole (3-AT) at 1 mM to induce histidine

starvation and to derepress the general control system of amino acid biosynthesis (Hilton *et al.*, 1965; Bode *et al.*, 1990). Specific DAHP synthase activities (EC 4.1.2.15) determined in crude extracts of RB11 grown in the absence or presence of 3-AT, respectively, were used as a control and showed an increase by a factor of two (data not shown), indicating that the general control of amino acid biosynthesis had been induced by the false feedback-inhibitor (Teshiba *et al.*, 1986). The specific chorismate mutase activity was unaffected by the absence or presence of 3-AT (data not shown). Total RNA was prepared from cultures in mid-log phase (OD_{546nm}≈1.2) and subjected to Northern analysis. Quantification of signal strength revealed no significant increase of *HARO7* transcript levels after the shift to starvation conditions (Fig. 14). We conclude, therefore, that *HARO7* transcription is not triggered by the general control system of amino acid biosynthesis.

Chorismate mutase of *H. polymorpha* is allosterically regulated by tyrosine and tryptophan

The *HARO7* gene product is a key enzyme in the biosynthesis of aromatic amino acids. Chorismate mutase activity has to be regulated stringently to control the flux through the branch-point. As no regulation of expression is evident with respect to amino acid availability, we were interested to see whether certain amino acids might influence catalytic activity. To determine its enzymatic properties the *HARO7* gene product was overproduced and purified. The *HARO7* coding sequence was cloned into the expression vector pFPMT121 where it is fused to the promoter of the *H. polymorpha FMD* gene coding for formate dehydrogenase (Hollenberg and Janowicz, 1989) and flanked by the termination region of the *MOX* gene (Ledeboer *et al.*, 1985). *H. polymorpha* strain RB11 was transformed with this expression plasmid (pME1686) and sequentially grown in selective and rich medium to obtain mitotically stable transformants (Gatzke *et al.*, 1995). One clone (RH2408) analyzed by Southern hybridization was identified to harbor approximately 50 copies of the expression construct ectopically integrated into the genome of the host strain (data not shown). Cultivation in minimal medium containing glycerol as sole carbon source derepressed the *FMD*-driven expression of *HARO7*. The resulting chorismate mutase activity was purified to homogeneity from this overexpressing strain by the purification procedure described in Experimental Procedures (Fig. 15A, B). In a gradient PAGE under nondenaturating conditions, the purified protein displayed an apparent molecular mass of approximately 70 kDa (Fig. 15A). This indicates that the native enzyme consists of two protomers combined to form a dimeric quaternary structure. Kinetic stop assays for determination of catalytic parameters were performed at 37°C which is the optimal

temperature for growth of *H. polymorpha* (Fig. 15C, Table III). In the absence of effectors the enzyme showed positive cooperativity towards its substrate chorismate resulting in a sigmoid substrate saturation curve. A $[S]_{0.5}$ value of 16.7 mM and a maximal turnover rate of 319.1 s^{-1} per active site were determined. The calculated Hill coefficient n_H of 1.56 clearly supports positive cooperativity. Additionally, the regulatory properties of the enzyme were determined by kinetic assays in the presence of allosteric effectors. Tryptophan at 10 µM concentration acts as strong heterotropic positive effector on enzymatic activity. A break-down of cooperativity was observed (n_H=0.97) resulting in a Michaelis-Menten-type kinetic with a K_m of 1.6 mM and a maximum turnover value of 303.8 s^{-1}. In contrast, tyrosine acts as inhibitor of chorismate mutase activity: the turnover rate decreased to 89.3 s^{-1} and a $[S]_{0.5}$ value of 12.0 mM was calculated at a concentration of 100 µM of this heterotropic effector. A Hill coefficient of 1.32 indicates retained cooperativity.

In summary, the *HARO7*-encoded chorismate mutase enzyme of *H. polymorpha* is strictly regulated in its activity. Whereas *HARO7* transcription is constitutive with respect to amino acid starvation and derepressed in the presence of methanol, catalytic turnover is triggered in an allosterical manner by homotropic and heterotropic effectors specific for the biosynthetic pathway of aromatic amino acids.

TABLE III: **Kinetic parameters of chorismate mutase enzyme from *Hansenula polymorpha*.** Values for k_{cat}, K_m, and $[S]_{0.5}$ were defined by fitting initial velocity data to equations describing hyperbolic or cooperative saturation, respectively. Hill coefficients (n_H) were calculated from Hill plots by linear regression.

	Inhibited (100 µM tyrosine)			Unliganded			Activated (10 µM tryptophan)		
	k_{cat} (s^{-1})	$[S]_{0.5}$ (mM)	n_H	k_{cat} (s^{-1})	$[S]_{0.5}$ (mM)	n_H	k_{cat} (s^{-1})	K_m (mM)	n_H
	89.3	12.0	1.32	319.1	16.7	1.56	303.8	1.6	0.97
k_{cat} / K_m ($mM^{-1}\cdot s^{-1}$)		7.44			19.1			188.1	

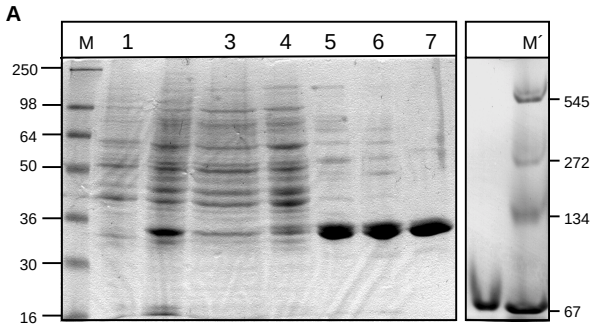

raction	total protein (mg)	spec. activity (U·mg^{-1})	ield (%)	purification (x-fold)
crude extract	127	9.7	100	
ammonium sulfate	55	17.3	77	1.8
ethylamino sepharose	24	36.3	71	3.7
1st MonoQ (HR 16/10)	4.4	66.1	24	6.8
2nd MonoQ (HR 5/5)	2.6	87.4	18	9.0
Superdex 200pg	0.5	168	7	17

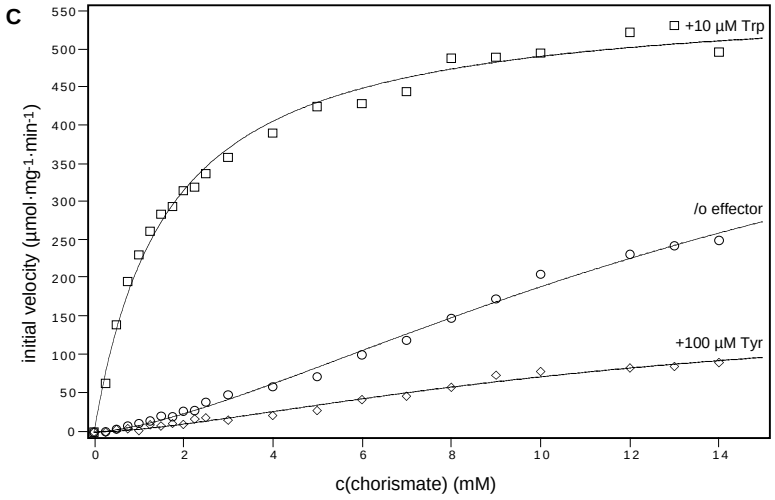

Figure 15: Purification of chorismate mutase of *H. polymorpha* and enzymatic properties. *A*, SDS-polyacrylamide gel of the purification of chorismate mutase of *H. polymorpha*, Haro7p. M, Marker proteins with the indicated molecular mass in kilodaltons; 1, crude extract of RB11; 2, crude extract of RH2409; 3, supernatant of ammonium sulfate precipitation; 4, ethylamino sepharose pool; 5, first MonoQ pool; 6, second MonoQ pool; 7, Superdex 200pg pool. 5 µg of total protein was loaded on each lane. *B*, Purification protocol for *H. polymorpha* chorismate mutase. Enzyme assays were performed in the presence of 500 µM tryptophan, 1 mM chorismate was used as substrate concentration, and catalytic turnover was carried out for 10 minutes. *C*, Substrate saturation plot of enzyme assays. *H. polymorpha* chorismate mutase was assayed with 10 µM tryptophan (squares), without effector (circles), or in the presence of 100 µM tyrosine (diamonds). The data were fitted to functions describing cooperative or Michaelis-Menten-type saturation. Specific activities are mean values of at least five independent measurements with a standard deviation not exceeding 20%.

Unliganded *H. polymorpha* chorismate mutase shows a higher optimal temperature for catalytic turnover than its *S. cerevisiae* counterpart despite lower thermal stability

Kinetic stop assays with the unliganded enzyme were carried out to characterize the temperature profile of catalytic activity of the *HARO7*-encoded chorismate mutase and purified yeast chorismate mutase from *S. cerevisiae* was subjected to identical assays for comparison (Fig. 16A). For the enzyme derived from the thermotolerant yeast *H. polymorpha* maximum enzymatic activity was achieved at a temperature of 48°C. In comparison, the *S. cerevisiae* enzyme shows a decrease in catalytic turnover at temperatures higher than 38°C. With respect to the different maxima of catalytic turnover at elevated temperatures we were interested in the stability of both enzymes upon incubation at different temperatures. To determine the rate constants in the decrease of catalytic activity due to irreversible denaturation, aliquots of both enzymes were preincubated different time periods at respective temperatures before residual chorismate activity was determined in stop assays at low temperature with 2 mM substrate concentration and no effectors present (Fig. 16B). Both enzymes displayed thermal stability at 37°C. After preincubation at 50°C a decrease in catalytic activity was determined for the *H. polymorpha* chorismate mutase with a calculated half-life ($t_{1/2}$) at this temperature of approximately 8 minutes. At 55°C the $t_{1/2}$ decreased to a value of 2 minutes and in preincubation experiments at 60°C catalytic activity displayed a significant decrease over the recorded time period with a $t_{1/2}$ of nearly 1 minute. For the *S. cerevisiae* chorismate mutase $t_{1/2}$ values of 7 minutes and 2.74 minutes were determined at 55°C and 60°C, respectively. After pre-incubation at 65°C also for this enzyme a sharp drop in catalytic activity was observed with a deduced $t_{1/2}$ of 13 seconds. In conclusion, the chorismate mutase of *H. polymorpha* diplays a lower thermal stability in comparison to its *S. cerevisiae* homologue as deduced from the higher rate constants of inactivation at respective temperatures.

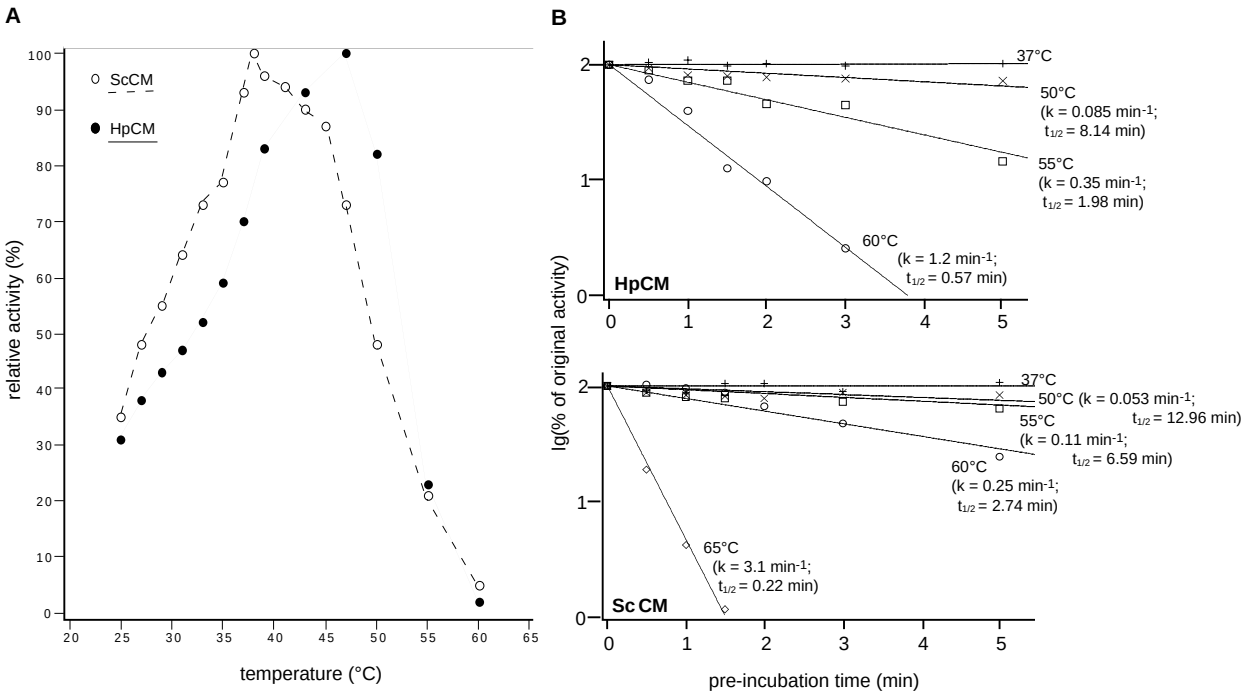

Figure 16: Temperature profiles and thermal stabilities of chorismate mutases from *H. polymorpha* and *S. cerevisiae*. *A,* Determination of optimum temperatures for catalytic turnover. Catalytic activities were quantified with purified chorismate mutase enzymes of *S. cerevisiae* (ScCM, open circles) and of *H. polymorpha* (HpCM, filled circles) in the absence of effectors. Enzyme samples in buffer were pre-incubated for 5 minutes at the respective temperature before chorismate was added to a final concentration of 1 mM to start catalytic turnover. Reactions were stopped after 10 minutes. Each measurement was performed twice with a standard deviation not exceeding 20%. 100% activity equals 13.1 U ($\mu mol \cdot mg^{-1} \cdot min^{-1}$) for ScCM and 5.6 U for HpCM, respectively. *B,* Analysis of rate constants for thermal inactivation. Enzyme samples of purified chorismate mutase of *H. polymorpha* (HpCM, upper panel) and of *S. cerevisiae* (ScCM, lower panel) were pre-incubated in the absence of effectors for different time periods at the respective temperature, chilled on ice and residual activities were determined in stop assays at 37°C (HpCM) and 30°C (ScCM), respectively, with 2 mM substrate concentration and 2 minutes catalytic turnover after 1 min incubation at the respective assay temperature. 100% of original activity equals 49.8 U for ScCM and 15.4 U for HpCM, respectively, and each measurement was performed twice with a standard deviation not exceeding 20%.

Discussion

Chorismic acid, the formerly 'elusive branch-point compound' (Gibson, 1999) is an intermediate of several metabolic pathways, like biosynthesis of ubiquinone and other quinones, 4-aminobenzoate, or aromatic amino acids, in which it is the last common compound of a branched biosynthetic cascade. Conversion of chorismate to prephenate, finally resulting in tyrosine and phenylalanine, is an extraordinary chemical reaction in primary metabolism that is accelerated by chorismate mutase enzymes up to a factor of 10^6. In addition, especially eukaryotic chorismate mutases have been established as model enzymes for allosteric regulation of catalytic turnover.

We have cloned the *H. polymorpha HARO7* gene coding for the chorismate mutase activity of this methylotrophic yeast. This newly identified enzyme extends the number of described sequences that constitute chorismate mutases. The *H. polymorpha* chorismate mutase is highly similar to the enzyme of the related yeast *S. cerevisiae*, placing the *HARO7* gene product into the AroQ class of chorismate mutases. Additionally, in aligning the published primary sequences of chorismate mutases, a consolidated consensus sequence can be deduced, indicating invariant residues for catalytic activity as well as for regulatory properties. For the yeast enzyme derived from *S. cerevisiae*, several residues have been identified and characterized in detail with respect to enzymatic function (Schnappauf *et al.*, 1997; Graf *et al.*, 1995; Schnappauf *et al.*, 1998b). Almost all of these specific amino acids are conserved in the *H. polymorpha* enzyme, except for the effector-binding residue at position 143. In *S. cerevisiae*, this position corresponds to the Thr^{145} residue, whereas a methionine is found at this position in the *H. polymorpha* enzyme. Nevertheless, overall alignment with other enzymes reveals that this particular position is variable in primary sequence. In contrast, a highly conserved region is present within the primary structures, spanning from Cys^{148} to Phe^{167} in the *H. polymorpha* enzyme. Based on crystal structures of the *S. cerevisiae* enzyme, this protein segment constitutes a helix (helix 8) that is part of the active site as well as of the regulatory site at the dimer interface and that contributes to the strong hydrophobic interaction between the monomers. The general importance of this secondary structure element accounts for its strictly conserved primary sequence. In the global alignment of cloned eukaryotic chorismate mutases, the *H. polymorpha* enzyme has a unique C-terminal extension. Molecular modeling studies based on the crystal structures determined for the *S. cerevisiae* enzyme imply an additional turn in the C-terminal helix (not shown) but functionality of this extension with respect to catalytic or regulatory properties remains to be elucidated.

Using a *loxP-ODC1MX-loxP* cassette we were able to construct a *H. polymorpha* strain disrupted in its *HARO7* locus (RH2409). Retransformation of *HARO7*, either as linear DNA fragment or plasmid-bound, restored growth of the disruptant on the complex medium YEPD. This clearly supports the idea that the observed growth defect of strain RH2409 is linked to its *haro7Δ* genotype and not to a background mutation. Surprisingly, the mutant strain only showed auxotrophy for tyrosine but not for phenylalanine with no residual chorismate mutase activity detectable in crude extracts of the disruption strain. One explanation, that the *HARO7* gene might encode a bifunctional enzyme like a chorismate mutase-prephenate dehydrogenase activity (T-protein), was ruled out as the *HARO7* gene was not able to complement a *tyr1* mutant strain of *S. cerevisiae* which lacks prephenate dehydrogenase activity (Mannhaupt *et al.*, 1989). We conclude, therefore, that the *HARO7*-encoded activity is the only chorismate mutase enzyme in *H. polymorpha* and that no other redundant catalytic activity is encoded by a homologous gene. This is in agreement with results determined by Bode and Birnbaum (1991), who found no evidence for the occurrence of isoenzymic chorismate mutases in yeasts, among them *H. polymorpha*. The reasons for the unexpected Phe^+ phenotype remain obscure but it may be speculated that spontaneous, non-catalytic rearrangement of chorismate to prephenate is sufficient in *H. polymorpha* to feed the phenylalanine-specific branch, implying a higher affinity of prephenate to the dehydratase activity than to the dehydrogenase enzyme. Alternatively, *H. polymorpha* might be able to synthesize phenylalanine via additional routes or from exogenous tyrosine, but both possibilities are unlikely, as no catalytic activities sufficient for such pathways have been described so far. By transient expression of the Cre recombinase we were able to rescue the genetic marker in the *haro7* disruption strain RH2409 due to excision of the *ODC1* expression construct. The resulting strain, RH2410, showed identical growth phenotypes to its progenitor but, additionally, required uracil. Concerning biotechnological aspects, this strain is a new suitable recipient in the vector-host system of *H. polymorpha* as it is able to harbor two expression plasmids carrying different metabolic marker genes. Furthermore, we have demonstrated for the first time that the Cre-*loxP* recombination system can be applied in *H. polymorpha* providing an efficient tool for repeated marker rescue following gene disruptions.

Taking advantage of the vector-host system of *H. polymorpha* we were able to overexpress the *HARO7* gene in a homologous way and to purify the encoded chorismate mutase to homogeneity in order to characterize its enzymatic properties in detail. Catalytic activity of a given enzyme is generally linked to temperature. We have shown that the

H. polymorpha chorismate mutase reaches maximal turnover at a temperature 10°C higher than that of the related yeast *S. cerevisiae*. In experiments like these elevated turnover based on increased enzyme-substrate collisions is superimposed by irreversible denaturation of the enzyme. We therefore addressed the question about thermal stability of both enzymes. Surprisingly, the *H. polymorpha* enzymes displayed higher rate constants of inactivation upon incubation at elevated temperatures in comparison to its *S. cerevisiae* counterpart. We therefore conclude that the higher optimum temperature for the former one is mainly based on increased turnover at the catalytic site. In its allosteric regulation of catalytic activity the *H. polymorpha* chorismate mutase fits well in the theory of concerted transition as proposed by Monod, Wyman, and Changeux in 1965 (Monod *et al.*, 1965). The substrate chorismate acts as homotropic, positive effector that shifts the equilibrium between tense (T-) and relaxed (R-) state to the more active R-state, indicated by a sigmoid curvature of initial velocities as determined in saturation assays as well as by a Hill coefficient of 1.56. Additionally, this value for n_H indicates that the enzyme contains at least two binding sites for the substrate. Furthermore, regulation of catalytic turnover is achieved by heterotropic effects of two aromatic amino acids. Tyrosine, one end product of the chorismate mutase-specific branch, reduces catalytic efficiency by a factor of 2.6 (k_{cat}/K_m = 7.44 versus 19.1 $mM^{-1} \cdot s^{-1}$), whereas tryptophan, the final product of the opposite branch, increases the k_{cat}/K_m value by a factor of 9.8 to 188.1 $mM^{-1} \cdot s^{-1}$ and abolishes cooperativity. The overall modulation range of catalytic efficiency is given by a factor of 25. Altering catalytic efficiency is one mode of regulation for a given enzyme. An additional and more general way to tune the flux through a metabolic pathway is based on altered expression levels of a gene product. For the *HARO7* gene we have shown that transcription is not increased upon the environmental signal amino acid starvation, as induced by the false feedback inhibitor 3-amino-1,2,4-triazole. This is not unusual for chorismate mutase-encoding genes, as neither *ARO7* from *S. cerevisiae* nor *aroC* from *A. nidulans* are targets of a cross-pathway control system acting on amino acid starvation in fungi (Schmidheini *et al.*, 1990b; Krappmann *et al.*, 1999). In contrast to this constitutive expression pattern, *HARO7* transcription is induced upon methanol utilization, a specific metabolic feature of *H. polymorpha,* whereas glycerol as non-optimal carbon source slightly derepresses *HARO7* transcription. Both effects are abolished in the presence of glucose, which accounts for a repression system acting on *HARO7* transcription. This is the first example for transcriptional regulation of a eukaryotic chorismate mutase-encoding gene. As methanol utilization is accompanied by drastically increased expression of

enzymes specific for this pathway, this mode of chorismate mutase expression might reflect the general need for larger amino acid pools in the yeast cell. A putative binding site for the MOX binding factor (Mbf1p) has been identified in the *HARO7* promoter region. This sequence elements differs from the characterized upstream activating sequence found in the *MOX* promoter by one transversion and one insertion (Gödecke *et al.*, 1994). Nevertheless, this conserved motif is a promising candidate for a positive, *cis*-acting element triggering *HARO7* transcription.

References

Anderson L. H., Borg, H., and Mikaelsson, M. (1972) Molecular weight estimation of proteins by electrophoresis in polyacrylamide gel of graded porosity. *FEBS Lett.* **20:** 199-202.

Bode, R. and Birnbaum, D. (1991) Regulation of chorismate mutase activity of various yeast species by aromatic amino acids. *Antonie van Leeuwenhoek* **59:** 9-13.

Bode, R., K. Schüssler, H. Schmidt, T. Hammer, and D. Birnbaum (1990) Occurrence of the general control of amino acid biosynthesis in yeasts. *J. Basic Microbiol.* **30:** 31-35.

Boeke J.D., J. Trueheart, G. Natsoulis, and G.R. Fink (1987) 5-Fluoroorotic acid as a selective agent in yeast molecular genetics. *Methods Enzymol.* **154:** 164-175.

Bradford, M.M. (1976) A rapid and sensitive method for the quantitation of microgram quantities of protein utilizing the principle of protein-dye binding. *Anal. Biochem.* **72:** 248-254.

Chook, Y.M., H. Ke, and W.N. Lipscomb (1993) Crystal structures of the monofunctional chorismate mutase from *Bacillus subtilis* and its complex with a transition state analog. *Proc. Natl. Acad. Sci. USA* **90:** 8600-8603.

Cross, F.R., and A. Tinkelenberg (1991) A potential positive feedback loop controlling *CLN1* and *CLN2* gene expression at the start of the yeast cell cycle. *Cell* **65:** 875-883.

Didion, T., and R. Roggenkamp (1992) Targeting signal of the peroxisomal catalase in the methylotrophic yeast *Hansenula polymorpha*. *FEBS Lett.* **303:** 113-116.

Eberhard, J., H.-R. Raesecke, J. Schmid, and N. Amrhein (1993) Cloning and expression in yeast of a higher plant chorismate mutase. *FEBS Lett.* **334:** 233-236.

Eggeling, L., and H. Sahm (1981) Regulation of alcohol oxidase synthesis in *Hansenula polymorpha*: oversynthesis during growth on mixed substrates and induction by methanol. *Arch. Microbiol.* **127:** 119-124.

Egli, H., J.P. van Dijken, M. Veenhuis, W. Harder, and A. Fiechter (1980) Methanol metabolism in yeasts: regulation of the synthesis of catabolytic enzymes. *Arch. Microbiol.* **124:** 115-121.

Elble, R. (1992) A simple and efficient procedure for transformation of yeasts. *BioTechniques* **13:** 18-20.

Faber, K.N., G.J. Swaving, F. Faber, G. Ab, W. Harder, M. Veenhuis, and P. Haima (1992) Chromosomal targeting of replicating plasmids in the yeast *Hansenula polymorpha*. *J. Gen. Microbiol.* **138:** 2405-2416.

Faber, K.N., P. Haima, W. Harder, M. Veenhuis, and G. Ab (1994) Highly-efficient electrotransformation of the yeast *Hansenula polymorpha*. *Curr. Genet.* **25:** 305-310.

Faber, K.N., P. Haima, C. Gietl, W. Harder, G. Ab, and M. Veenhuis (1995) Methylotrophic yeasts as factories for the production of foreign proteins. *Yeast* **11:**1331-1344.

Fisher, F., and C.R. Goding (1992) Single amino acid substitutions alter helix-loop-helix protein specificity for bases flanking the core CANNTG motif. *EMBO J.* **11:** 4103-4109.

Ganem, B. (1996) The mechanism of the Claisen rearrangement: déjà vu all over again. *Angew. Chem. Int. Ed. Engl.* **35:** 936-945.

Gatzke, R., U. Weydemann, Z.A. Janowicz, and C.P. Hollenberg (1995) Stable multicopy integration of vector sequences in *Hansenula polymorpha*. *Appl. Microbiol. Biotechnol.* **43:** 844-849.

Gellissen, G., C.P. Hollenberg, and Z.A. Janowicz (1994) Gene expression in methylotrophic yeasts p. 395-439. *In* A. Smith (ed.), *Gene expression in recombinant microorganisms.* Dekker, New York.

Gellissen, G., G. Braus, R. Pries, S. Krappmann, and A.W. Strasser (1999) Nukleinsäuremolekül, umfassend eine für ein Polypeptid mit Chorismatmutase-Aktivität kodierende Nukleinsäure. German Patent Application 19919124.7.

Gibson, F. (1999) The elusive branch-point compound of aromatic amino acid biosynthesis. *Trends Biochem. Sci.* **24:** 36-38.

Gödecke, S., M. Eckart, Z.A. Janowicz, and C.P. Hollenberg (1994) Identification of sequences responsible for transcriptional regulation of the strongly expressed methanol oxidase-encoding gene in *Hansenula polymorpha*. *Gene* **139:** 35-42.

Graf, R., Y. Dubaquié, and G.H. Braus (1995) Modulation of the allosteric equilibrium of yeast chorismate mutase by variation of a single amino acid. *J. Bacteriol.* **177:** 1645-1648.

Güldener, U., S. Heck, T. Fiedler, J. Beinhauer, and J.H. Hegemann (1996) A new efficient gene disruption cassette for repeated use in budding yeast. *Nucleic Acids Res.* **24:** 2519-2524.

Guthrie, C., and G.R. Fink (eds.) (1991) Guide to yeast genetics and molecular biology. *Methods Enzymol* **194**: 15.

Hansen H., and C.P. Hollenberg (1996) *Hansenula polymorpha* (*Pichia angusta*), p. 293-311. In K. Wolf (ed.), *Nonconventional Yeasts in Biotechnology*, Springer-Verlag, Berlin.

Haslam, E. (1974) *The skikimate pathway*. Butterworth & Co., London.

Heiner, C.R., K.L. Hunkapiller, S. Chen, J.I. Glass, and E.Y. Chen (1998) Sequencing multimegabase-template DNA with BigDye terminator chemistry. *Genome Research* **8:** 557-561.

Hilton, J.L., P.C. Kearney, and B.N. Ames (1965) Mode of action of the herbicide 3-amino-1,2,4-triazole (amitrole): inhibition of an enzyme of histidine biosynthesis. *Arch. Biochem. Biophys.* **112:** 544-547.

Hoffmann, C.S., and F. Winston (1987) A ten-minute DNA preparation from yeast efficiently releases autonomous plasmids for transformation of *Escherichia coli*. *Gene* **57:** 267-272.

Hollenberg, C.P., and Z.A. Janowicz. (1989) DNA molecules coding for *FMDH* control region and structured gene for a protein having *FMDH*-activity and their uses. European Patent, EP 0299108-A1.

Hong, W.K., H.A. Kang, J.H. Shon, E.S. Choi, and S.K. Rhee (1998) Cloning and analysis of *ACT* gene encoding actin from methylotrophic yeast *Hansenula polymorpha*. Direct submission to GenBank, Acc. No. AF085278.

Inoue, H., H. Nojima, and H. Okayama (1990) High efficiency transformation of *Escherichia coli* with plasmids. *Gene* **96:** 23-28.

Janowicz, Z., M. Eckart, C. Drewke, R. Roggenkamp, C.P. Hollenberg, J. Maat, A.M. Ledeboer, C. Visser, and C.T. Verrips (1985) Cloning and characterization of the *DAS* gene encoding the major methanol assimilatory enzyme from the methylotrophic yeast *Hansenula polymorpha*. *Nucleic Acids Res.* **13:** 3043-3062.

Janowicz, Z.A., K. Melber, A. Merckelbach, E. Jacobs, N. Harford, M. Comberbach, and C.P. Hollenberg (1991) Simultaneous expression of the S and L surface antigens of hepatitis B, and formation of mixed particles in the methylotrophic yeast, *Hansenula polymorpha*. *Yeast* **7:** 431-443.

Krappmann, S., K. Helmstaedt, T. Gerstberger, S. Eckert, B. Hoffmann, M. Hoppert, G. Schnappauf, and G.H. Braus (1999) The *aroC* gene of *Aspergillus nidulans* codes for a monofunctional, allosterically regulated chorismate mutase. *J. Biol. Chem.* **274:** 22275-22282.

Lämmli, U.K. (1970) Cleavage of structural proteins during the assembly of the head of the bacteriophage T4. *Nature* **227:** 680-685.

Ledeboer, A.M., L. Edens, J. Maat, C. Visser, J.W. Bos, C.T. Verrips, Z. Janowicz, M. Eckart, R. Roggenkamp, and C.P. Hollenberg (1985) Molecular cloning and characterization of a gene coding for methanol oxidase in *Hansenula polymorpha*. *Nucleic Acids Res.* **13:** 3063-3082.

Lee, J.-D., and K. Komagata (1980) Taxonomic study of methanol-assimilating yeasts. *J. Gen. Appl. Microbiol.* **26:** 133-158.

Lee, A., J.D. Stewart, J. Clardy, and B. Ganem (1995) New insight into the catalytic mechanism of chorismate mutases from structural studies. *Chemistry & Biology* **2:** 195-203.

Levine, D.W., and C.L. Cooney (1973) Isolation and characterization of thermotolerant methanol-utilizing yeasts. *Appl. Microbiol.* **26:** 982-990.

Lipman, D.J., and W.R. Pearson (1985) Rapid and sensitive protein similarity searches. *Science* **227:** 1435-1441.

Ma, J., X. Zheng, G. Schnappauf, G. Braus, M. Karplus, and W.N. Lipscomb (1998) Yeast chorismate mutase in the R state: simulations of the active site. *Proc. Natl. Acad. Sci. USA* **95:** 14640-14645.

MacBeath, G., P. Kast, and D. Hilvert (1998) A small, thermostable, and monofunctional chorismate mutase from the archeon *Methanococcus jannaschii*. *Biochemistry* **37:** 10062-10073.

Maniatis, T., E.F. Fritsch, and J. Sambrook (1982) *Molecular Cloning, a laboratory manual*, 2nd edn., Cold Spring Harbor Laboratory Press, Cold Spring Harbor, New York.

Mannhaupt, G., R. Stucka, U. Pilz, C. Schwarzlose, and H. Feldmann (1989) Characterization of the prephenate dehydrogenase-encoding gene, *TYR1*, from *Saccharomyces cerevisiae*. *Gene* **85:** 303-311.

Merckelbach, A., S. Gödecke, Z.A. Janowicz, and C.P. Hollenberg (1993) Cloning and sequencing of the *ura3* locus of the methylotrophic yeast *Hansenula polymorpha* and its use for the generation of a deletion by gene replacement. *Appl. Microbiol. Biotechnol.* **40:** 361-364.

Monod, J., J. Wyman, and J.-P. Changeux (1965) On the nature of allosteric transitions: a plausible model. *J. Mol. Biol.* **12:** 88-118.

Oliver, K., D. Harris, B.G. Barrell, M.A. Rajandream, and V. Wood (1995) *Schizosaccharomyces pombe* chromosome I sequencing project. Direct submission to GenBank, Acc. No. Z98529.

Rave, N., R. Crkvenjakov, and H. Bödtker (1979) Identification of procollagen mRNAs transferred to diazobenzoyloxymethyl paper from formaldehyde agarose gels. *Nucleic Acids Res.* **6:** 3559-3567.

Roggenkamp, R., Z. Janowicz, B. Stanikowski, and C.P. Hollenberg (1984) Biosynthesis and regulation of the peroxisomal methanol oxidase from the methylotrophic yeast *Hansenula polymorpha*. *Mol. Gen. Genet.* **194:** 489-493.

Romero, R.M., M.F. Roberts, and J.D. Phillipson (1995) Chorismate mutase in microorganisms and plants. *Phytochemistry* **40:** 1015-1025.

Rymond B.C., and M. Rosbash (1992) Yeast pre-mRNA splicing. pp. 143-192 In J.R. Broach, J.R. Pringle, and E.W. Jones (eds.) *The Molecular and Cellular Biology of the Yeast Saccharomyces*, Volume 2: Gene Expression., Cold Spring Harbor Laboratory Press, Cold Spring Harbor, New York.

Saiki, R.K., S. Scharf, F. Faloona, K.B. Mullis, G.T. Horn, H.E. Erlich, and N. Arnheim (1985) Enzymatic amplification of β-globin genomic structures and restriction sites analysis for diagnosis of sickle cell anemia. *Science* **230:** 1350-1354.

Sauer, B. (1987) Functional expression of the Cre-*lox* site-specific recombination system in the yeast *Saccharomyces cerevisiae*. *Mol. Cell. Biol.* **7:** 2087-96.

Schmidheini, T., P. Sperisen, G. Paravicini, R. Hütter, and G. Braus (1989) A single point mutation results in a constitutively activated and feedback-resistant chorismate mutase of *Saccharomyces cervisiae*. *J. Bacteriol.* **171:** 1245-1253.

Schmidheini, T., H.-U. Mösch, , J.N.S. Evans, and G. Braus (1990a) Yeast allosteric chorismate mutase is locked in the activated state by a single amino acid substitution. *Biochemistry* **29:** 3660-3668.

Schmidheini, T., H.-U. Mösch, R. Graf, and G.H. Braus (1990b) A GCN4 protein recognition element is not sufficient for GCN4-dependent regulation of transcription in the *ARO7* promoter of *Saccharomyces cerevisiae*. *Mol. Gen. Genet.* **224:** 57-64.

Schnappauf, G., N. Sträter, W.N. Lipscomb, and G. Braus (1997) A glutamate residue in the catalytic center of the yeast chorismate mutase restricts enzyme activity to acidic conditions. *Proc. Natl. Acad. Sci. USA* **94:** 8491-8496.

Schnappauf, G., W.N. Lipscomb, and G.H. Braus (1998a) Separation of inhibition and activation of the allosteric yeast chorismate mutase. *Proc. Natl. Acad. Sci. USA* **95:** 2868-2873.

Schnappauf, G., S. Krappmann, and G.H. Braus (1998b) Tyrosine and tryptophan act through the same binding site at the dimer interface of yeast chorismate mutase. *J. Biol. Chem.* **273:** 17012-17017.

Sikorski, R.S., and P. Hieter (1989) A system of shuttle vectors and yeast host strains designed for efficient manipulation of DNA in *Saccharomyces cervisiae*. *Genetics* **122:** 19-27.

Southern, E.M. (1975) Detection of specific sequences among DNA fragments separated by gel electrophoresis. *J. Mol. Biol.* **98:** 503-517.

Sternberg, N., and D. Hamilton (1981) Bacteriophage P1 site-specific recombination. I. Recombination between *loxP* sites. *J. Mol. Biol.* **150:** 467-486.

Sternberg N., B. Sauer, R. Hoess, and K. Abremski (1986) Bacteriophage P1 *cre* gene and its regulatory region. Evidence for multiple promoters and for regulation by DNA methylation. *J. Mol. Biol.* **187:** 197-212

Sträter, N., G. Schnappauf, G. Braus, and W.N. Lipscomb (1997) Mechanism of catalysis and allosteric regulation of yeast chorismate mutase from crystal structures. *Structure* **5:** 1437-1452.

Teshiba, S., R. Furter, P. Niederberger, G. Braus, G. Paravicini, and R. Hütter (1986) Cloning of the *ARO3* gene of *Saccharomyces cerevisiae* and its regulation. *Mol. Gen. Genet.* **205:** 353-357.

Veenhuis, M., J.P. van Dijken, S.A.F. Pilon, and W. Harder (1978) Development of crystalline peroxisomes in methanol-grown cells of the yeast *Hansenula polymorpha* and its relation to environmental conditions. *Arch. Microbiol.* **117:** 153-163.

Weiss, U., and J.M. Edwards (1980) *The Biosynthesis of Aromatic Amino Acids*, Wiley, New York.

Weydemann, U., P. Keup, M. Piontek, A.W. Strasser, J. Schweden, G. Gellissen, and Z.A. Janowicz (1995) High-level secretion of hirudin by *Hansenula polymorpha* – authentic processing of three different preprohirudins. *Appl. Microbiol. Biotechnol.* **44:** 377-385.

Woodcock, D.M., P.J. Crowther, J. Doherty, S. Jefferson, E. DeCruz, M. Noyer-Weidner, S.S. Smith, M.Z. Michael, and M.W. Graham (1989) Quantitative evaluation of *Escherichia coli* host strains for tolerance to cytosine methylation in plasmid and phage recombinants. *Nucleic Acids Res.* **17:** 3469-3478.

Xue, Y., W.N. Lipscomb, R. Graf, G. Schnappauf, and G. Braus (1994) The crystal structure of allosteric chorismate mutase at 2.2 Å resolution. *Proc. Natl. Acad. Sci. USA* **91:** 10814-10818.

Chapter 4

The *aroC* Gene of *Aspergillus nidulans* Codes for a Monofunctional, Allosterically Regulated Chorismate Mutase

Abstract

The cDNA and the chromosomal locus of the *aroC* gene of *Aspergillus nidulans* were cloned which is the first representative of a filamentous fungal gene encoding chorismate mutase (E.C. 5.4.99.5), the enzyme at the first branch point of aromatic amino acid biosynthesis. The *aroC* gene complements the *S. cerevisiae aro7Δ* as well as the *A. nidulans aroC* mutation. The gene consists of three exons interrupted by two short intron sequences. The expressed mRNA is 0.96 kb in length and *aroC* expression is not regulated on the transcriptional level under amino acid starvation conditions. *aroC* encodes a monofunctional polypeptide of 268 amino acids. Purification of this 30 kDa enzyme allowed determination of its kinetic parameters (k_{cat}=82 s^{-1}, n_H=1.56, $[S]_{0.5}$=2.3 mM), varying pH dependencies of catalytic activity in different regulatory states, and an acidic pI value of 4.7. Tryptophan acts as heterotropic activator and tyrosine as negative-acting, heterotropic feedback-inhibitor with a K_i of 2.8 μM. Immunological data, homology modeling as well as electron microscopy studies indicate that this chorismate mutase has a dimeric structure like the *S. cerevisiae* enzyme. Site-directed mutagenesis of a crucial residue in loop220s (D233) revealed differences concerning the intramolecular signal transduction for allosteric regulation of enzymatic activity.

Introduction

Chorismic acid is the last common compound in the biosynthesis of aromatic amino acids. The metabolic branch leading to L-tryptophan is initiated by its conversion to anthranilate catalyzed by the enzyme anthranilate synthase (E.C. 4.1.3.27), whereas the catalytic reaction to prephenate finally leads to L-phenylalanine and L-tyrosine (Weiss and Edwards, 1980; Braus, 1991). The latter reaction is the only known Claisen rearrangement in primary metabolism of living organisms and is catalyzed by a unique enzyme, the chorismate mutase (E.C. 5.4.99.5) (Andrews *et al.*, 1973). Chorismate mutases are found in archaea, bacteria, fungi, and plants (Romero *et al.*, 1995). Based on primary sequence information and determination of the crystal structure of three natural enzymes, chorismate mutases are classified into two groups: the chorismate mutase of *Bacillus subtilis* represents the AroH class and is characterized by its trimeric pseudo α/β-barrel structure (Chook *et al.*, 1993; Chook *et al.*, 1994). In contrast, polypeptides of the AroQ class are all-helix-bundle proteins and are often part of a bifunctional enzyme containing a chorismate mutase domain (Gu *et al.*, 1997). According to Hilvert and co-workers (MacBeath *et al.*, 1998), eukaryotic chorismate mutases, which additionally contain regulatory domains, also fall into the latter class despite of the rare primary amino acid sequence similarity with their prokaryotic counterparts. The enzymatic properties of some eukaryotic chorismate mutases have been studied in detail, but only a limited number of the corresponding genes have been cloned yet (Romero *et al.*, 1995).

The chorismate mutase of the baker's yeast *Saccharomyces cerevisiae* is the most prominent member of the AroQ class and has been characterized in extensive studies (Schmidheini *et al.*, 1989; Schnappauf *et al.*, 1997; Schnappauf *et al.*, 1998). Its allosteric modulation by tyrosine and tryptophan serves as a model in understanding the regulatory properties of a branch point enzyme. Determination of different crystal structures has given insight into the structural basis for the regulatory processes controlling the flux of chorismate into one of the two branches in the biosynthesis of aromatic amino acids (Sträter *et al.*, 1997 and references therein). In addition, molecular dynamics studies have given hints to understand the mechanism of the enzymatic conversion performed by this enzyme (Ma *et al.*, 1998). The homodimeric yeast enzyme consists of 2x12 helices with the catalytically active domain built up by three helices of each subunit. The loop preceding one of these helices has turned out to be crucial for transmitting the signal of T to R state transition. Conversion of one residue in this loop (T226I) results in a constitutively activated enzyme that is unresponsive to its inhibitor tyrosine (Schmidheini *et al.*, 1990).

To date, no gene coding for a chorismate mutase of a filamentous fungus has been characterized. Here we present the characterization of the chorismate mutase-encoding gene *aroC* of *Aspergillus nidulans*. This filamentous fungus has become a model organism concerning metabolism as well as differentiation in recent decades (Martinelli *et al.*, 1994; Adams *et al.*, 1998). The *aroC* gene product was overexpressed in yeast using recombinant DNA technology and then purified for kinetic assays and regulatory analysis. The quarternary structure was determined by computer modeling and compared to the yeast enzyme. Additionally, site-directed mutagenesis was applied to investigate the role of a putatively crucial residue (D233) in allosteric transition as this amino acid residue corresponds to residue T226 in the yeast chorismate mutase. We found that the newly characterized chorismate mutase shares structural similarities with its yeast homologue, but that the molecular basis of the mechanism for T-R transition is not conserved.

Experimental Procedures

Materials

Chorismic acid as barium salt was purchased from SIGMA (St. Louis, MO, USA). Ethylamino-Sepharose was prepared following the protocol for activation of Sepharose CL-4B (Dimroth, 1986) and by coupling of the ligand ethylamine-HCl to the activated matrix. Protein solutions were concentrated by using stirred cells (volumes of 180 ml and 10 ml) with PM-10 ultrafiltration membranes from MILLIPORE (Eschborn, Germany). The Mini 2D SDS-polyacrylamide gel electrophoresis system and the Bradford protein assay solution for determination of protein concentrations originated from BIO-RAD LABORATORIES (Hercules, CA, USA). VENT polymerase (BIOLABS, Schwalbach, Germany) was used for PCR reactions.

All other chemicals were supplied by FLUKA (Neu-Ulm, Germany) or SIGMA-ALDRICH Chemie GmbH (Steinheim, Germany).

Strains, Media, cDNA library, Plasmids, Growth Conditions

The *S. cerevisiae* strain RH2185 (*MATa, suc2-Δ9, ura3-52, leu2-3, leu2-112, his4-519, aro7::LEU2, GAL2*) (Schnappauf *et al.*, 1997) with the genetic background of the laboratory strain X2180-1A (*MATa, gal2, SUC2, mal, CUP1*) was used as recipient for cloning of an *aroC* cDNA out of an inducible expression library. The expression library provided by B. Hoffmann was constructed after mRNA isolation from *A. nidulans* strain FGSC A234 (*yA2, pabaA1, veA1*) using the Superscript™ cDNA Synthesis Kit from GIBCO (Gaithersburg, MD, USA). cDNAs were ligated as *Sal*I/*Not*I fragments in the shuttle vector pRS316-*GAL1* (Liu *et al.*, 1992) and propagated in *E. coli*. Yeast transformation was carried out as described in (Elble, 1992). Transformation of *A. nidulans* was carried out according to Punt and van den Hondel (1992). For overexpression, a derivative of plasmid p426MET25 (Mumberg *et al.*, 1994) was used in the *S. cerevisiae* strain RH2192 (*MAT**a**, pra1-1, prb1-1, prc1-1, cps1-3, ura3Δ5, leu2-3, 112, his*$^-$*, aro7::LEU2*) which is a derivative of the protease-deficient strain c13-ABYS-86 (Heinemeyer *et al.*, 1991). The *A. nidulans* strain G1100 (*aroC1248, riboA1, adG14, yA2*) was described earlier (Roberts, 1969) and was obtained from J. Clutterbuck, Glasgow, UK. MV minimal medium for the cultivation of yeast was described earlier (Miozzari *et al.*, 1978) and minimal medium for the cultivation of *A. nidulans* strains was prepared according to Käfer (1977).

Site-directed Mutagenesis

A polymerase chain reaction (PCR) based method was used for site-directed mutagenesis of *aroC* (Giebel and Spritz, 1990). The PCR-generated fragments were sequenced (Sanger *et al.*, 1977) to confirm the presence of the mutations and to rule out second-site mutations.

RNA preparation and analysis

Total RNA was prepared from vegetatively growing *A. nidulans* cultures using the TRIzol™ reagent from GIBCO following the supplier's instructions. Transcript levels were analyzed by Northern hybridization (Alwine *et al.*, 1977) using a Bio-Imaging Analyzer from FUJI PHOTO FILM Co. Ltd. (Tokyo, J). Transcript length was determined using the 0.16-1.77 kb RNA ladder from GIBCO.

Overexpression and Purification of *Aspergillus nidulans* chorismate mutase

Plasmid-carrying yeast strains were grown at 30°C in 10 l rotatory fermentors under aeration. Cells were harvested in mid-log phase at an OD_{546nm} of 4 - 6, washed twice with 50 mM K-phosphate buffer, pH 7.6 and stored in 1 ml buffer per g wet cells at -20°C in the presence of protease inhibitors (0.1 mM phenylmethylsulfonylfluoride (PMSF), 0.2 mM ethylenediaminetetraacetate (EDTA) and 1 mM DL-dithiothreitol (DTT)). For purification, 80-110 g of cells were thawed and run three times through a French Pressure Cell (18,000 psi). Cell debris was sedimented by centrifugation at 30,000xg for 20 min.

The chorismate mutase was purified according to the protocol of Schmidheini *et al.* (1990) with the following modifications: in all steps 10 mM K-phosphate buffer, pH 7.6 was used as solvent, ammonium sulfate precipitation was carried out at 47% saturation, PMSF was added to the equilibration buffer for the ethylamino sepharose column, dialysis was used to desalt protein extracts, and a second run on a MonoQ column at pH 5.8 in 10 mM K-phosphate buffer was performed. Chorismate mutase was detected by SDS-PAGE (Laemmli, 1970) and by enzymatic activity assays. Measurements of protein concentrations were performed using the Bradford assay (Bradford, 1976).

Enzyme assays

Chorismate mutase activity was measured as described previously (Schmidheini *et al.*, 1989) with some modifications. The enzymatic conversion is stopped after 1 minute by addition of HCl and the product of the enzymatic reaction, prephenate, is converted to phenylpyruvate through a chemical reaction. Enzymatic activity is measured spectrophotometrically, determining the concentration of phenylpyruvate. Since absorbance

of phenylpyruvate is temperature-dependent due to a keto-enol equilibrium, the assay was standardized by keeping the enzymatic reactions at 30°C and equilibrating the spectrophotometer cell to the same temperature. Reaction volumes of 250 µl containing 100 mM K-phosphate, pH 7.6, 2 mM EDTA, 20 mM DTT, optionally 50 µM tyrosine or 5 µM tryptophan, chorismate mutase enzyme and chorismate in a range from 0.25 to 13 mM were used. The reaction was started by adding the mix of all ingredients to the pre-warmed chorismate solution. The reaction was stopped by adding 250 µl 1 M HCl. After an incubation time of 10 min, 4 ml of 1 M NaOH were added and extinction at 320 nm was measured against H_2O. To exclude absorbance caused by the uncatalyzed rearrangement of chorismate, blanks of increasing chorismate concentrations without enzyme were prepared and absorbance was measured. These blank absorbances were subtracted from optical densities measured for enzyme activities. A calibration curve was drawn using different known phenylpyruvate concentrations that were treated the same way as the enzyme reactions. The molecular extinction coefficient at 30ºC was determined as 13095 $M^{-1} \cdot cm^{-1}$. For determination of the pH optima, a universal buffer solution with a pH range of 2.5-12 containing 30 mM citric acid, 30 mM KH_2PO_4, 30 mM H_3BO_4, 30 mM diethylbarbituric acid and different amounts of NaOH was used.

The collected data were transformed to international units ($\mu mol \cdot min^{-1}$) per mg enzyme. The maximum velocity V_{max}, the Hill-coefficient n_H, and the substrate concentration at half maximal velocity $[S]_{0.5}$ or K_m were determined using a computer program which applied the Quasi-Newton method (Davidon-Fletcher-Powell algorithm) to fit optimal curves to the data (Fletcher and Powell, 1963). To draw substrate saturation curves, the data were fitted either to the Michaelis-Menten equation ($v=V_{max} \cdot [S] \cdot (K_m+[S])^{-1}$) or to the Hill equation ($v=V_{max} \cdot [S]^n \cdot ([S]^n + S')^{-1}$), where $S'^{(1/n)}=S_{0.5}$. Eadie-Hofstee plots ($v \cdot [S]^{-1}$ vs. v) were drawn to decide to which equation a set of kinetic data had to be applied. Enzyme kinetics without cooperativity result in a linear curve, whereas even small degrees of cooperativity result in concave curvatures of the kinetic data (Newell and Schachmann, 1990). Hill plots ($\log(v \cdot (V_{max}-v)^{-1})$ vs. $\log[S]$) were used to calculate Hill coefficients. The resulting V_{max} values were transformed to catalytic constants ($k_{cat}=V_{max} \cdot M_r \cdot E_0^{-1} \cdot (60s)^{-1}$; substrate turnover per active site). The inhibitor constant K_i for tyrosine was determined according to Dixon (1953) by plotting v^{-1} versus inhibitor concentration.

Determination of the Native Molecular Weight

The native molecular weight of the chorismate mutase was estimated by gel filtration on a Superdex200 prep grade column using 50 mM K-phosphate, 150 mM NaCl, pH 7.6 as elution buffer. The void volume of the column was determined with Blue Dextran and a calibration plot was defined using a gel filtration chromatography standard from BIO-RAD (Hercules, CA, USA) containing thyroglobulin, bovine γ-globulin, chicken ovalbumin, equine myoglobin, and vitamin B-12. In addition, the molecular weight was determined independently by sedimentation equilibrium at 50,000 rpm (16°C) and calculation of the sedimentation coefficient and the molecular mass. Three different concentrations of the enzyme in 20 mM K-phosphate buffer, pH 7.6 were used and all ultracentrifugal analyses were performed on a BECKMANN XLA. To confirm the results obtained by gel filtration and analytical ultracentrifugation, the molecular weight was estimated by native polyacrylamide gel electrophoresis using a gradient from 4% to 20% polyacrylamide (Andersson *et al.*, 1972).

Determination of the Isoelectric Point

The isoelectric point of the chorismate mutase enzyme was determined using the BIO-RAD Rotofor system according to the supplier's instructions. A pH gradient in 18 ml of 10 mM K-phosphate buffer, pH 7.6 was set up by a Bio-Lyte® ampholyte ranging from pH 3.5 to 9.5 in a concentration of 0.5%. 100 µg of purified protein were applied to the focusing chamber and after 4 hours the run was completed. The content of the focusing chamber was fractionated and the pH of each fraction was measured. Before detection of chorismate mutase, NaCl was applied to 1 M final concentration and fractions were dialyzed against 10 mM K-phosphate, pH 7.6. Chorismate mutase was detected by enzyme assays as well as by SDS-PAGE.

Electron Microscopy

Negative staining of protein samples was performed as described in (Valentine *et al.*, 1968) with 4% uranyl acetate solution. Electron microscopic images were taken at a EM 301 transmission electron microscope (PHILIPS, Eindhoven, Netherlands) at an acceleration potential of 80 kV. Magnification was calibrated using a crossgrid replica.

Western Blot analysis

Immunological detection of chorismate mutase proteins was performed using a polyclonal rabbit antibody raised against purified yeast chorismate mutase (Schnappauf *et al.*, 1997) and a second antibody with horseradish peroxidase activity. Detection was carried out using the ECL method (Tesfaigzi *et al.*, 1994).

Sequence Alignment and Homology Modeling Studies

All sequence analyses were performed using the LASERGENE Biocomputing software from DNASTAR (Madison, WC, USA). Alignments were created based on the Lipman-Pearson method (Lipman and Pearson, 1985). For homology modeling, the deduced primary structure of the *A. nidulans* chorismate mutase was aligned to the crystallographic data of yeast chorismate mutases described in the Brookhaven protein database (Sträter *et al.*, 1997) by ProModII (Peitsch, 1996) and refined by the SWISS-MODEL service (Peitsch, 1995; Guex and Peitsch, 1997). Using the MOLMOL software (Koradi *et al.*, 1996), a three-dimensional structure model could be established by calculation of secondary structures.

Results

Isolation of the *aroC* gene from *Aspergillus nidulans*

The *aroC* gene from *Aspergillus nidulans* was cloned by functional complementation of a *Saccharomyces cerevisiae aro7Δ* mutant strain (Schnappauf *et al.*, 1997). Yeast strains with a deleted *ARO7* gene do not contain any chorismate mutase activity and therefore were unable to grow on minimal medium lacking tyrosine or phenylalanine. Yeast strain RH2185 (*aro7::LEU2, ura3-52*) was transformed with *A. nidulans* cDNA expressed from the *GAL1* promoter (Liu *et al.*, 1992) and transformants were selected by growth on medium lacking tyrosine and phenylalanine containing 2% galactose as sole carbon source. A total of 80 colonies were obtained, from which plasmids were isolated that could complement the Phe/Tyr auxotrophy of the recipient *aro7Δ* yeast strain. One of the plasmids (pME1498) was further analyzed by DNA sequencing of the *Sal*I/*Not*I fragment containing the cDNA insert. The cDNA without poly(A) tail is 927 bp in length and includes an open reading frame of 804 bp with 267 codons which correspond to a polypeptide with a calculated M_r of 30,660. Alignment of the deduced amino acid sequence shows strong homology to the chorismate mutase sequence of *S. cerevisiae* with 44% identity (Fig. 17). The homology goes up to 67% when conservative changes are taken into account.

The genomic region encoding the cDNA insert of pME1498 was isolated and analyzed. Southern blot analysis of this region, using the cDNA of pME1498 as a probe, revealed that the corresponding gene exists as single copy in the *A. nidulans* genome (data not shown). A sublibrary of *A. nidulans* genomic *Hin*dIII fragments of 4 to 6 kb in size was screened by colony hybridization with the *aroC* cDNA probe and resulted in a 5 kb fragment which was subjected to DNA sequence analyses (Fig. 18A). The genomic fragment contains the same open reading frame as the cDNA, flanked by a 1.2 kb 5'-region and a 2.7 kb 3'-region, and is interrupted by two short intron sequences. Intron I is located 70 bp downstream of the translational start site and is 113 bp in length, while intron II is located 77 bp upstream of the stop codon UAG and 49 bp in size. Both show the conserved 5' splicing, internal, and 3' splicing sequences described for *A. nidulans* introns (May *et al.*, 1987). Sequence analysis for upstream regulatory sequences in the promoter region of *aroC* indicated a putative STUA binding site 560 nucleotides upstream of the translational start codon. This sequence element (5'-ACGCGAAA-3') matches the described consensus for STUA response elements (StRE, 5'-$^{A}/_{T}$CGCG$^{T}/_{A}$N$^{A}/_{C}$-3') (Dutton *et al.*, 1997). In addition, a sequence element (5'-GAGTCA-3') was identified 571 bp upstream of the translational

start codon that matches the described consensus sequence for a Gcn4p binding site (GCRE, 5'- TGACTC-3') in reverse orientation (Hinnebusch, 1988).

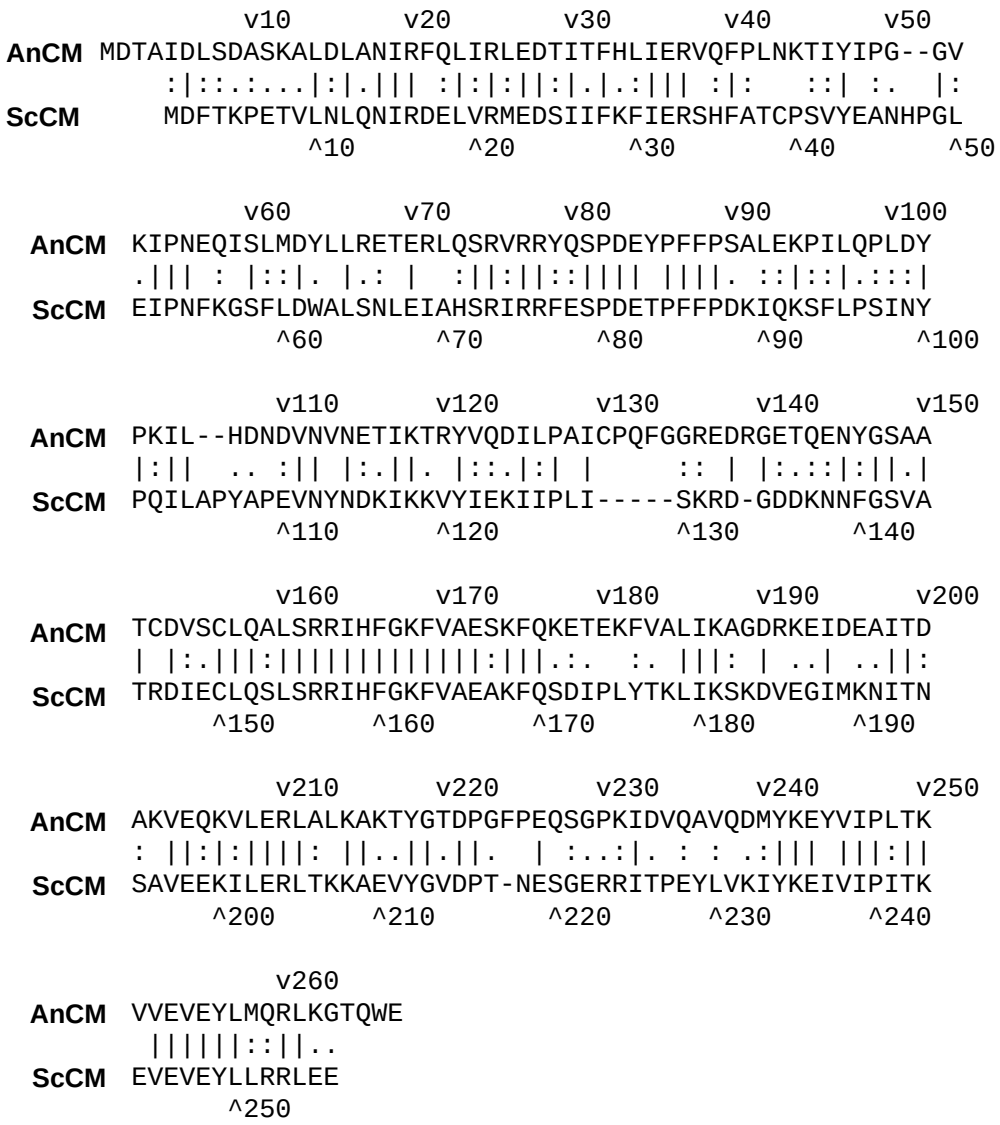

Figure 17: The chorismate mutase of *Aspergillus nidulans* shows homology to the *Saccharomyces cerevisiae* enzyme. The alignment shows a comparison of the deduced amino acid sequence of *A. nidulans* chorismate mutase (AnCM) with that of *S. cerevisiae* (ScCM). Identical residues are indicated by vertical bars, conservative replacements by colons, and neutral changes by periods.

A. nidulans mutant strains auxotrophic for phenylalanine and tyrosine have been isolated before (Roberts, 1969). One complementation class of these mutants was named *aroC* and mapped to linkage group I (Zaudy, 1969). The described phenotype of *aroC* mutant strains prompted us to test whether the gene isolated was able to complement the auxotrophy of *aroC* mutants. For this purpose, the genomic *Hin*dIII fragment was transformed into strain G1100 (*aroC1248, riboA1, adG14, yA2*) for ectopic integration and transformants were selected on medium lacking phenylalanine and tyrosine. For 90% of the isolated transformants a complementation of the Phe/Tyr auxotrophy was observed, indicating that we had isolated the *aroC* gene of *A. nidulans*, which codes for the chorismate mutase enzyme.

aroC expression is not regulated transcriptionally upon amino acid starvation.

By Northern blot analysis using an RNA size standard the transcript length of *aroC* was determined to be approximately 0.96 kb (not shown). As the *aroC* gene product is an enzyme of the aromatic amino acid biosynthetic pathway and because of the existence of a putative GCRE in its promoter region we were interested in whether *aroC* expression is affected by amino acid starvation conditions. For that purpose, *A. nidulans* strain FGSC A234 (*yA2, pabaA1, veA1*) was cultivated in liquid minimal medium for 20 hours and mycelia were transferred to fresh medium containing 3-amino-1,2,4-triazole (3AT). This reagent acts as false feedback-inhibitor on the histidine biosynthesis and therefore mimics amino acid starvation by depletion of the histidine pool within the fungus (Hilton *et al.*, 1965). After different time points mycelium was harvested and total RNA was prepared. Following Northern blot the *aroC* transcript levels were determined by probing with the cDNA fragment. Additionally, the levels of the *gpdA* (Punt *et al.*, 1988) and the *trpC* (Yelton *et al.*, 1983) transcripts were detected with specific probes serving as internal controls (Fig. 18B). *gpdA*, which encodes an enzyme of glycolysis (glyceraldehyde-3-phosphate dehydrogenase, EC 1.2.1.12), is known to be unregulated in its transcription upon 3AT addition. In contrast, *trpC*, which codes for a trifunctional enzyme of tryptophan biosynthesis, has been shown to be transcriptionally regulated by amino acid starvation conditions. Quantification of signal strength reveals constant expression of *aroC* after shifting to amino acid starvation conditions. Expression of *gpdA* shows the identical pattern, whereas *trpC* transcription is increased by a factor of 15 eight hours after the onset of the environmental stimulus. Therefore we conclude that transcription of the *aroC* gene is not affected by a regulatory network that acts upon the environmental signal amino acid starvation.

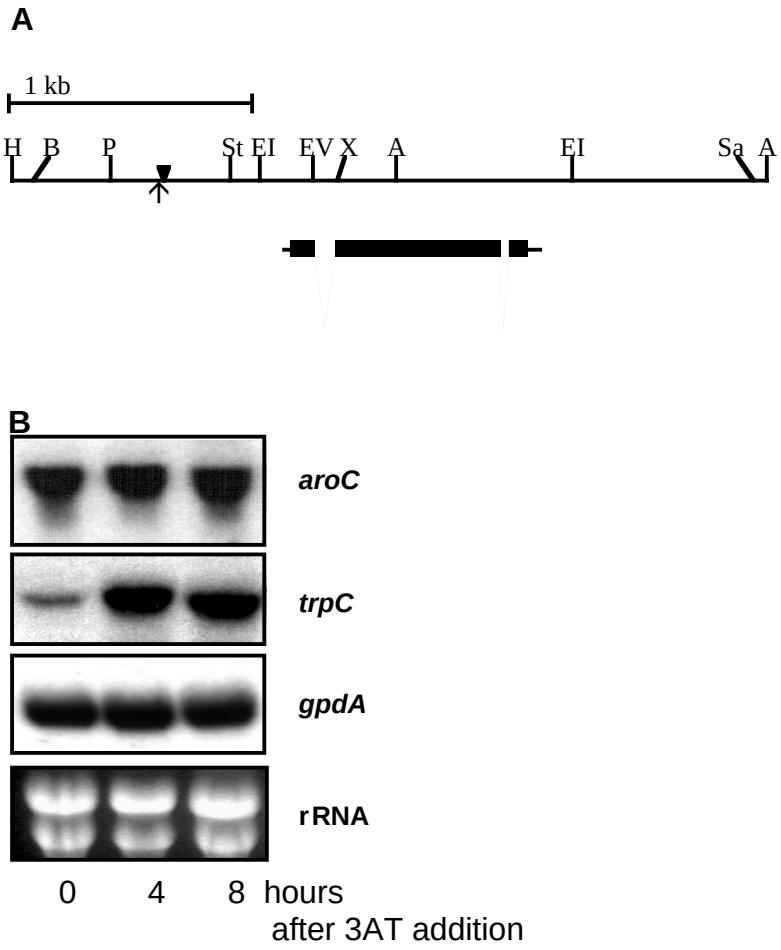

Figure 18: Structure of the *aroC* gene and expression under amino acid starvation conditions. *A*, schematic drawing of a genomic *Hin*dIII/*Aat*II DNA fragment containing the *aroC* gene. The GenBank accession number for this sequence is AF133241. Solid boxes indicate the open reading frame interrupted by two introns. A putative STUA binding site is indicated by the solid triangle and a Gcn4p response element in reverse orientation by the open triangle. A, *Aat*II; B, *Bst*EII; EI, *Eco*RI; EV, *Eco*RV; H, *Hin*dIII; P, *Pvu*II; Sa, *Sal*I; St, *Stu*I; X, *Xba*I. *B*, Northern analysis of total RNA prepared from *A. nidulans* strain FGSC A234 (*yA2, pabaA1, veA1*) different time points after shifting to medium containing 3-amino-1,2,4-triazole (3AT). Each lane was loaded with 20 µg total RNA and probed successively with probes specific for *aroC, trpC,* and *gpdA.* Ethidium bromide-stained total RNA is included as control.

Chorismate mutase of *A. nidulans* is regulated by tyrosine and tryptophan.

The enzyme was purified by overexpression in *S. cerevisiae* strain RH2192 (*aro7::LEU2, ura3-52*) from a high-copy plasmid carrying the *A. nidulans aroC* cDNA fragment driven by the *MET25* yeast promoter. The protein was enriched 64-fold and purified to homogeneity to determine the properties of the *aroC* gene product. Kinetic stop assays with the unliganded enzyme were performed to reveal the catalytic properties of the *A. nidulans*

chorismate mutase (Fig. 19A, Tab. IV). In the absence of effectors the enzyme shows positive cooperativity towards its substrate chorismate leading to a sigmoidal substrate saturation curve. A $[S]_{0.5}$ value of 2.3 mM and a Hill coefficient n_H of 1.56 were determined and the maximal turnover rate k_{cat} was calculated to be 82 s^{-1} per active site. By isoelectric focusing, the pI of the protein was determined to be at an acidic pH of 4.7 (data not shown). The solvent pH also has an influence on the catalytic activity of the enzyme (Fig. 19C). Without any effector bound, chorismate mutase activity reaches its maximum at a pH of 5.9.

To reveal the regulatory behaviour of the enzyme, kinetic assays were performed in the presence of allosteric effectors (Fig. 19A, Tab IV). Tryptophan at 5 μM concentration has a strong effect on the catalytic rate. Cooperativity is lost (n_H=0.95), leading to a Michaelis-Menten-type kinetic with a K_m of 0.1 mM and the maximal turnover number is increased to 92 s^{-1}. In contrast, tyrosine acts as inhibitor of chorismate mutase activity. 50 μM of this amino acid resulted in a $[S]_{0.5}$ value of 6.4 mM with a turnover rate of 82.5 s^{-1}. The Hill coefficient of 1.69 indicates the retained cooperativity. The influence of tyrosine was further examined by kinetic assays in the presence of different amounts of this effector. Evaluation of these data according to Dixon (1953) leads to a set of linear curves, one for each chorismate concentration (Fig. 19B). The point of intersection reveals an inhibitory constant K_i of 2.8 μM and further indicates the type of mixed inhibition. In summary, chorismate mutase of *A. nidulans* is tightly regulated in its catalytic activity by tryptophan and tyrosine, with tryptophan as positive effector having a stronger influence on enzymatic behaviour. This is indicated by the fact that alteration of enzyme kinetics is achieved at 10-fold lower concentration (5 μM) compared to the inhibitory concentration of tyrosine (50 μM). The allosteric effectors also show an influence on enzymatic activity with respect to solvent pH (Fig. 19C). Tyrosine shifts the catalytic maximum to a value of 5.4, whereas in the presence of tryptophan maximal catalytic activity is achieved at pH 7.1. In addition, tryptophan broadens the pH range of detectable catalytic activity.

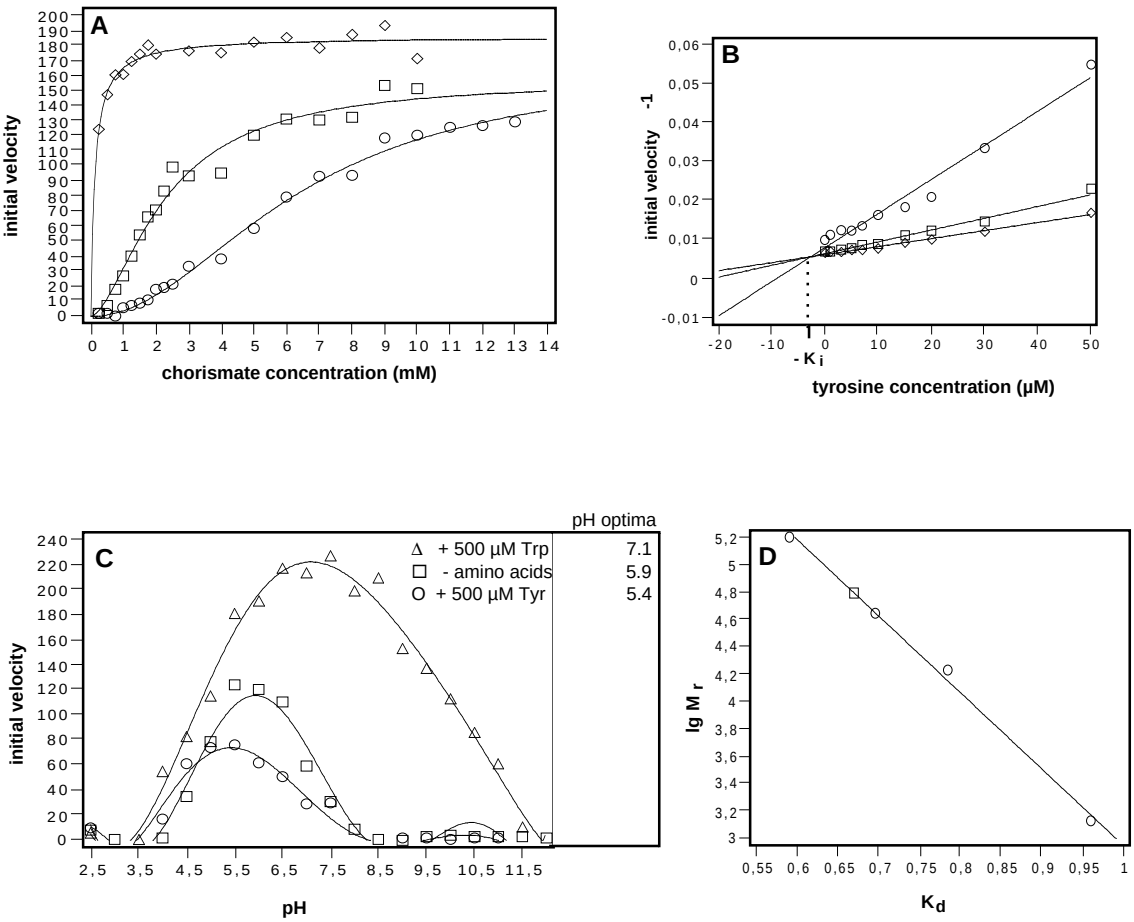

Figure 19: Characteristics of *Aspergillus nidulans* chorismate mutase. *A*, substrate saturation plot of enzyme assays. The enzyme was assayed with 5 µM tryptophan (◊), without effector (□), or in the presence of 50 µM tyrosine (O). The data were fitted to functions describing cooperative or Michaelis-Menten-type saturation. Specific activities are mean values of five independent measurements with a standard deviation not exceeding 20%. *B*, Dixon plot of enzyme assays in the presence of tyrosine at different concentrations. Specific activities were measured in the presence of 2 mM (◊), 3 mM (□), and 4 mM (O) substrate and plotted reciprocally versus tyrosine concentrations. The point of intersection determines the inhibitory constant K_i for tyrosine. *C*, pH optima for chorismate mutase activities under different effector conditions at 1 mM chorismate concentration. The optima are given on the right side. *D*, determination of native molecular weight by gelfiltration. Calibration of a Superdex200 column was performed as described in Experimental Procedures. Using a void volume of 47.19 ml as determined by Blue Dextran and a total column volume of 120 ml, the K_d of the native chorismate mutase (□) was calculated to be 0.67. This value corresponds to a polypeptide with an apparent molecular weight of 62 187 Da. Enzymatic activities are indicated as initial velocities ($\mu mol \cdot min^{-1} \cdot mg^{-1}$) as determined by kinetic stop assays

TABLE IV: **Kinetic parameters of chorismate mutase enzyme from *Aspergillus nidulans*.** Values for k_{cat}, K_m, $[S]_{0.5}$ were defined by fitting initial velocity data to equations describing hyperbolic or cooperative saturation, respectively. Hill coefficients (n_H) were calculated from Hill plots by linear regression.

	Inhibited (50 µM tyrosine)			Unliganded			Activated (5 µM tryptophan)		
	k_{cat} (s^{-1})	$[S]_{0.5}$ (mM)	n_H	k_{cat} (s^{-1})	$[S]_{0.5}$ (mM)	n_H	k_{cat} (s^{-1})	K_m (mM)	n_H
	82.5	6.4	1.69	82	2.3	1.56	92	0.1	0.95
k_{cat} / K_m ($mM^{-1} \cdot s^{-1}$)		12.9			35.7			920	

The chorismate mutase of *A. nidulans* is a dimer

In order to elucidate the quaternary structure of the *aroC* gene product, different approaches were carried out. By analytical ultracentrifugation a mean sedimentation constant S of 4.35±0.2 was determined (data not shown). Using a calculated molecular mass of 30.0 kDa for one single chorismate mutase polypeptide, this S value indicates the existence of a homodimeric structure. Gel filtration analysis supports this result (Fig. 19D). The purified protein eluted from a calibrated Superdex200 column at a defined elution volume corresponding to a K_d value of 0.67. This value matches the estimated K_d for a protein of 62.2 kDa, therefore the chorismate mutase had passed the column as a dimer. Additionally, gradient polyacrylamide gelelectrophoresis under non-denaturing conditions indicated an apparent molecular mass of the native enzyme of approximately 65 kDa (data not shown).

To analyze the structure of AROC, electron microscopic images of the purified enzyme were taken at a magnification of $1 : 3.1 \cdot 10^5$ (Fig. 20A). The images show the presence of a globular protein, approximately 13 nm x 7 nm in size. Different projections of the protein show a cleft between two subunits, indicating a structure where two identical subunits are connected by a dimeric interface.

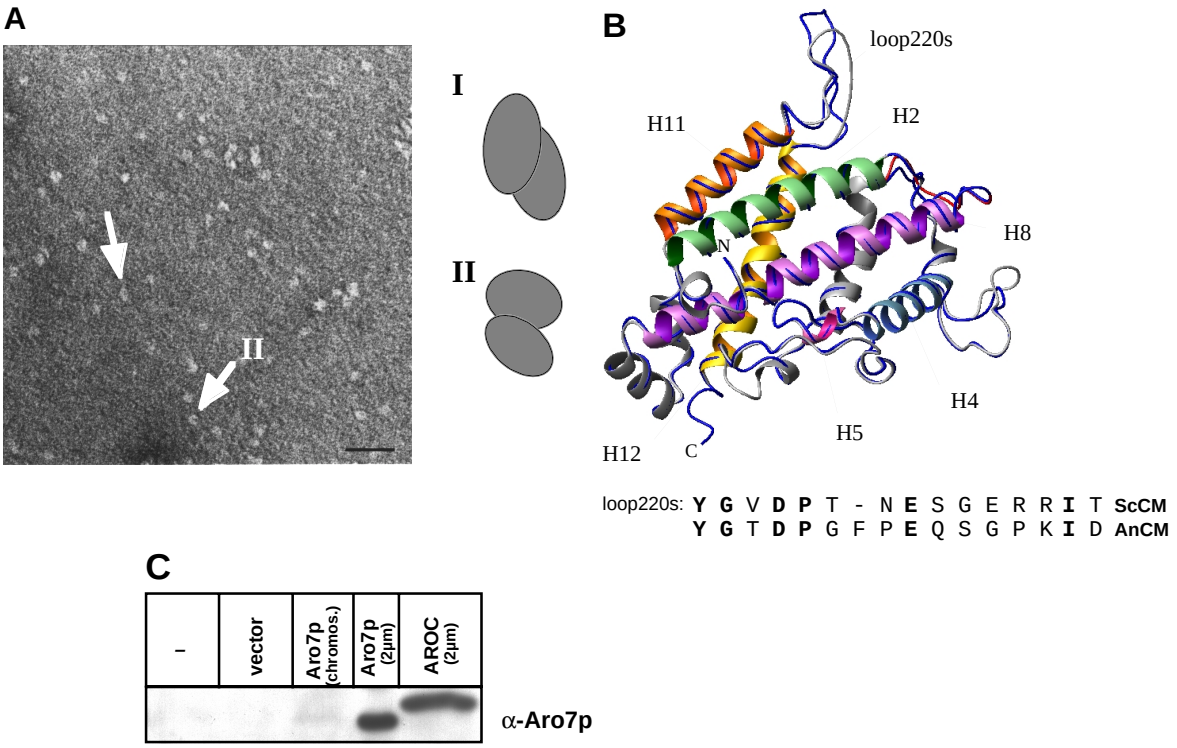

Figure 20: The *A. nidulans* chorismate mutase shares structural similarities with its yeast homologue and is bound with high affinity by a polyclonal antibody against the yeast enzyme. *A*, electron microscopy images show a globular tertiary structure of chorismate mutase built up by two spherical subunits. Pictures of the purified protein were taken at $3.1 \cdot 10^5$-fold magnification. Arrows point out two molecules for which schematic models are shown on the right side. Scale bar equals 32 nm. *B*, homology modeling of *A. nidulans* chorismate mutase based on crystal structures of the yeast enzyme. The primary sequence of the *aroC* gene product was modeled on known 3D structures of yeast chorismate mutase monomers by SWISS-MODEL. In the superimposition the tertiary structure of the yeast protein is represented as colored ribbons, structures of AROC are indicated as blue line. C indicates the C-terminus of the protein, N its N-terminus. Important helices (H) are indicated as well as loop220s connecting helix11 and helix12. The alignment shows a section of both enzymes compromising the region of loop220s with identical residues in bold. *C*, a polyclonal rabbit antibody raised against yeast chorismate mutase binds the AROC enzyme with high affinity. The immunoblot shows 15 µg of crude extracts of yeast strain RH2192 (*aro7::LEU2*) harboring different 2 µm expression plasmids. Lane 3 contains crude extract from yeast strain RH2191 carrying one chromosomal copy of the *ARO7* gene. Proteins cross-reacting with polyclonal antiserum raised against purified yeast chorismate mutase were detected using enhanced chemiluminescence.

Antibodies against the yeast chorismate mutase recognize the *A. nidulans* enzyme

Given the globular, homodimeric structure of the chorismate mutase from *A. nidulans* and its similarity in the deduced amino acid sequence to the yeast enzyme, we performed molecular modeling studies based on the homology to known crystal structures. A three-dimensional structure of the *A. nidulans* enzyme was deduced on the basis of the crystal structures of the yeast chorismate mutases and the secondary structure elements of this newly created structure were calculated. The proposed 3D-structure of the enzyme from *A. nidulans* shows an all-helical structure (Fig. 20B) consisting of 12 helices which resembles that of the yeast protein. Superposition of both structures points out the similarity between them which is highest for the helical elements. Differences between the structures exist in the loops that connect these helices, especially for the loop preceding helix 12 (loop220s).

The modeling studies suggest that similar epitopes exist on the *A. nidulans* chorismate mutase in comparison to the yeast enzyme. To test this hypothesis, we performed immunoblotting with a polyclonal rabbit antibody raised against purified yeast chorismate mutase. Western blots of cell extracts of yeast strain RH2192 harboring the coding cDNA for *aroC* or the *ARO7* gene of *S. cerevisiae*, respectively, on a 2 µm overexpression plasmid revealed a high affinity of this antibody to the *A. nidulans* enzyme (Fig. 20C). Therefore, we conclude that similar epitopes exist on both chorismate mutases and that the structure of the *A. nidulans* enzyme resembles that of the yeast protein.

A crucial region for allosteric regulation of the yeast enzyme is not conserved in the *A. nidulans* chorismate mutase

Given the strong homology of the *aroC* gene product to yeast chorismate mutase, we were interested in whether the mechanism of allosteric transition is conserved in these related proteins. For the Aro7p of *S. cerevisiae*, it has been shown that a single threonine residue in loop220s (T226) is important for proper signal transduction from the effector binding sites to the catalytic centers of the homodimer (Schmidheini *et al.*, 1990a). Exchange of that amino acid residue to isoleucine ($ARO7^{T226I}$) leads to a constitutively activated enzyme that is locked in the R state. Upon alignment of the primary structures of AROC and Aro7p, an aspartate residue (D233) corresponds to that position in the *A. nidulans* enzyme (Fig. 20B). By site-directed mutagenesis, this residue was changed to threonine and isoleucine, respectively, in the *aroC* gene product. Both alleles ($aroC^{D233T}$, $aroC^{D233I}$) were able to

complement the yeast *aro7Δ* deletion indicating that they are expressed properly in the recipient strain. After overexpression in the yeast *aro7Δ* mutant strain RH2192, desalted crude extracts were prepared and specific chorismate mutase activities were determined in the absence or presence of effectors, respectively. In addition, the corresponding *ARO7* alleles, $ARO7^{wt}$, $ARO7^{T226I}$, and $ARO7^{T226D}$, were expressed from the same plasmid in the *aro7Δ* strain and the specific activities were determined in desalted crude extracts under identical conditions (Tab. V).

Generally, the *A. nidulans* chorismate mutase enzymes showed higher specific activities in these assays than their yeast homologues. For the AROC wild-type enzyme a specific activity of 32.5 Units per mg total protein was measured, which is repressed 3.9-fold to 8.4 $U \cdot mg^{-1}$ in the presence of 100 μM tyrosine, whereas tryptophan at 500 μM concentration leads to a 2.7-fold increase in specific activity to a value of 88.5 $U \cdot mg^{-1}$. In contrast, yeast chorismate mutase activity expressed from the $ARO7^{T226D}$ allele was measured to be 3.7 $U \cdot mg^{-1}$. In its inhibited form the enzyme is slightly repressed in its activity (3.3 $U \cdot mg^{-1}$). In the presence of tryptophan activity is increased 3-fold to 11.1 $U \cdot mg^{-1}$. The proteins with a substitution to isoleucine clearly differ in their enzymatic properties. The unliganded $aroC^{D233I}$ gene product shows a specific activity of 30.3 $U \cdot mg^{-1}$, which is repressed 2.3-fold when liganded by tyrosine (13.4 $U \cdot mg^{-1}$) and increased 2.1-fold to 63.0 $U \cdot mg^{-1}$ by its activator tryptophan. The yeast counterpart $Aro7^{T226I}p$ has a specific activity of 20.6 $U \cdot mg^{-1}$ and shows almost no regulatory response to both effectors which is characteristic for this constitutively activated enzyme. Substitution of residue 233 in the *A. nidulans* enzyme to threonine leads to a chorismate mutase with a reduced regulatory range. The uneffected enzymatic activity of 41.3 $U \cdot mg^{-1}$ is decreased 1.9-fold to 22.0 $U \cdot mg^{-1}$ by tyrosine and increased 1.6-fold to 64.3 $U \cdot mg^{-1}$ by tryptophan. The corresponding wt-Aro7p enzyme shows a specific activity of 4.8 $U \cdot mg^{-1}$ in its unliganded state. This value is decreased 4-fold to 1.2 $U \cdot mg^{-1}$ in the presence of tyrosine, whereas tryptophan leads to a 8.4-fold increase of specific activity to 40.2 Units per mg protein.

TABLE V: **Specific enzyme activities of mutant chorismate mutases.** Catalytic activities were determined in desalted crude extracts of yeast strain RH2192 expressing different chorismate mutase-encoding alleles on a 2μm overexpression plasmid driven by the *MET25* promoter. The values measured for each enzyme were standardized for plasmid copy number by Southern analyses.

Protein	Specific activity[a] ($nmol \cdot min^{-1} \cdot mg^{-1}$)			
	Unliganded	Inhibited	Activated	Range of modulation
AROC	32.5	8.4	88.5	**11**
AROC^{D233I}	30.3	13.4	63.0	**4.7**
AROC^{D233T}	41.3	22.0	64.3	**2.9**
Aro7p	4.8	1.2	40.2	**34**
Aro7^{T226I}p	20.6	21.7	26.4	**1.3**
Aro7^{T226D}p	3.7	3.3	11.1	**3.4**

[a] Assay conditions were 50 μg total protein and 2 mM chorismate, 3 min reaction time, and 100 μM tyrosine or 500 μM tryptophan, respectively. Each value is the mean of three independent measurements with a standard deviation not exceeding 20%.

In summary, both AROC mutant proteins exhibit a reduced range of regulatory properties in comparison to the wild-type enzyme. In the wild-type enzyme, carrying the charged amino acid aspartate at position 233, modulation of chorismate mutase activity by the heterotropic effectors tyrosine and tryptophan, respectively, is given by a factor of 11. In the protein derived from the *aroC^{D233I}* mutant allele, the substitution to an apolar amino acid residue leads to reduced modulation and enzymatic activity is within a range of 5. The AROC^{D233T} protein shows almost no response to the effectors with a narrow window of regulation by a factor of 3. The exchange of the aspartate residue to the polar amino acid threonine therefore seems to disturb the intramolecular signal transduction pathway for the allosteric switch.

Taken together, the data clearly show that the chorismate mutase enzymes of the baker's yeast and of the filamentous fungus *A. nidulans* share regulatory and structural properties. Despite these similarities the intramolecular signal transduction pathway for allosteric transition as proposed for the yeast enzyme seems to be not conserved in the AROC protein.

Discussion

The metabolic pathway of aromatic amino acid biosynthesis is a conserved reaction cascade converting two compounds of primary metabolism to phenylalanine, tyrosine, and tryptophan. The flux of compounds through this pathway has to be strictly regulated as synthesis of aromatic amino acids is an energy-consuming process. One mode of regulation lies in controlling the activity of branch point enzymes within a pathway, either by altering their catalytic properties or via altered enzyme levels within a cell. In the aromatic amino acid biosynthetic pathway, the chorismate mutase enzyme is one major point of attack in regulating the flux of chorismic acid into the tyrosine/phenylalanine-specific branch.

We have demonstrated that the protein specified by the *aroC* gene of *A. nidulans* is the chorismate mutase enzyme of this filamentous fungus. According to its high sequence similarity to the monofunctional chorismate mutase of *S. cerevisiae* the *A. nidulans* enzyme has to be classified as member of the AroQ class of chorismate mutases. The kinetic properties of this enzyme demonstrate that the *aroC* gene product is tightly regulated in its activity. The substrate, chorismate, serves as homotropic, positive effector as deduced from positive cooperativity in substrate saturation assays. The determined Hill coefficient of 1.56 clearly indicates that the enzyme contains at least two substrate binding sites. In addition, two aromatic amino acids show heterotropic effects on enzymatic activity. Tyrosine, one end product of the chorismate mutase-specific branch, influences catalytic efficiency negatively, whereas tryptophan, end product of the opposite branch, strongly increases catalytic turnover. Therefore this chorismate mutase enzyme fits well in the model of allosterism as established by Monod and co-workers (Monod *et al.*, 1963). In this simple model a given enzyme exists in two (or more) structural states, tense (T-) state or relaxed (R-) state, with different catalytic activities. The equilibrium between these states is changed upon substrate binding to the active site or by binding of inhibitory or activating ligands at distinct allosteric sites. Further reference to allosterism is given by the homodimeric structure of the *A. nidulans* chorismate mutase since allosteric enzymes are often multimeric proteins.

pH dependency of catalytic activity of the chorismate mutase from *A. nidulans* shows three distinct optima. For the unliganded enzyme the pH optimum of 5.9 fits quite well the intracellular pH in filamentous fungi, which is in a range of 5.7 to 6.5 (Caddick *et al.*, 1986). The negative effector tyrosine shifts this optimum only slightly to a value of 5.4, whereas tryptophan alters the range of catalytic activity dramatically: maximum turnover is achieved at neutral pH of 7.1 and catalytic activity is present over a pH range between 4

and 12. This pH-dependent catalytic behaviour is contrary to that known from bacterial chorismate mutases where highest catalytic activities are achieved at alkaline pH (Schmit and Zalkin, 1969; Dopheide *et al.*, 1972). On the other hand the catalytic activities of the *A. nidulans* enzyme at different pH values resemble that of yeast chorismate mutase. For the *A. nidulans* chorismate mutase, similar absolute catalytic activities were determined as described for the yeast enzyme (Schnappauf *et al.*, 1997). Without any effector present, enzymatic activity was measured over 4.5 pH units and tyrosine restricted catalytic activity to a range of 3 pH units (Fig. 3C). One difference concerning pH dependency is the range of detectable catalytic activity in the presence of tryptophan. The heterotropic positive effector broadens the pH range of activity to 8 pH units compared to a value of 6 units as reported for the *S. cerevisiae* enzyme. In the yeast protein the active site residue E246 has been identified to be important in restricting enzyme activity to acidic conditions (Schnappauf *et al.*, 1997). Upon alignment, this particular residue is conserved within the primary structure of the *A. nidulans* enzyme (E253).

In yeast chorismate mutase, different domains within the dimeric structure have been identified (Sträter *et al.*, 1996). Upon effector binding, the two subunits rotate relative to each other and the allosteric signal is transmitted towards the polypeptide to the catalytic domain. The dimeric structure and all specific amino acids of the yeast enzyme which are important for binding of effectors (R75, R76, N139, S142, T145) and allosteric signal transduction (E23, D24, F28, Y234), as well as active site residues (R16, R157, K168, E198, T242) are conserved in the chorismate mutase of *A. nidulans* (Fig. 1B). Additionally, *in silico* studies showed that AROC can be modeled quite closely onto the tertiary structure of the yeast protein. Therefore, it was surprising that one particular residue, T226, of the yeast enzyme is not conserved in its *A. nidulans* counterpart, as this residue had been characterized as molecular switch in transmitting the signal for T to R state transition (Schmidheini *et al.*, 1989). By site-directed mutagenesis we created two mutant AROC enzymes. None of these enzymes turned out to be locked in either allosteric state, but both proteins showed decreased regulatory properties upon effector binding. We conclude that this narrow window of regulatory modulation represents intermediate states between tense and relaxed state. The role of loop220s in transmitting the intramolecular signal from the effector binding sites to the catalytic domains is obviously different in the chorismate mutases of *S. cerevisiae* and *A. nidulans*. Whereas in the yeast protein substitution of one particular residue in loop220s locks the whole enzyme in its activated state, we did not find such a behaviour in the AROC mutant enzymes. Taking into account that the *A. nidulans*

enzyme resembles its yeast homologue with respect to catalytic and regulatory behaviour as well as structural properties this difference is surprising. It implicates that the structure of this loop preceding helix12, which is part of the catalytic domain, is more flexible in the *A. nidulans* enzyme than in the yeast chorismate mutase. Additionally, we suggest that alternative pathways within the molecule could exist for signal transduction to the active site in contrast to one exclusive via loop220s.

Allosterism is one possible way in regulating enzymatic activity. In living systems additional mechanisms of flux control through a metabolic pathway exist which affect the rate of expression of a given enzyme. For the *aroC* gene product data indicate that its expression is not regulated transcriptionally via the cross-pathway-control network (Piotrowska, 1980). Amino acid starvation conditions showed no influence on *aroC* transcript levels which is consistent with data obtained for *S. cerevisiae* (Schmidheini *et al.*, 1990b). Sequence analysis for upstream regulatory sequences indicated a putative STUA binding site 560 nucleotides upstream of the translational start codon of *aroC*. This sequence element matches the described consensus for STUA response elements (Dutton *et al.*, 1997). As a filamentous fungus *Aspergillus nidulans* has developed additional regulatory networks that constitute differentiation processes. Preliminary transcript level analyses indicate that *aroC* expression is downregulated drastically after the developmental program of asexual conidiation is initiated (not shown). Future research will have to identify *trans* factors as well as *cis* elements responsible for this type of regulation and elucidate whether this is specific for chorismate mutase expression or, in contrast, is a general effect after the developmental program has been established.

References

Adams, T.H., J.K. Wieser, and J.-H. Yu (1998) Asexual sporulation in *Aspergillus nidulans*. *Microbiol. Mol. Biol. Rev.* **62:** 35-54.

Alwine, J.C., D.J. Kemp, and G.R. Stark (1977) Method for detection of specific RNAs in agarose gels by transfer to diazobenzyloxymethyl-paper and hybridization with DNA probes. *Proc. Natl. Acad. Sci. USA* **74:** 5350-5354.

Andersson, L.O., H. Borg, and M. Mikaelsson (1972) Molecular weight estimation of proteins by electrophoresis in polyacrylamide gel of graded porosity. *FEBS Lett.* **20:** 199-202.

Andrews, P.R., G.D. Smith, and I.G. Young (1973) Transition state stabilization and enzyme catalysis. Kinetic and molecular orbital studies of the rearrangement of chorismate to prephenate. *Biochemistry* **12:** 3492-3498.

Bradford, M.M. (1976) A rapid and sensitive method for the quantitation of microgram quantities of protein utilizing the principle of protein-dye binding. *Anal. Biochem.* **72:** 248-254.

Braus, G.H. (1991) Aromatic amino acid biosynthesis in the yeast *Saccharomyces cerevisiae*: a model system for the regulation of a eukaryotic biosynthetic pathway. *Microbiol. Rev.* **55:** 349-370.

Caddick, M.X., A.G. Brownlee, and H.N. Arst Jr. (1986) Regulation of gene expression by pH of the growth medium in *Aspergillus nidulans*. *Mol. Gen. Genet.* **203:** 346-353.

Chook, Y.M., H. Ke, and W.N. Lipscomb (1993) Crystal structures of the monofunctional chorismate mutase from *Bacillus subtilis* and its complex with a transition state analog. *Proc. Natl. Acad. Sci. USA* **90:** 8600-8603.

Chook, Y.M., J.V. Gray, H. Ke, and W.N. Lipscomb (1994) The monofunctional chorismate mutase from *Bacillus subtilis*. *J. Mol. Biol.* **240:** 476-500.

Dimroth, P. (1986) Preparation, characterization and reconstitution of oxalacetate decarboxylase from *Klebsiella aerogenes*, a sodium pump. *Methods Enzymol.* **125:** 530-540.

Dixon, M. (1953) *J. Biochem.* **55:** 170-171.

Dopheide, T.A.A., P. Crewther, and B.E. Davidson (1972) Chorismate mutase-prephenate dehydratase from *Escherichia coli* K12. II. Kinetic properties. *J. Biol. Chem.* **247:** 4447-4452.

Dutton, J.R., S. Johns, and B.L. Miller (1997) StuAp is a sequence-specific transcription factor that regulates developmental complexity in *Aspergillus nidulans*. *EMBO J*. **16:** 5710-5721.

Elble, R. (1992) A simple and efficient procedure for transformation of yeasts. *BioTechniques* **13:** 18-20.

Fletcher, R., and M.J.D. Powell (1963) A rapidly convergent descent method for minimization. *Computer Journal* **6:** 163-168.

Giebel, L.B., and R.A. Spritz (1990) Site-directed mutagenesis using a double-stranded DNA fragment as a PCR primer. *Nucl. Acids Res.* **18:** 4947.

Gu, W., D.S. Williams, H.C. Aldrich, G. Xie, D.W. Gabriel, and R.A. Jensen (1997) The *aroQ* and *pheA* domains of the bifunctional P-protein from *Xanthomonas campestris* in a context of genomic comparison. *Microb. Comp. Genomics* **2:** 141-158.

Guex, N., and M.C. Peitsch (1997) SWISS-MODEL and the Swiss-PdbViewer: An environment for comparative protein modelling. *Electrophoresis* **18:** 2714-2723.

Heinemeyer, W., J.A. Kleinschmidt, J. Saidowsky, C. Escher, and D.H. Wolf (1991) Proteinase yscE, the yeast proteasome/multicatalytic-multifunctional proteinase: mutants unravel its function in stress induced proteolysis and uncover its necessity for cell survival. *EMBO J.* **10:** 555-562.

Hilton, J.L., P.C. Kearney, and B.N. Ames (1965) Mode of action of the herbicide 3-amino-1,2,4-triazole (amitrole): inhibition of an enzyme of histidine biosynthesis. *Arch. Biochem. Biophys.* **112:** 544-547.

Hinnebusch, A.G. (1988) Mechanisms of gene regulation in the general control of amino acid biosynthesis in *Saccharomyces cerevisiae*. *Microbiol. Rev.* **52:** 248-273.

Käfer, E. (1977) Meiotic and mitotic recombination in Aspergillus and its chromosomal aberrations. *Adv. Gen.* **19:** 33-131.

Koradi, R., M. Billeter, and K. Wüthrich (1996) MOLMOL: a program for display and analysis of macromolecular structures. *J. Mol. Graphics* **14:** 51-55.

Laemmli, U.K. (1970) Cleavage of structural proteins during the assembly of the head of the bacteriophage T4. *Nature* **227:** 680-685.

Lipman, D.J., and W.R. Pearson (1985) Rapid and sensitive protein similarity searches. *Science* **227:** 1435-41.

Liu, H., J. Krizek, and A. Bretscher (1992) Construction of a *GAL1*-regulated yeast cDNA expression library and its application to the identification of genes whose overexpression causes lethality in yeast. *Genetics* **132:** 665-673.

Ma, J., X. Zheng, G. Schnappauf, G. Braus, M. Karplus, and W.N. Lipscomb (1998) Yeast chorismate mutase in the R state: simulations of the active site. *Proc. Natl. Acad. Sci. USA* **95:** 14640-14645.

MacBeath, G., P. Kast, and D. Hilvert (1998) A small, thermostable, and monofunctional chorismate mutase from the archeon *Methanococcus jannaschii*. *Biochemistry* **37:** 10062-10073.

Martinelli, S.D., and J.R. Kinghorn (ed.) (1994) *Aspergillus: 50 years on* Elsevier Science B. V., Amsterdam.

May, G.S., M.L.-S. Tsang, H. Smith, S. Fidel, and N.R. Morris (1987) *Aspergillus nidulans* β-tubulin genes are unusually divergent. *Gene* **55:** 231-243.

Miozzari, G., P. Niederberger, and R. Hütter (1978) Tryptophan biosynthesis in *Saccharomyces cerevisiae*. Control of the flux through the pathway. *J. Bacteriol.* **134:** 48-59.

Monod, J., J.P. Changeux, and F. Jacob (1963) Allosteric proteins and cellular control systems. *J. Mol. Biol.* **6:** 306-329.

Mumberg, D., R. Müller, and M. Funk (1994) Regulatable promoters of *Saccharomyces cerevisiae*: comparison of transcritional activity and their use for heterologous expression. *Nucl. Acid Res.* **22:** 5767-5768.

Newell, J.O., and H.K. Schachmann (1990) Amino acid substitutions which stabilize aspartate transcarbamoylase in the R state disrupt both homotropic and heterotropic effects. *Biophys. Chem.* **37:** 183-196.

Peitsch, M.C. (1995) Protein modeling by E-mail. *Bio/Technology* **13:** 658-660.

Peitsch, M.C. (1996) ProMod and Swiss-Model: Internet-based tools for automated comparative protein modelling. *Biochem. Soc. Trans.* **24:** 274-279.

Piotrowska, M. (1980) Cross-pathway regulation of ornithine carbamyltransferase synthesis in *Aspergillus nidulans*. *J. Gen. Microbiol.* **116:** 335-339.

Punt, P.J., M.A. Dingemanse, B.J.M. Jacobs-Meijsing, P.H. Pouwels, and C.A.M.J.J. van den Hondel (1988) Isolation and characterization of the glyceraldehyde-3-phosphate dehydrogenase gene of *Aspergillus nidulans*. *Gene* **69:** 49-57.

Punt, P.J., and C.A.M.J.J. van den Hondel (1992) Transformation of filamentous fungi based on hygromycin B and phleomycin resistance markers. *Methods Enzymol.* **216:** 447-457.

Roberts, C.F. (1969) Isolation of multiple aromatic amino acid mutants in *Aspergillus nidulans*. *Aspergillus Newsletter* **10:** 19-21.

Romero, R.M., M.F. Roberts, and J.D. Phillipson (1995) Chorismate mutase in microorganisms and plants. *Phytochemistry* **40:** 1015-1025.

Sanger, F., S. Nicklen, and A.R. Coulson (1977) DNA sequencing with chain-terminating inhibitors. *Proc. Natl. Acad. Sci. USA* **74:** 5463-5467.

Schmidheini, T., P. Sperisen, G. Paravicini, R. Hütter, and G. Braus (1989) A single point mutation results in a constitutively activated and feedback-resistant chorismate mutase of *Saccharomyces cervisiae*. *J. Bacteriol.* **171:** 1245-1253.

Schmidheini, T., H.-U. Mösch, , J.N.S. Evans, and G. Braus (1990a) Yeast allosteric chorismate mutase is locked in the activated state by a single amino acid substitution. *Biochemistry* **29**: 3660-3668.

Schmidheini, T., H.-U. Mösch, R. Graf, and G.H. Braus (1990b) A GCN4 protein recognition element is not sufficient for GCN4-dependent regulation of transcription in the *ARO7* promoter of *Saccharomyces cerevisiae*. *Mol. Gen. Genet.* **224:**57-64.

Schmit, J.C., and H. Zalkin (1969) Chorismate mutase-prephenate dehydratase. Partial purufication and properties of the enzyme from *Salmonella typhimurium*. *Biochemistry* **8:** 174-181.

Schnappauf, G., N. Sträter, W.N. Lipscomb, and G.H. Braus (1997) A glutamate residue in the catalytic center of the yeast chorismate mutase restricts enzyme activity to acidic conditions. *Proc. Natl. Acad. Sci. USA* **94:** 8491-8496.

Schnappauf, G., S. Krappmann, and G.H. Braus (1998) Tyrosine and tryptophan act through the same binding site at the dimer interface of yeast chorismate mutase. *J. Biol. Chem.* **273:** 17012-17017.

Sträter, N., K. Håkansson, G. Schnappauf, G. Braus, and W.N. Lipscomb (1996) Crystal structure of the T state of allosteric yeast chorismate mutase and comparison with the R state. *Proc. Natl. Acad. Sci. USA* **93:** 3330-3334.

Sträter, N., G. Schnappauf, G.H. Braus, and W.N. Lipscomb (1997) Mechanism of catalysis and allosteric regulation of yeast chorismate mutase from crystal structures. *Stucture* **5:** 1437-1452.

Tesfaigzi, J., W. Smith-Harrison, and D.M. Carlson (1994) A simple method for reusing western blots on PVDF membranes. *BioTechniques* **17:** 268-269.

Valentine, R.C., P.M. Shapiro, and E.R. Stadtman (1968) Regulation of glutamine synthetase. XII. Electron microscopy of the enzyme from *Escherichia coli*. *Biochemistry* **7:** 2143-2152.

Weiss, U., and J.M. Edwards (1980) *The Biosynthesis of Aromatic Amino Acids* Wiley, New York.

Yelton, M.M., J.E. Hamer, E.R. deSouza, E.J. Mullaney, and W.E. Timberlake (1983) Developmental regulation of the *Aspergillus nidulans trpC* gene. *Proc. Natl. Acad. Sci. USA* **80:** 7576-7580.

Zaudy, G. (1969) The location of some multiple aromatic mutants in *Aspergillus nidulans*. *Aspergillus Newsletter* **10:** 22.

Conclusions

Chorismate Mutases: Unique Enzymes Accelerating an Unusual Chemical Reaction of Primary Metabolism

The intramolecular conversion of chorismic acid to prephenic acid is a rare example of an enzyme-catalysed pericyclic reaction in nature. It resembles formally a Claisen rearrangement and is accelerated *in vivo* by the action of chorismate mutases. These enzymes, which are solely found in microorganisms and plants, enhance the one-step process by a factor of up to 10^6. Whereas for the non-enzymatic reaction a negative activation entropy is observed which is typical for [3,3] sigmatropic rearrangements, the mutase-catalysed reaction displays an activation entropy of almost zero (Görisch, 1978; Ganem, 1996). This indicates that the conformation of chorismate is highly restricted within the enzyme/substrate complex to support catalysis. For both the spontaneous as well as the enzymatic reaction a chair-like transition state has been proposed that can be mimicked by a stable *endo*-oxabicyclic analogue (Bartlett and Johnson, 1985). Further insight concerning the mechanism of the enzymatic rearrangement has been gained from structural studies. The X-ray structures of three chorismate mutases have been solved. By comparison of the binding mode of the stable transition state analogue the molecular environment established at the active sites was deduced. Despite low similarities with respect to primary structure, binding of the inhibitor is similar in all three enzymes derived from *Bacillus subtilis*, *Escherichia coli*, and *Saccharomyces cerevisiae* (Chook *et al.*, 1994; Lee *et al.*, 1995; Sträter *et al.*, 1997). Detailed analysis based on molecular dynamics simulations of the yeast active site in complex with the inhibitor has yielded specific knowledge concerning the molecular environment of the active site cavity (Ma *et al.*, 1998).

In this work, two additional chorismate mutases derived from fungal sources, the yeast *Hansenula polymorpha* and the filamentous fungus *Aspergillus nidulans*, were isolated and characterized. On the basis of the encoding genes, both enzymes were overexpressed and purified to homogeneity. It will be of special interest to obtain crystallographic data of both eukaryotic chorismate mutases and to compare their structural properties with the available structures. Furthermore, by construction of a chorismate mutase-deficient strain of the methylotrophic yeast *H. polymorpha*, a well-suited vector-host system for overexpression and purification of chorismate mutases in general is now available.

Fungal Chorismate Mutases Are Highly Conserved

Chorismate mutases initiate the tyrosine/phenylalanine-specific branch of aromatic amino acid biosynthesis. Besides the *ARO7*-encoded chorismate mutase of the baker's yeast *S. cerevisiae*, no further eukaryotic CM activities have been characterized in great detail. Here, the enzymatic activities derived from two fungi were cloned and isolated to extend the $AroQ_r$ class of chorismate mutases (MacBeath *et al.*, 1998).

Upon aligning the deduced primary structures of fungal chorismate mutases, a variety of conserved residues are evident with overall similarities ranging from 63% to 70% (see Chapter 3, Fig. 12). For the baker's yeast enzyme, specific residues have been mapped and assigned to different functions like effector binding, allosteric signal transduction, and catalysis (for review see Helmstaedt *et al.*, 2000). Besides one exception, all these side chains are invariant in fungal primary sequences. The effector binding residue Thr^{145} of Aro7p is not conserved as in the Haro7p enzyme a methionine is found at the respective position, whereas the AROC protein displays a valine side chain. Based on structural studies, Thr^{145} of Aro7p was proposed to contribute to binding of the negative effector tyrosine. Replacement of this residue by valine resulted in an enzyme that was partially impaired in tyrosine binding whereas binding of the allosteric activator was not affected. The AROC protein displays a lower inhibitory constant K_i for tyrosine in comparison to the *S. cerevisiae* enzyme. This accounts for other residues at the effector binding side that contribute to tight tyrosine binding in the *A. nidulans* chorismate mutase. Of special interest is a glutamate side chain (Glu^{246} of Aro7p) that has been shown to restrict enzymatic activity to acidic conditions (Schnappauf *et al.* 1997). In both Haro7p and AROC this residue is conserved (Glu^{247} and Glu^{253}, respectively) and for the *A. nidulans* chorismate mutase it has been shown in this thesis that pH dependency of catalytic turnover is similar to the *ARO7* gene product of *S. cerevisiae*. In conclusion, fungal chorismate mutases are generally well adapted to the acidic intracellular pH found in these microorganisms (Caddick *et al.*, 1986; Cimprich *et al.*, 1995).

Allosteric regulation by homotropic and heterotropic effectors requires distinct features of a given enzyme. Oligomerisation is one of these, and it has been demonstrated here for the Hansenula as well as the Aspergillus enzyme that both chorismate mutases display dimeric quaternary structures like their *S. cerevisiae* counterpart. In the Aro7p enzyme, the binding site, which is identical for both heterotropic effectors, is built up at the dimeric interface between the two protomers (Schnappauf et al., 1998). In conclusion, dimerisation of identical subunits to form the chorismate mutase holoenzyme is

evolutionary conserved in fungi and contributes to the regulatory behaviour of these model enzymes for allostery. Allosteric signal transduction from the effector binding sites to the active sites is mediated along alternative pathways within the *S. cerevisiae* holoenzyme (Sträter *et al.*, 1997). A specific structural element, loop220s, was identified to contribute to the T-to-R transition (Schmidheini *et al.*, 1990; Graf *et al.*, 1995). In the global alignment of fungal chorismate mutases it becomes evident that this loop is not conserved in primary structure. Additionally, we were not able to mimic a specific, unregulated Aro7p mutant enzyme by site-directed mutagenesis of the *aroC* gene. Therefore, it is likely that the overall structural properties of loop220s are important for serving as an intramolecular hinge with no specific side chains contributing to the flexible nature of this polypeptide segment. It will be interesting to test the interchangeability of loops from different fungal chorismate mutases concerning allosteric signal transduction.

The Regulatory Pattern Triggering Chorismate Mutase Activity Is a Common Theme in Fungi

Regulation of chorismate mutase activity is necessary, as this enzyme lies at a branch point in primary metabolism. Chorismic acid is the last common intermediate of aromatic amino acid biosynthesis and feeds two main branches. To regulate the flux into the tyrosine/phenylalanine-specific branch, tight regulation of chorismate mutase activity is strictly necessary. The two fungal enzymes characterized in this study display cooperative kinetics and are regulated by the heterotropic effectors tyrosine and tryptophan, respectively. No inhibitory effect of phenylalanine was determined at physiological concentrations (not shown). In conclusion, this allosteric regulation is identical to the one described for the *S. cerevisiae* enzyme. Activation by tryptophan, the end product of the competing branch, has been also reported for the chorismate mutase of the filamentous fungus *Neurospora crassa* as well as for a variety of other yeast species (Baker, 1966; Bode and Birnbaum, 1991). Concerning inhibition, yeast chorismate mutases can be classified in four groups. Either no inhibition by phenylalanine or tyrosine is present, or by both amino acids or exclusively by one of them. The Haro7p gene product of *H. polymorpha* strain RB11 is solely inhibited by tyrosine. This is in contrast to the results described by Bode and Birnbaum (1991) which additionally found inhibition by phenylalanine in the *H. polymorpha* strain SBUG 500. In their study a high concentration of 1 mM phenylalanine was used. Using 100 µM of this amino acid in enzymatic assays, no significant inhibition of enzymatic activity was detected and therefore phenylalanine as a physiological inhibitor of chorismate mutase in *H. polymorpha* is very unlikely.

Transcriptional regulation of gene expression is an additional mechanism to trigger enzymatic activity. For none of the fungal chorismate mutase-encoding genes described in this study an induction of transcription has been determined upon amino acid starvation. This is of general importance as fungi have developed a specific regulatory network to counteract this particular environmental condition. Most of the genes involved in amino acid biosynthesis are targets of the cross-pathway/general control of amino acid biosynthesis (Hinnebusch, 1996). The fact that neither in the yeasts *S. cerevisiae* and *H. polymorpha* nor in the filamentous fungus *A. nidulans* the chorismate mutase-encoding genes are regulated by this control system accounts for a general necessity that has evolved from a common ancestor. No transcriptional regulation of chorismate mutase expression in the methylotrophic yeast *H. polymorpha* was found. There, *HARO7* transcription is the target of a regulatory system involved in methanol utilization. This reflects that although the regulatory properties of chorismate mutases in fungi are well conserved and quite similar, specific differences have evolved to meet specific needs of the individual microorganism.

Co-Evolution of Allosteric and Transcriptional Regulation of Chorismate Mutase Activity

The *ARO7*^{c} allele of *S. cerevisiae* used in this study reflects a chorismate mutase activity that is not regulated allosterically. This is reminiscent to bacterial chorismate mutases, which are found to display Michaelis-Menten-like kinetics in substrate saturation assays. Furthermore, catalytic efficiency (k_{cat}/K_m) of this unregulated yeast CM activity of 13.1 $min^{-1} \cdot \mu M^{-1}$ is in the same range as the one reported for the *E. coli* P-protein CM activity with 10.4 $min^{-1} \cdot \mu M^{-1}$ (Schmidheini *et al.*, 1990a; Zhang *et al.*, 1998). The allelic situation with an allosterically unregulated chorismate mutase expressed in a general control-dependent manner might reflect an early evolutionary situation as the existence of a reversed Gcn4p recognition element in the *ARO7* promoter region that is able to bind the transcriptional activator *in vitro* implies that this gene formerly was subjected to the general control system (Schmidheini *et al.*, 1990b). This sequence element is also found in the 5' region of the *aroC* gene of *A. nidulans*. From structural studies it has been deduced that the dimeric, allosterically regulated chorismate mutase might have evolved from a monomeric, unregulated ancestor by a gene duplication/gene fusion event (Sträter *et al.*, 1997). Given the drastic effects observed for the *ARO7*^{c} allele when being subjected to the general control, it can be speculated that chorismate mutase expression was removed from the general control system before this gene duplication and fusion. As the absence of

transcriptional regulation upon amino acid starvation conditions is likely to be conserved among fungi, it might be suggested that this event occurred before the evolutionary separation of fungal species. By dimerization and remodelling of distinct domains, allosteric behavior was achieved for the fungal chorismate mutases. In bacterial systems, alternative strategies have evolved to achieve regulation of chorismate mutase activity. In *E. coli*, two isoenzymes are expressed in which the CM domains are fused to additional enzymatic activities. Due to the fusion events, feedback regulation by end products has been established.

References

Bartlett, P.A., and C.R. Johnson (1985) An inhibitor of chorismate mutase resembling the transition-state conformation. *J. Am. Chem. Soc.* **107:** 7792-7793.

Braus, G.H. (1991) Aromatic amino acid biosynthesis in the yeast *Saccharomyces cerevisiae*: a model system for the regulation of a eukaryotic biosynthetic pathway. *Microbiol. Rev.* **55:** 349-370.

Caddick, M.X., A.G. Brownlee, and H.N. Arst Jr. (1986) Regulation of gene expression by pH of the growth medium in *Aspergillus nidulans*. *Mol. Gen. Genet.* **203:** 346-353.

Chook, Y.M., H. Ke, and W.N. Lipscomb (1993) Crystal structures of the monofunctional chorismate mutase from *Bacillus subtilis* and its complex with a transition state analog. *Proc. Natl. Acad. Sci. USA* **90:** 8600-8603.

Cimprich, P., J. Slavik, and A. Kotyk (1995) Distribution of individual cytoplasmatic pH values in a population of the yeast *Saccharomyces cerevisiae. FEMS Microbiol. Lett.* **130:** 245-252.

Ganem, B. (1996) The mechanism of the Claisen rearrangement: déjà vu all over again. *Angew. Chem. Int. Ed. Engl.* **35:** 936-945.

Görisch, H. (1978) On the mechanism of the chorismate mutase reaction. *Biochemistry* **17:** 3700-3705.

Graf, R., Y. Dubaquie, and G.H. Braus (1995) Modulation of the allosteric equilibrium of yeast chorismate mutase by variation of a single amino acid residue. *J. Bacteriol.* **177:** 1645-1648.

Helmstaedt, K., S. Krappmann, and G.H. Braus (2000) Yeast chorismate mutase as model enzyme for allosteric regulation of catalytic activity. Submitted for publication.

Hinnebusch, A. (1992) General and pathway-specific regulatory mechanisms controlling the synthesis of amino acid biosynthetic genes in *Saccharomyces cerevisiae*. In *The Molecular and Cellular Biology of the Yeast Saccharomyces.* Vol. 2: Gene expression.

(E.W. Jones, J.R. Pringle, and J.R. Broach, eds), pp. 319-414. Cold Spring Harbor Laboratory Press, Cold Spring Harbor, New York.

Lee, A.Y., P.A. Karplus, B. Ganem, and J. Clardy (1995) Atomic structure of the buried catalytic pocket of *Escherichia coli* chorismate mutase. *J. Am. Chem. Soc.* **117:** 3627-3628

Ma, J., X. Zheng, G. Schnappauf, G. Braus, M. Karplus, and W.N. Lipscomb (1998) Yeast chorismate mutase in the R state: simulations of the active site. *Proc. Natl. Acad. Sci. USA* **95:** 14640-14645.

MacBeath, G., P. Kast, and D. Hilvert (1998) A small, thermostable, and monofunctional chorismate mutase from the archeon *Methanococcus jannaschii*. *Biochemistry* **37:** 10062-10073.

Schmidheini, T., H.-U. Mösch, J.N. Evans, and G. Braus (1990a) Yeast allosteric chorismate mutase is locked in the activated state by a single amino acid substitution. *Biochemistry* **29:** 3660-3668.

Schmidheini, T., H.-U. Mösch, R. Graf, and G.H. Braus (1990b) A GCN4 protein recognition element is not sufficient for GCN4-dependent regulation of transcription in the *ARO7* promoter of *Saccharomyces cerevisiae*. *Mol. Gen. Genet.* **224:** 57-64.

Schnappauf, G., N. Sträter, W.N. Lipscomb, and G.H. Braus (1997) A glutamate residue in the catalytic center of the yeast chorismate mutase restricts enzyme activity to acidic conditions. *Proc. Natl. Acad. Sci. USA* **94:** 8491-8496.

Schnappauf, G., S. Krappmann, and G.H. Braus (1998) Tyrosine and tryptophan act through the same binding site at the dimer interface of yeast chorismate mutase. *J. Biol. Chem.* **273:** 17012-17017.

Sträter, N., G. Schnappauf, G. Braus, and W.N. Lipscomb (1997) Mechanisms of catalysis and allosteric regulation of yeast chorismate mutase from crystal structures. *Structure* **5:** 1437-1452.

Zhang, S., G. Pohnert, P. Kongsaeree, D.B. Wilson, J. Clardy, and B. Ganem (1998) Chorismate mutase-prephenate dehydratase from *Escherichia coli*. Study of catalytic and regulatory domains using genetically engineered proteins. *J. Biol. Chem.* **273:** 6248-6253.

Curriculum vitae

Sven Krappmann, Dipl.-Chem. Univ.

born on October, 15th 1969 in Hanau, Germany

Education:

1976-1980	**Primary education** in Nürnberg and Oberasbach
1980-1989	**Secondary education** at the Dietrich-Bonhoeffer-Gymnasium, Oberasbach

Scientific Background:

Oct. 1990-April 1996	**Study** of Chemistry at the Friedrich-Alexander-University, Erlangen/Nürnberg
Sept. 1995-April 1996	**Diploma** thesis in Biochemistry: "Characterization of a *HIS7* Promoter-binding Protein of the Baker's Yeast *Saccharomyces cerevisiae*"
Oct. 1996-Nov. 2000	**Scientific assistant** at the Institute of Microbiology & Genetics, Georg-August-University, Göttingen